TOJSAT
The Online Journal of Science and Technology

ISSN 2146-7390

# The Online Journal of Science and Technology

*Volume 5 Issue 1*

*January 2015*



www.tojsat.net
January 2015

Published in TURKEY

**Contact Address:**

Prof. Dr. Mustafa Şahin Dündar - TOJSAT, Editor Sakarya-Turkey

**Message from the Editor-in-Chief**

TOJSAT welcomes you. TOJSAT would like to thank you for your online educational interest. We are delighted that more educators, teachers, parents, and students from around the world had visited the last issue. It means that TOJSAT has continued to educate academic people about new developments on science around the world. We hope that the new issue will also successfully accomplish our global science goal.

TOJSAT, Sakarya University Governor State University and other international universities will organize International Science and Technology Conference –ISTEC-2015 in Saint Petersburg, Russia in September, 2015.

For any suggestions and comments on the international online journal TOJSAT, please do not hesitate to fill out the comments & suggestion form.

**January 1, 2015**
**Editor-in-Chief**
**Prof. Dr. Aytekin İŞMAN**
**Sakarya University**

Dear Journal Readers,

As an editör, I wish you 2015 filled with peace, joy, health and happiness. Now, we welcome you the 5th volume of the jornal. We carried out a conference in Doha, Qatar and the selected, peer-reviewed papers were accepted for publication apart from contributions from all over the World. The accepted and published papers are from Toxicology to computer science.

**Prof. Dr. M. Şahin DÜNDAR**

**Editor, TOJSAT**

## Table of Contents

# Assessing the Efficient Utilization of Electricity by Domestic Consumers in the Agona District in Central Region

Enock A. Duodu and J. D. Owusu-Sekyere

Department of Agricultural Engineering, University of Cape Coast, Ghana
enock.duodu@ucc.edu.gh

**Abstract**
The study assessed the efficient utilization of electricity by domestic consumers in the Agona District. Descriptive survey design was employed in the study. Purposive and simple random sampling techniques were used in selecting five (5) towns and 100 respondents, respectively. A questionnaire as well as interview and observation methods were used in data collection. The data obtained from respondents were analyzed using frequencies and percentages. The study revealed that almost two-thirds (63%) of the respondents in the condominium consume electricity from a single central credit meters. Again, the study showed that lack of access to energy efficient technologies have contributed to the waste of electricity in the households. The results also revealed that consumers have little or no knowledge about some basic energy conservation tips. It is recommended that all households in such condominium should be provided with separate meters preferably the pre-paid meters so as to encourage consumers to conserve energy. Also, consumers are to use modern appliances with energy efficient standards and label codes. Finally, energy conservation tips should be known and practiced by all the domestic consumers of electricity.

**Keywords:** Condominium; Credit meters; Pre-paid meters; Electricity Bills

## Introduction

Electricity supply in Ghana suffered a serious decline as a result of several factors but mainly due to poor inflows for water into the Volta basin, which until then accounted for 95% of Ghana's electricity supply. Industry including the Volta Aluminum Company (VALCO) accounts for the largest consumption of electricity in the country. VALCO alone takes about 59% of total electricity consumption. After the industrial sector has taking 79% of the country's total electricity consumption, the residential, commercial and government sector account for the remaining 21% (Energy Foundation, 1999).

Until recently, Ghana's total energy requirement was produced from hydro generation. This is now complemented by thermal generation and imports. For example, in 1999 Volta River Authority (VRA) produced the total energy requirement of the country with 60% from hydro generation 25% from thermal generation and 15% import from La Cote d'Ivoire (Donkor, 2001).

Though power from hydro plants is relatively cheap to produce, its availability depends on the rainfall pattern, hence the need to diversify supply base from hydro to other bases such as thermal power system. Such an approach could help minimize the effect of decline in electricity generation resulting from drought in the Volta River basin, forcing the power utilities to embark on a power curtailment exercise, which adversely affect the economic growth of the country.

According to VRA (2001), the authority operates a total installed power generation capacity of 1,432MW. This is made up of two hydro-electric plants on the Volta River with installed capacities of 912 MW at Akosombo and 160MW at Kpong, a 30MW diesel plant at Tema, and a 330MW combined cycle thermal power plant at Takoradi.

## Background to the Study

The annual growth in the demand for electrical energy before 1986 was low as 2%. However, for the period 1986 – 1997, Ghana moved into a higher energy consuming bracket with a 10-15% annual demand growth rate. The phenomenal growth in the demand for electricity was mostly due to the economic policies of the 1980's (economic recovery programme and structural adjustment programme) which brought about profound changes – production level of factories going up and new private enterprise opening by the day in every community which need to be connected to the national grid. Also, at the current annual growth rate of 10-15%, the demand for electricity energy is expected to increase to at least seven times (7x) the present level of demand by the year 2020. However, Ghana lacks the energy resources to satisfy the ever-increasing demand, building new power capacity plants is extremely expensive and the need to import fuel to run new thermal plants is also not an attractive option. Report by Donkor (2001) indicated that in 1998, Ghana imported electrical energy from Cote d'Ivoire at much higher cost than is available domestically due to inability to produce sufficient electrical energy.

Research conducted by Energy Foundation (1999) observed that it has been estimated that the level of waste in the use of electrical energy by consumers is over 20%, indicating that consumers waste the entire generation of Kpong hydro

power plant. This is due to the use of obsolete equipment, inadequate maintenance on appliances and lack of knowledge about the very steps that can be taken to improve the efficient use of electrical energy.

## Statement of the Problem

Electrical energy is one of the pre-requisite for national development. As the government is doing all it can to ensure an uninterrupted power supply for industrial and commercial consumers, there is a need to save energy as much as possible. For example, in March 2003 an increase in electricity tariff in the country saw many domestic consumers paying huge electricity bills; however, consumers are ignorant about how to use electricity efficiently to reduce their energy consumption. As stated by a consumer "why do I consumed so much of electricity and pay so much".

## Purpose of the Study

The purpose of the study was to assess the efficient utilization of electricity by domestic consumers in the Agona District. Again, to evaluate the benefits derived from judicious use of energy by consumers.

The key issues of the study were therefore to find out;

i. the consumption pattern of electrical appliances.
ii. the availability of energy efficient technology.
iii. the energy saving tips and measures.

## Research Questions

The research questions that guided the study were as follow:

1. what methods of billing systems are being employ by service providers?
2. how do consumers know that an appliance is energy efficient?
3. what strategies can be put in place to reduce the waste of electricity consumption in the households?

## Significance of the Study

The study aimed at finding out how energy is dissipated by domestic consumers. It will also help to identify the most suitable practices and measures to put in place to reduce energy in the households. Moreover, it would help erase the erroneous impression consumers have on the staff of ECG as thieves thinking that the huge bills they pay are due to illegal increment of bills. Finally, the study may serve as an operative level for further research into certain aspect of the efficient use of electricity.

## Methodology

## Study Area

The Agona District is situated in the eastern portion of the central region with a total land size of 540sq km and a population of about 15,8995(GSS, 2001). The district is bordered on the east by Awutu-Effutu-Senya District; on the west by Asikuma-Odoben-Brakwa District; on the north east by Akim West District; on the north west by Birim South District and to the south by the Gomoa District with Agona Swedru as the district capital. The district has 862 settlements with 11 urban towns; and out of the total settlements, only 15 have been connected to the national electricity grid (AgonaDistrict, 2003). The first public electricity supply in the district commenced in 1947 from a diesel generating plant and in 1967 when the hydro plant at Akosombo became operational, the power station was linked to the national electricity grid of VRA (http://www.ecgonline.info/index.php/organisation/about-us. Retrieved February 1, 2002.).

## Research Design

A descriptive research design of the survey type was adopted for this study.

## Population and Sampling Procedure

The target population for this study was all the domestic consumers of electricity in the Agona District of the Central Region. The sample for the study was limited to five (5) towns in the district. Purposive random sampling method was used to select the towns; these included Swedru, Nyakrom, Kwanyako, Nsaba and Duakwa. Twenty (20) respondents from each of the towns were randomly selected.

## Instrumentation

The data collection instrument included questionnaire, interview and observation schedules. The questionnaire was administered by the researcher to the respondents and the return rate was 95%.For the interview section, the researcher

posed the questions and the responses given were written in a note book. Finding from observations were also recorded.

## Data Analysis

Frequencies and simple percentages were used to analyze the data of the study. A narrative summary including direct quotes was made to further explain the data.

## Results

**Research Question 1:**

This section ascertains the billing systems employed on the consumers by the service providers. The result in table 1 shows that more than half 66 (69%) of the respondents live in the compound houses while 29 (21%) live in bungalows.

**Table 1**: Type of dwellings

| **Type** | **Frequency** | **Percentage %** |
|---|---|---|
| Compound house (rooms) | 66 | 69.0 |
| Flat/Apartment | 29 | 21.0 |
| **Total** | **95** | **100.0** |

**Source:** Field Data, 2003

The data in table 2 records that all 95(100%) of the respondents consume energy from credit meters with no respondent calibrates with prepaid meter.

**Table 2**: Method of billing systems

| **Method** | **Frequency** | **Percentage %** |
|---|---|---|
| Credit meter | 95 | 100.0 |
| Prepaid meter | - | - |
| **Total** | **95** | **100.0** |

**Source:** Field Data, 2003

The statistics in figure 1 illustrate that 16% of consumers monitor their meter readings daily, 32% check their consumptions weekly, 42% monitor consumptions monthly while10% never check their energy consumption pattern.

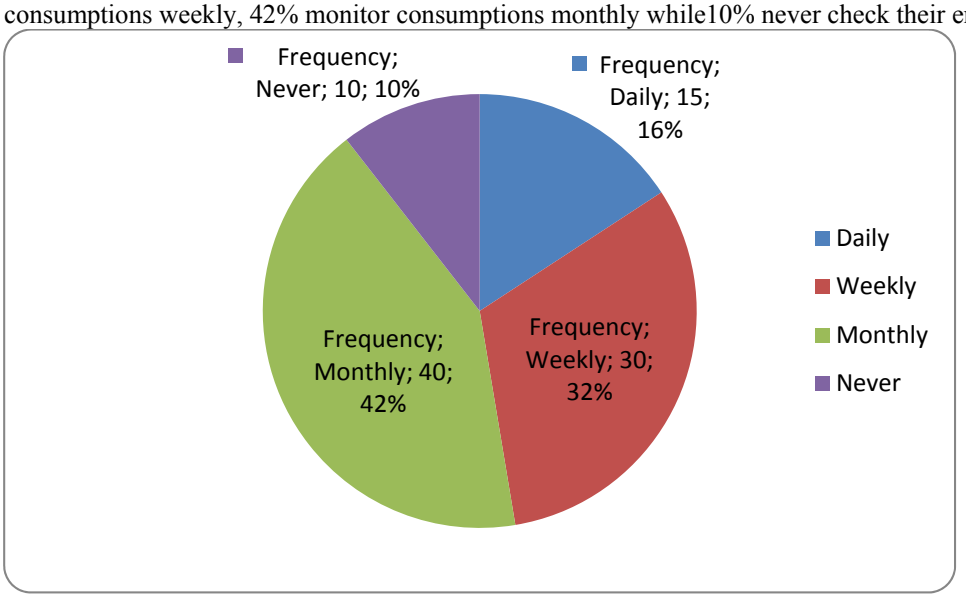


**Figure 1**: Monitoring of energy consumption (**Source:** Field Data, 2003)

The data in table 3 indicates that only 10 (11%) of the respondents fall within the 0-50 kWh consumption brackets while 40 (42%) and 45 (47%) consumers fall within the 51-300 kWh bracket and300+ kWh bracket, respectively.

**Table 3**: Energy consumption bracket of consumers

| **Consumption bracket (kWh)** | **Frequency** | **Percentage %** |
|---|---|---|

| | | |
|---|---|---|
| 0 – 50kWh | 10 | 11.0 |
| 51 – 300kWh | 40 | 42.0 |
| 300+ kWh | 45 | 47.0 |
| **Total** | **95** | **100.0** |

**Source:** Field Data, 2003

The information in figure 2 shows that majority 80 (84%) of the respondents pay their own bills while 15 (16%) of the consumption borne by their employers.

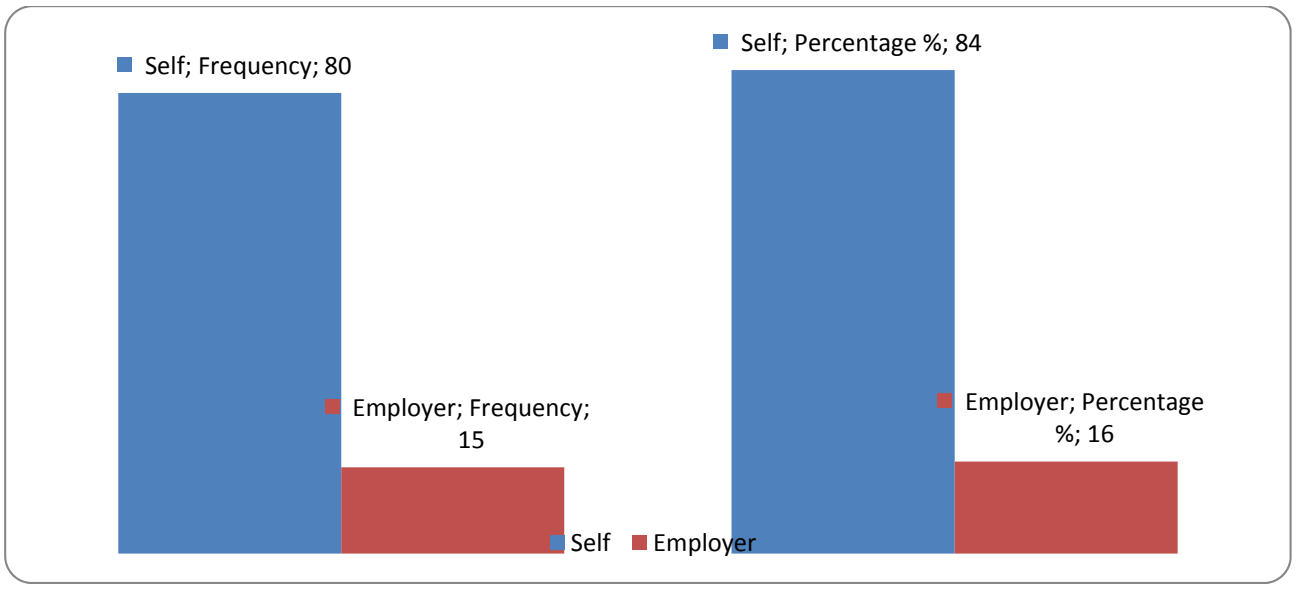


**Figure 2**: Mode of payment of electricity bills
**Source:** Field Data, 2003

The result in table 4 postulates that majority 80 (84%) of the respondents share bills according to the number of points with 10 (11%) and five (5%) share tariff according to number of rooms and size of the households, respectively.

**Table 4**: Method of sharing electricity bills

| **Method** | **Frequency** | **Percentage %** |
|---|---|---|
| No. of point(s) | 80 | 84.0 |
| No. of room(s) | 10 | 11.0 |
| Size of household(s) | 5 | 5.0 |
| **Total** | **95** | **100.0** |

**Source:** Field Data, 2003

The information in table 5 records that almost all 85 (89%) of the respondents submit that they do not know their appliance energy consumptions with only 10 (11%) indicate that they do know their appliance ratings.

**Table5**: Knowledge of consumption rate of household appliances

| **Response** | **Frequency** | **Percentage %** |
|---|---|---|
| Yes | 85 | 89.0 |
| No | 10 | 11.0 |
| **Total** | **95** | **100.0** |

**Source:** Field Data, 2003

**Research Question 2:**
This section finds out some of the energy efficient technologies and practices being use by domestic consumers. The data in table 6 shows that majority 80 (84%) of consumers strongly agree that energy efficient technologies be made accessible to consumers as well as the purchase of energy efficient appliances while few15 (16%) opposed to the assertions. All 95 (100%) of the respondents strongly agree that electrical appliance importers and manufacturers conformed to energy efficient standards and codes. About three-fifth 65 (68%) of the population strongly affirmed that

second hand electrical appliances consume more electrical energy than the modern type as compare to 30 (32%) who disagree to the response. More than three-forth 80 (84%) of respondents strongly agreed that television sets must be put off when nobody is watching with only 15 (16%) opposing the assertion. All 95 (100%) of consumers strongly agree that lights should be put off when not in use. More than half 60 (63%) of the respondents strongly disagree that the doors to refrigerators be opened frequently while 35 (37%) agree to the statement. The data also shows that all 95 (100%) of consumers strongly agree that consumption rates in the households must be monitored.

**Table 6**: Energy efficient technology and practices

| S/N | Statements | Responses | | | |
|---|---|---|---|---|---|
| | | SA/A | | SD/D | |
| | | Freq. | % | Freq. | % |
| 1 | Energy efficient technologies should be made accessible to consumers | 80 | 84 | 15 | 16 |
| 2 | It is good to purchase energy efficient appliances | 80 | 84 | 15 | 16 |
| 3 | Electrical appliance importers and manufacturers should conform to energy efficient standards and codes | 95 | 100 | - | - |
| 4 | Second hand electrical appliance consumes more energy | 65 | 68 | 30 | 32 |
| 5 | Television should be put off when nobody is watching | 80 | 84 | 15 | 16 |
| 6 | Light should be put off when not in use | 95 | 100 | - | - |
| 7 | Refrigerator doors should be opened frequently | 35 | 37 | 60 | 63 |
| 8 | It is important to monitor how electricity is use in the households | 95 | 100 | - | - |

SA= Strongly Agree, A= Agree, SD= Strongly Disagree, D= Disagree
**Source:** Field Data, 2003

**Research Question 3:**
This section finds out the strategies which can be put in place to minimize waste of electricity in the households.
The study in table 7 shows that one-third 20 (21%) of the respondents do iron their clothes daily while 40 (42%) iron their clothes twice in a week with 35 (37%) iron their clothes once in a week.

**Table 7**: Rate of ironing clothes

| Rate | Frequency | Percentage % |
|---|---|---|
| Daily | 20 | 21.0 |
| Twice weekly | 40 | 42.0 |
| Weekly | 35 | 37.0 |
| **Total** | **95** | **100.0** |

**Source:** Field Data, 2003

The result in table 8 records that less than one-third 25 (26%) of the respondents defrost their refrigerators weekly; more than half 30 (32%) and 35 (37%) defrost their refrigerators monthly and quarterly, respectively, however, only five (5%) do not defrost the apartment at all.

**Table 8**: Rate of defrosting refrigerators

| Rate | Frequency | Percentage % |
|---|---|---|
| Weekly | 25 | 26.0 |
| Monthly | 30 | 32.0 |
| Quarterly | 35 | 37.0 |
| Never | 5 | 5.0 |
| **Total** | **95** | **100.0** |

Source: Field Data, 2003

The statistics in figure 3 suggest that less than quarter 15 (16%) and 35 (37%) of the consumers use 25W and 40W incandescent bulbs lavatories respectively, while 40 (42%) and five (5%) use the 40W and 100W incandescent bulbs respectively.

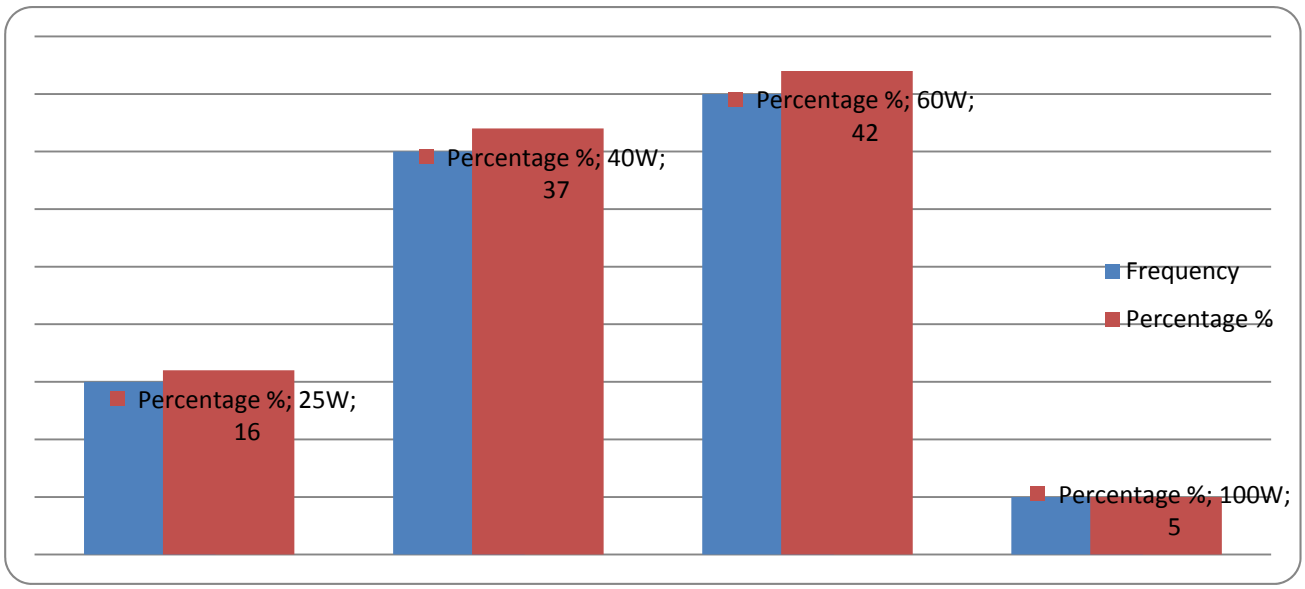


**Figure 3**: Type of incandescent bulbs use in lavatories (Source: Field Data, 2003)

The data in table 9 shows that out of the 700 lamps indicated by consumers, more than two-thirds 550 (79%) use incandescent lamps, 100 (14%) use fluorescent lamps with only 50 (7%) using compact fluorescent lamps (CFLs) for lighting.

**Table 9**: Type and number of lamps in the households

| Lamp | Quantity | Percentage % |
|---|---|---|
| Incandescent | 550 | 79.0 |
| Fluorescent | 100 | 14.0 |
| CFL | 50 | 7.0 |
| **Total** | **95** | **100.0** |

**Source:** Field Data, 2003

## Discussion

The study revealed that most compound houses have been bridged to a central bulk meters which tend to force condominium electricity users into high consumption bracket, hence end up paying huge amount of electricity bills. Under such circumstances, consumers who feel that they pay more than they consume deliberately waste energy. Also, some consumers may waste energy since they know that others will pay for the waste. However, when consumers only pay for what they use they tend to be more conservative and every resident become an active participant in energy management of the condominium or institution (ECG, 2002: February; Schwaller and Gilberti, 1996).The finding confirms the assertion made by ECG (2002: August), Donkor (2001) and Energy Foundation (n.d) that lack of individual electricity meters to monitor the exact amount of electricity used by consumers encourages waste. The research added that though the progressive tariff structure could discourage waste by the rich, however it could also be a burden for consumers sharing common meters. This is because a condominium with a number of families may have a higher meter reading causing them to pay more per unit of electricity consumed. This presupposes that if each household in condominium is provided with separate credit meters, preferably pre-paid meters instead of central credit meters, consumption can be monitored and reduced, thereby conserving energy waste (VRA, 2003; 2002; ECG, 2002: June; Energy Commission, 1999).

The study further revealed that old equipment and appliances waste energy. This confirms report by Donkor (2001) and ECG (2002: July) that modern equipment such as lighting systems, air conditioners, refrigerators, cookers, washing machines and heating systems reduce energy consumption by 20% compared with standard ones. The study added that compact fluorescent lamps consume less energy and last longer as compared to the incandescent lamps of the same wattage. The research proved that currently no energy efficient standards and label codes laws to ensure that only energy efficient technologies are imported and sold in the country (Energy Foundation, n.d). This situation has led to the dumping of inefficient and obsolete technologies on the Ghanaian market and almost all the used appliances such as air conditioners, refrigerators and motors imported into the country are inefficient in every use and have been condemned in their country of origin therefore their high use has contributed to excess consumption of energy in the country.

The study also shows that consumers have little or no knowledge about some common energy conservation tips. This

buttresses research conducted by Donkor (2001) and ECG (2003: January) that practicing simple conservation tips could have a significant effect in the residential and commercial facilities to reduce energy consumption in the area of audio-visual appliances, lighting, refrigeration and heating systems.

## Conclusions

Evidence from the study indicates that majority of households in the condominium are using central credit meters instead of separate credit meters or the pre-paid meters. Feedbacks from respondents suggested that lack of access to energy efficient technologies have contributed to the waste of electricity, hence, the need to use modern efficient appliances and the enforcement of energy efficient codes and standards on end-use products. It was emerged from the study that consumers have little or no knowledge about some basic energy conservation tips.

## References

Agona District (2003). *Profile of Agona District* (June-August ed). Newsletter.1 (1), 2.

Donkor, F. (2001). *Energy Technology*: TEC 235 (Lecture notes), Kumasi, Ghana: UEW, Department of Technology Education.

Electricity Company of Ghana (2003).*Conserving electricity* (January ed). Newsletter. 44 (142), 5.

Electricity Company of Ghana (2002). *Billing meters* (August ed). Newsletter. 39 (137), 3.

Electricity Company of Ghana (2002). *Energy efficient campaign* (June ed). Newsletter.37 (135), 1.

Electricity Company of Ghana (2002). *Strategies for effective revenue and debt management* (February ed). Newsletter. 33 (131), 1.

Energy Commission (1999). *Development of energy efficiency standards and label codes.* A paper presented at the National Forum on Energy Efficiency. January, 27 – 28.

Energy Foundation (1999). *National forum on energy efficiency.*Accra: Ministry of Energy.

Energy Foundation (n.d). *Energy wise: Easy tips to reduce electricity consumption and save money*. Accra: Ministry of Energy.

GSS (2001). *2000 population and housing census report*. Accra: Ghana Statistical Service.

*http:// www.ecgonline.info/index.php/organisation/about-us. Retrieved February 1, 2002.*

Schwaller, A.E. and Gilberti, A.F. (1996). *Energy technology* (2nded).London: International Thomson Publishing.

Volta River Authority (2001). *40 years of powering Ghana's development*. 40 years Anniversaryprogramme. November 2-December 8.Accra: VRA Printing Unit

Volta River Authority (2002). *Voltabuy* (February ed). Accra: VRA Printing Unit

Volta River Authority (2003). *Voltabuy* (March ed). Accra: VRA Printing Unit.

# Comfort and structural (FEA) analysis on light weighted car seat design optimized with EPP material

[1]İbrahim Bahadır Çelik, [1]Bahadır Atmaca, [2]Ergün Nart

[1]Toyota Boshoku Turkey Co., 1st Organized Industrial Zone PK 190, 54580,Arifiye, Sakarya, Turkey, E-mail: bahadir.celik@toyota-boshokutr.com, bahadir.atamaca@toyota-boshokutr.com

[2]Sakarya University, Faculty of Technology, Dept. of Mechatronics Engineering, Esentepe Campus, 54187, Sakarya, Turkey, E-mail: enart@sakarya.edu.tr

**Abstract:** In this paper, comfort and strength performance of conventional and lightweight seat design which is developed by using EPP (expanded poly propylene) material is investigated by using FEA (finite elements analysis) method. The main goal is to contribute to reducing $CO_2$ emissions on passenger cars by providing weight reduction on car seats. To accomplish that, a special designed part made of EPP material, which has lower density and higher strength performance in compliance with PU (Polyurethane), is embedded in original car seats made of PU material, and the resulting composite material reinforces the structure and gives the similar performance compared to PU design, and in the meantime supporting metal frame's weight inside car seats is also reduced. In parallel with design optimization, a comparative analysis of strength and comfort performances between conventional seat design and lightweight seat design is studied correspondingly. Highly nonlinear contact analyses are performed with the dummy named "Manikin" (human model) to analyze comfort performance by looking at the pressure distribution on surface of seats. The results indicate that after design optimization by using new material technology, nearly same comfort and strength performance are achieved and weight of the car seats can be reduced remarkably.

**Key words:** Weight reduction on car seats, EPP material, Comparative comfort and strength analyses, FEA method

## Introduction

Reducing fuel consumption and $CO_2$ emissions on passenger cars is a subject of intensive research in automobile industry for better environment. One way of achieving this goal is to provide weight reduction on car bodies. Because the heaviest interior element among all others is car seat sets, ongoing research on weight reduction usually starts with car seats by using new engineering materials and optimization techniques. However, utilizing new engineering materials in designs is in need of verifications in terms of passengers' comfort and strength performance. In industry, these are usually done by series of tests after the prototypes are produced.

In 2012, the total global sales in the sector of automotive became 86.5 million by increasing 5%. In the same year, the most of total sales happened to be 68.3 million in automobile market (Reports,2012). Due to the intense use of automobiles, total consumption of fuel and $CO_2$ emission increased dramatically. Therefore, automobile industry seeks alternative energy sources due to devastating greenhouse gas effect for the environment, and starts decreasing the use of fossil fuel energy with standardization in fuel consumption because of new rules and regulations. According to the CAFÉ reports, the target fuel $CO_2$ emission complied by passenger car and vans manufactured in 2025 is shown in Figure 1. (NHTSA, 2012).

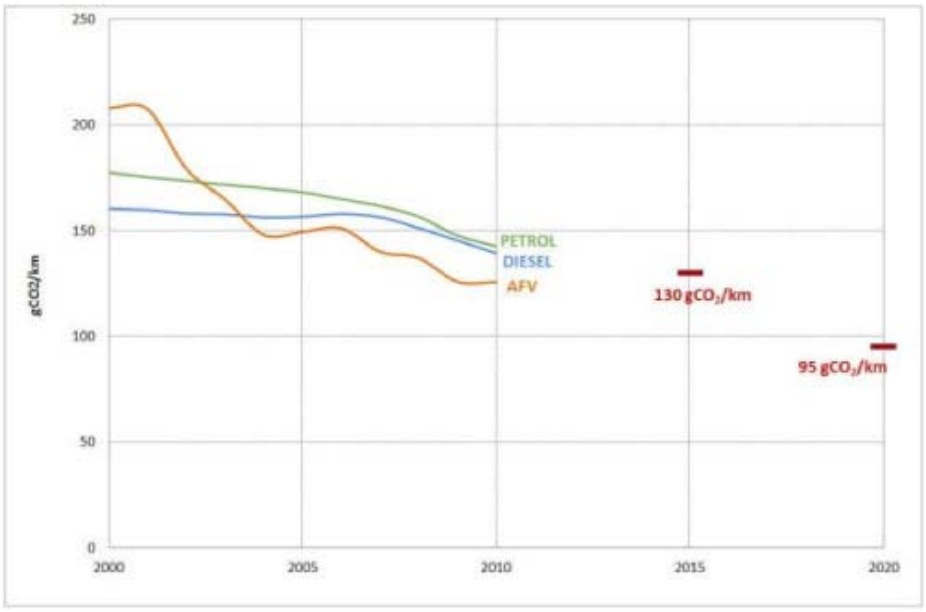


**Figure 1:** The target fuel CO2 emission by EU

In EU, it is aimed to have at least 130gr $CO_2$/km emission in accordance with the new rules for passenger cars (European Parliament and of the Council Regulation, 2009). As a general rule, the modification to have 100kg weight reduction provides approximately 0.005lt/km fuel cut. It is also corresponds to 10gr/km $CO_2$ emission. 1kg weight reducing for cars, which the required emission rate cannot be complied, costs roughly 10€. Therefore, with the help of reducing weight, developing new engines and transmissions, alternative fuels and other advancements, engineers are optimistic to reach the expected CO2 emission goals (Eureka Project-Lightweight Seatbacks, 2013).

The work on reducing weight to decrease the CO2 emission is usually performed by replacing the traditional engineering materials with the high-tech materials that provide both lightness and strength, and analyzing the design to eliminate the unnecessary materials usage. When the literature is curiously searched, it is easily seen that there is little work comparative research between traditional and new seat designs with respect to comfort and strength performances. In one of them, Grujicic et al study finite element models of a passenger-vehicle occupant's seat and of a dummy and used in the investigation of human/seat interactions and seating comfort. On the other hand, Siefert et al, work on a seat model in which static and dynamic properties of the structure are defined. Authors evaluate static comfort which is mainly determined by the seat pressure distribution. However optimization type of research works cannot be found easily in literature. Therefore, in this research, it is aimed to reduce % 22 of weights on car back seats by replacing PU with EPP material. To achieve that goal, finite element method is extensively used in both comparative works and design optimizations.

## Materials and Method

The procedure of weight reduction consists of three stages. In the first stage alternative material is selected and corresponding properties are determined. In our case, EPP is a material that fulfills most of the expectations. Meantime, in conventional seat design, PU foam and DIN 17223-B-type spiral high-carbon steel materials are widely used. On the other hand, selected EPP material has % 25 lower densities and better strength performance compared to PU material; therefore it is also expected to reduce steel wire material usage in the design optimization. In the second stage, various finite element analyses (FEA) are performed. In the modeling part of the FEA, AM50

(Adult Male 50) human model (manikin) is used to simulate the effect of passenger effect as a loading (SAE, Society of Automotive Engineers). Manikin is particularly placed on a car seat according to hip-point, heel-point and torso angle (Figure 2).

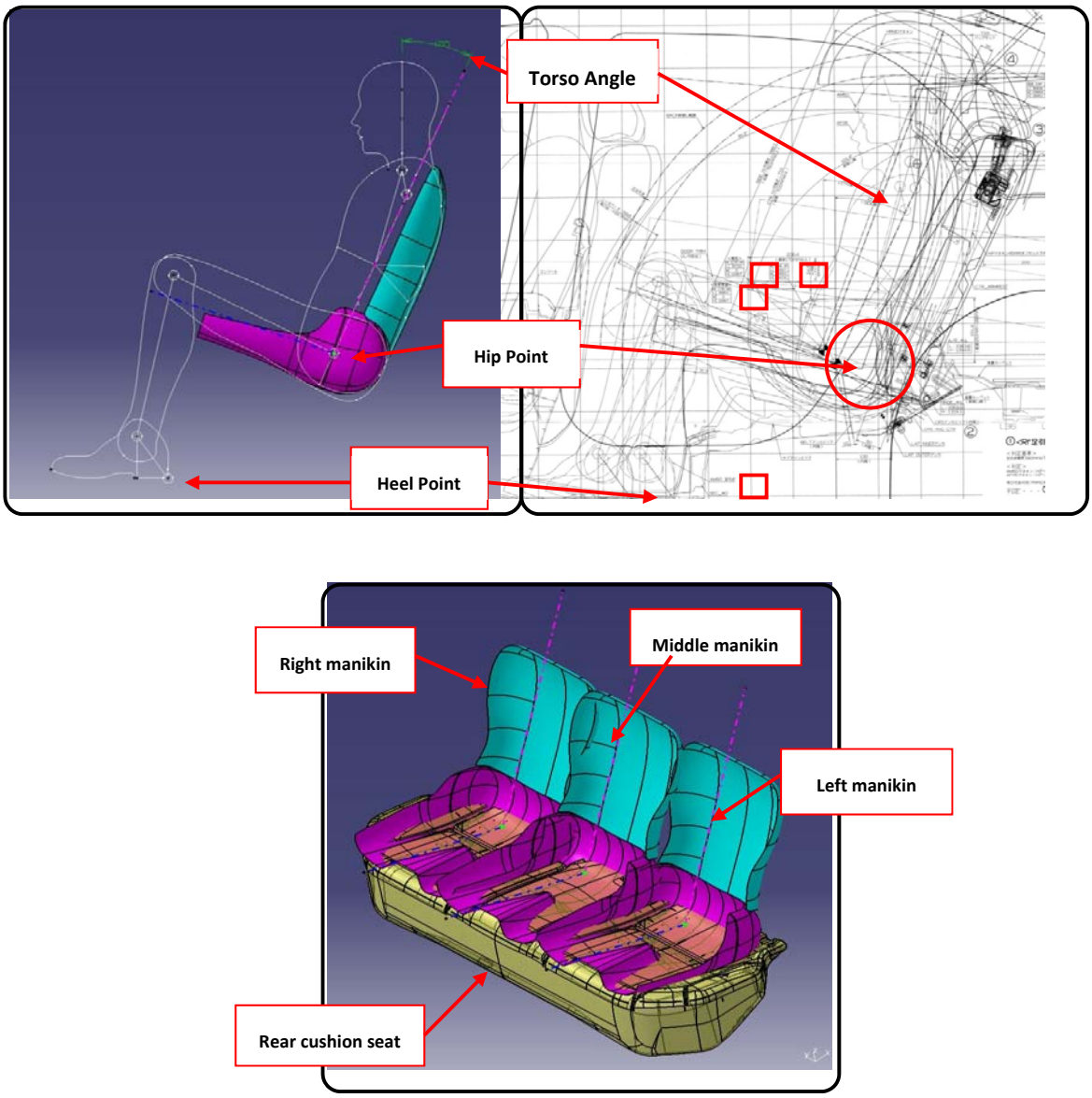


**Figure 2:** CAD model of AM50 dummies and their positions on the car back seat

Also new wire frame is design to be embedded in the EPP part (Figure 3). Therefore, the usage of steel wire can be reduced. Furthermore upper surface of the EPP part is designed by considering the manikin shape which directly affects the passenger comfort. Then, whole design of parts is completed in CATIA V5 CAD environment and transferred to finite element software (Figure 3).

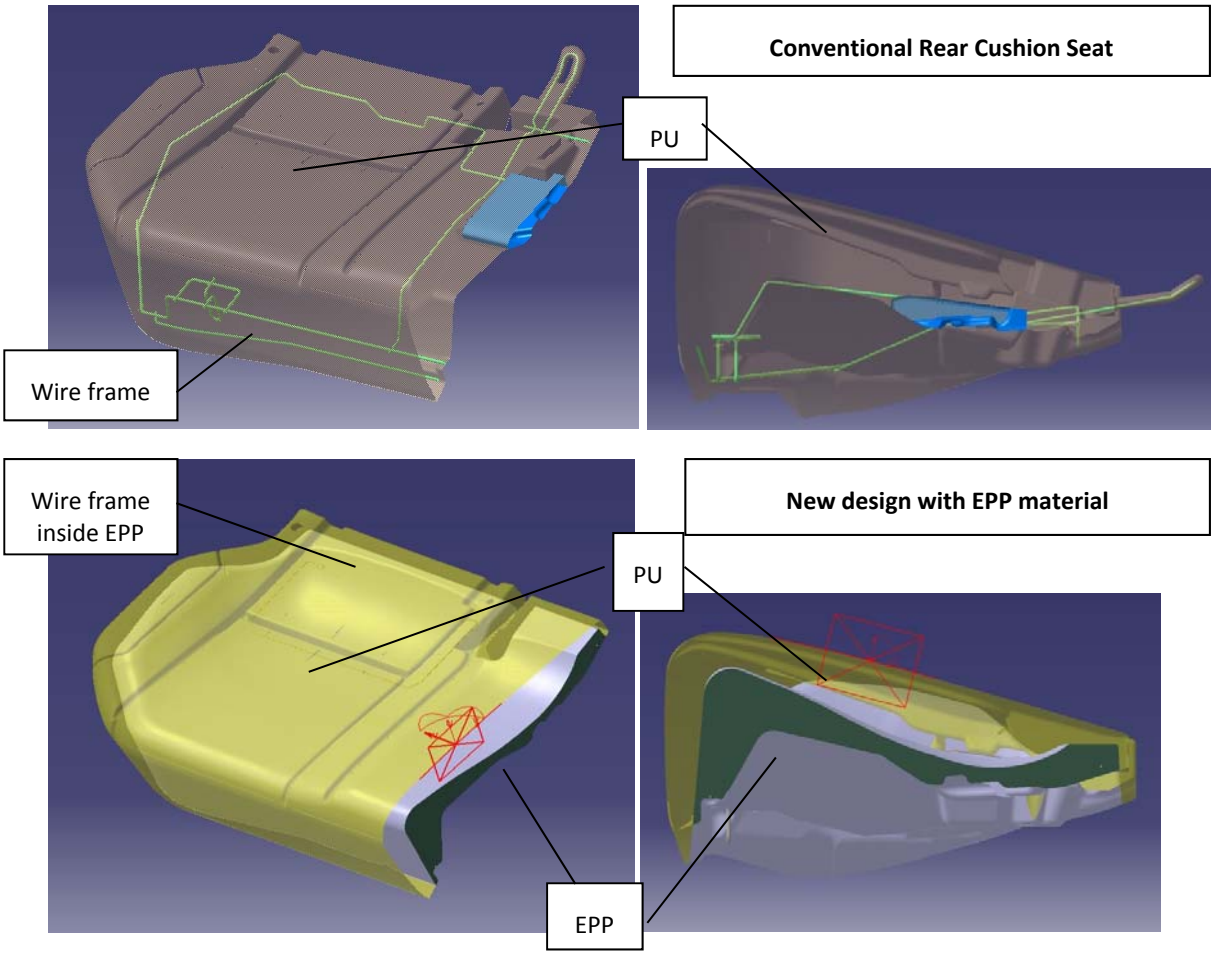


**Figure 3:** Current design and new design sections

After that, the models are meshed with tetrahedron elements due to the complex geometries. Meantime, tensile test results of EPP and PU materials are evaluated by finite element software, and hyper-elastic Marlow model is selected and assigned to EPP and PU parts. For the new composite design, embedded constraint between EPP and embedded wire frame, and non-linear contact between dummy and PU part are defined Both models are fixed from the same 3 fixation points of wire frame to car floor and corresponding boundary conditions are defined. Finally, loads are defined by applying 77 kg force (standard weight value of the AM50 Manikin) at the center of the gravity of dummy and body forces of the parts (Figure 4).

In the third stage, having finished the analyses for comparative strength and comfort analysis between current design and new design of rear seat cushion, comparative strength analysis is studied between composite structure of EPP + wire frame, which is developed in the new design, and the current wire frame, which reinforces whole strength in current design.

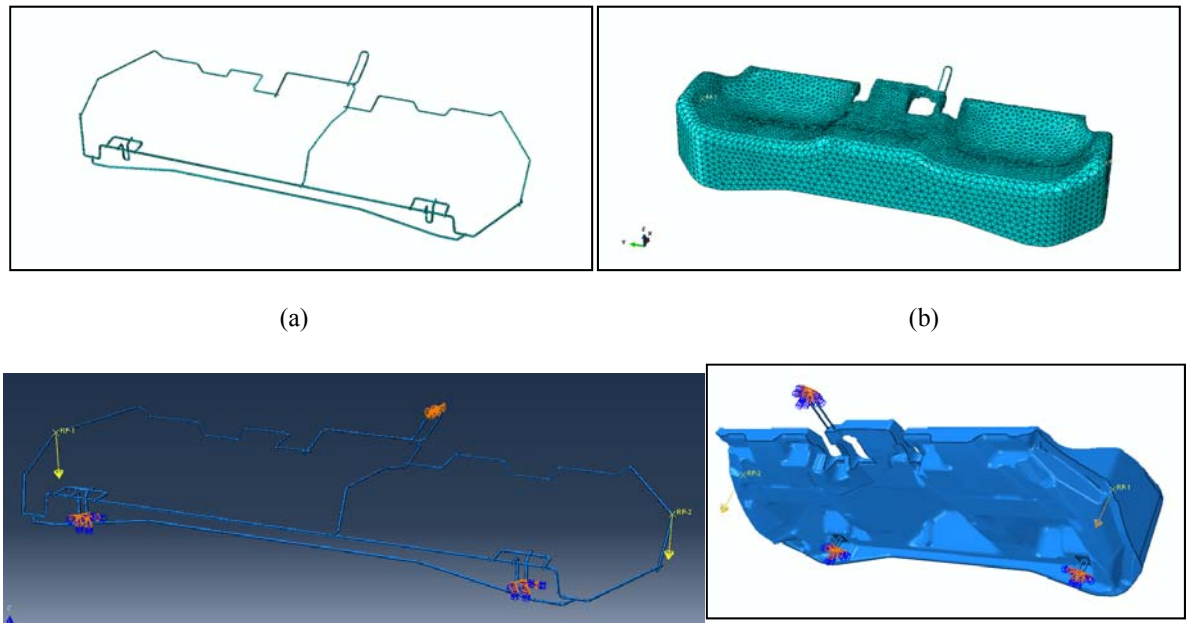

(a) (b)

(c) (d)

**Figure 4:** (a). Mesh system of current design (b) Mesh system of new design (c) Boundary and loading conditions of current design (d) Boundary and loading conditions of new design

To simulate the seating condition of a human, comfort analysis is performed by applying contact condition between manikin and PU surface. But both models are almost symmetrical, for the sake of comparison, half of the rear cushion seat is used to avoid unnecessary calculation. As a result symmetrical plane is applied as boundary condition by limiting degrees of freedom through normal to the plane (Figure 5).

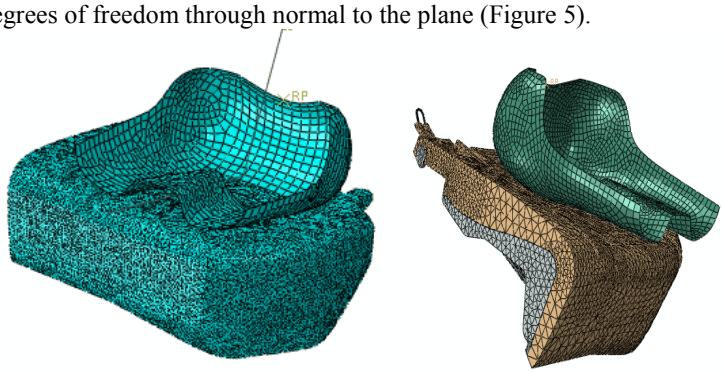

(a) (b)

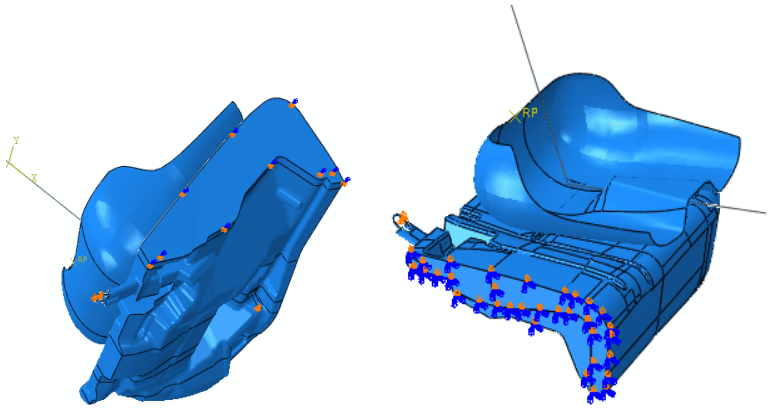

(c) (d)

**Figure 5:** (a). Mesh system of current design (b) Mesh system of new design
(c) Boundary and loading conditions of current design (d) Boundary and loading conditions of new design

## Results

Before the changes take place, the weight of traditional rear seat cushion is 4320g. According to the results of analyses, it is seen that %40 volume of PU material is replaced by EPP material in the new design. Due to %25 density difference between these materials, 350g weight reduction is provided. In addition, usage of steel wire is reduced 65%. Therefore, total weight of the rear seat cushion is reduced about % 22 compared to current designs, and the weight obtained for the new design reaches to 3372g total. (Figure 6).

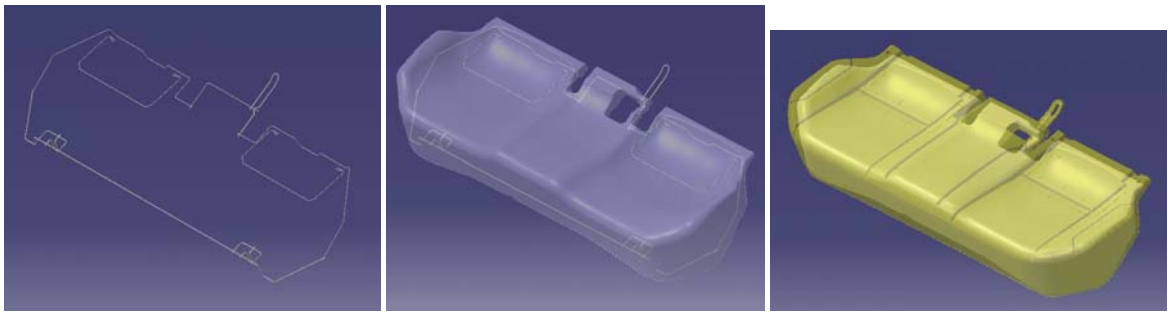

(a) (b) (c)

**Figure 6:** (a). Light weighted wire frame (b) EPP and embedded wire frame (c). New rear cushion design with EPP

Based on results of the strength analysis, both maximum strength generated in the current wire frame and maximum stresses for the EPP + wire frame composite structure in the new design is elastic. Maximum displacements for both configurations are almost same (Figure 7).

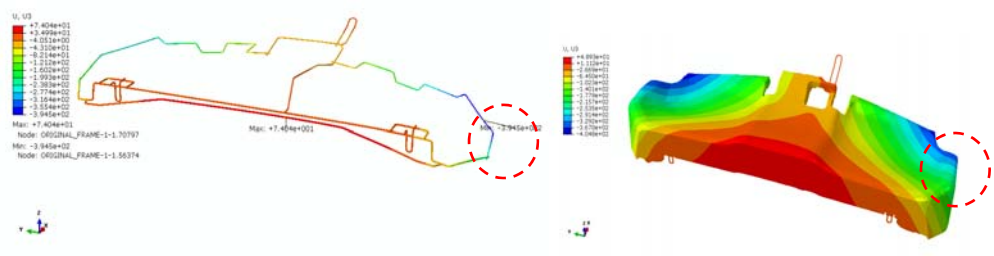

(a) (b)

| | **Current wire frame** | **New wire frame embedded in EPP** |
|---|---|---|
| **Maximum Displacement [mm]** | (c) -394 | (d) -404 |

**Figure 7:** Displacement distributions (a) on current wire frame (b) on EPP and embedded wire frame

For comfort analysis, pressure distributions on the upper surfaces of the both models are investigated. In the current model, average pressure values obtained as 2.66-03 MPa under the area of left leg, 2.60 MPa-03 on the hip area and 1.56-03 Mpa under the area of right leg. The average value of displacement on the legs are in the range of 33.2 to 9.3 mm and through (-) direction, for the hip area, displacement is obtained from 33.2 to 39.1 mm, also through (-) direction. In the new design, average value of pressure distribution is 2.91-03 Mpa on the left leg area, 3.10 MPa-03 on the hip area, 1,30-03 Mpa on the right leg area. The average value of displacement on the area of legs is through (-) direction and in the range of 26.4 to 5.8 mm, for the hip region it is through (-) direction and obtained between 26.4 - 31.6 mm (Figure 8).

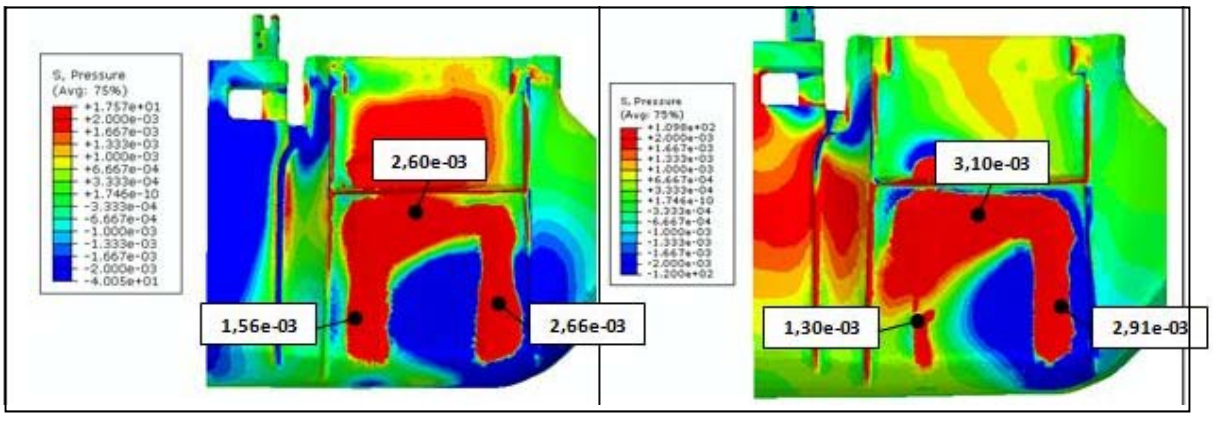


(a) (b)

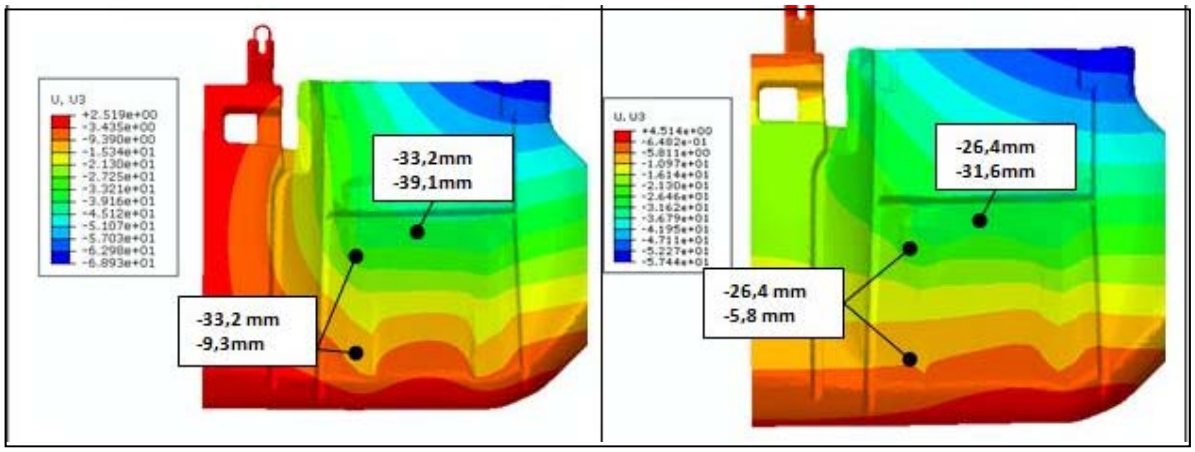


(c) (d)

| | Manikin Contact Area | Current Design | New Design |
|---|---|---|---|
| **Maximum Stress [Mpa]** | **Left leg** | (a) 2,66e-03 | (b) 2,91e-03 |
| | **Hip** | (a) 2,60e-03 | (b) 3,10e-03 |
| | **Right leg** | (a) 1,56e-03 | (b) 1,30e-03 |
| **Maximum Strain [mm]** | **Hip** | (a) -33,2 -39,1 | (b) -26,4 -31,6 |
| | **Legs** | (a) -33,2 -9,3 | (b) -26,4 -5,8 |

**Figure 8:** The average value of displacement on the area of legs

## Discussion

It is obvious that any reduction attempt by reducing wire frame usage in seat design causes reduced strength performance accordingly. In this study, this situation is compensated by developing a new EPP + wire frame composite structure. EPP is a new engineering material and has 25% lower density in comparison with PU. In the optimization part of the solution, the weight of traditional rear cushion seat is reduced about % 22 from the value of 4320g to 3372g. The weight of steel wire frame is decreased by % 65 by supporting the seat structure with EPP material, and the intended target for weight reduction of % 22 is reached.

Results of the analysis shows that strain/stress values of the EPP + wire frame composite structure appears to be around +/- % 2.5 compared to the current wire frame strain/stress performance. Regarding to these results, the new design, EPP + wire frame structure, is as stiff as the current wire frame.

In the process, it is also aimed to achieve same comfort performances between current and optimized seat design in maximum level. As a result of comparative comfort performance analyses, pressure distributions on the upper surfaces of the models shows that comfort performance of the new seat appears to be around -%17 / +%19 compared to current seat design. Even these results are not so close to each other, a small reduction on comfort performance is expected because of usage of such a rigid EPP material. Since the primary objective of the study is to reduce weight by 22%, the convergence of comfort performance is in the acceptable level. Considering all these results of comparative analyses, EPP material usage is optimized and % 22 of weight reduction is provided on rear cushion seat (Table 1).

**Table 1:** A comparison table between targets and results of design optimization

| | **TARGET** | **RESULT** |
|---|---|---|
| **Design optimization** | %22 Weight reduction | %22 Weight reduction |
| **1. Comparative Strength Analysis** | Current wire frame<br>vs.<br>EPP+wire frame | **Stress**<br>Difference: +%2,5<br>**Strain**<br>Difference: -%2,5 |
| **2. Comparative Comfort Analysis** | Current seat<br>vs.<br>New seat | **Pressure Distribution**<br>Difference: between -%17 / +%19<br><br>**Displacement**<br>Difference: between -%19 / -%20 |

## Conclusions

Weight reduction studies in cars are extremely important in terms of the reduction of CO2 emissions. Weight reduction on car seat sets is also an important part of these studies. But the challenge is to have a stabile comfort and strength performance of existing seat while weight is reduced, and do it at the design stage to avoid high prototype costs. Based on this study, the following recommendations and conclusions can be drawn;

1-Weight reduction studies are usually made for the front seat sets. In this study, weight reduction is studied for conventional rear cushion seat, and % 22 of weight reduction is obtained by using a new material which is EPP.

2- Pressure distributions based comfort analyses are usually studied for front seat sets. While reducing the weight highly nonlinear FEA analyses made for design optimization and strength/comfort performance is maintained.

3- Strength/comfort ratio of traditional seat is reached by that of optimized designs in strength/comfort performance analyses.

4- For further studies, finite element models can be detailed by applying car floor restrictions and vibration loads acting on the occupant while driving conditions.

## Acknowledgements

The technical support of Sakarya University is gratefully acknowledged.

## References

Republic of Turkey, Ministry Of Science, Industry And Technology (2012). *Automotive industry report*, Ankara, Turkey.

Grujicic, M. Pandurangan, B. Arakere, G. Bell, W.C. He, T, Xie, X. (2009). "*Seat-cushion and soft-tissue material modeling and a finite element investigation of the seating comfort for passenger-vehicle occupants"*, Materials and Design 30, 4273–4285

Siefert, A. Pankoke, S. Wölfel, H.-P.(2008)."*Virtual optimisation of car passenger seats: Simulation of static and dynamic effects on drivers' seating comfort"*, Int. J. Industrial Ergonomics 38, 410–424

National Highway Traffic Safety Administration (NHTSA) (2012). *Final Rule for CAFE Standards for Model Years 2017 and Beyond* , United States of America.

European Parliament and of the Council Regulation (2009). *Regulation (EC) No 443/2009 of setting emission performance standards for new passenger cars as part of the Community's integrated approach to reduce CO2 emissions from light-duty vehicles Text with EEA relevance*, European Union.

Eureka Project-*Lightweight Seatbacks* (2013),4920 Lıse, Styron Netherlands B.V. www.eurokanetwork.org/project, [access Oct. 2013]

Arpro physical properties (2013), http://www.arpro.com/tech-docs/europe, [access Oct. 2013]

# Effect of meteorological factors on the daily average levels of particulate matter in the Eastern Province of Saudi Arabia: A Cross-Sectional Study

Mahmoud Fathy El-Sharkawy[1], Gehan Raafat Zaki[2]

[1] Department of Environmental Health, College of Applied Medical Sciences, University of Dammam, Kingdom of Saudi Arabia
mfsharkawy2002@yahoo.com
[2] Assistant Professor of occupational hygiene and air pollution, Department of Occupational Health and air pollution, High Institute of Public Health, University of Alexandria, Egypt
gehanra@yahoo.com

**Abstract**: Particulate matter (PM) is a key indicator of air pollution. Particles with an aerodynamic diameter less than 10 μ ($PM_{10}$), and 2.5 μ ($PM_{2.5}$); are inhaled and deposited in the respiratory system. The fate of air pollutants, including PM, is highly dependent on meteorological parameters as they control natural emissions, transport, chemistry and deposition. This study was a cross-sectional one aimed at assessing the effect of meteorological factors on the daily average levels of PM in the Eastern Province of Saudi Arabia during year 2012. Two monitoring stations with the HORRIBA APDA-371 Continuous Particulate Monitors were distributed in Dammam and Khobar governorates for incessantly recording the hourly ambient levels of $PM_{10}$and $PM_{2.5}$. Simultaneously, the meteorological parameters (wind speed, wind direction, air temperature, relative humidity, barometric pressure, and precipitation) were recorded by the WS600-UMB weather parameters' sensor. The daily average levels $PM_{10}$, and $PM_{2.5}$ exceeded the U.S. National Ambient Air Quality Standards (NAAQS) for 19.5%, and 45.8% in the Dammam station measurement days and 27.1% and 36.1% in the Khobar measurement days respectively. They were correlated positively with wind speed and air temperature. Their relationships with wind direction, relative humidity, atmospheric pressure, and precipitation were negative.
**Key words:** air pollution, meteorological factors, particulate matter, Saudi Arabia.

## Introduction

Eastern Province has the largest and the most important governorates in the Kingdom of Saudi Arabia (KSA) from both the number of population and the developed economy points of view. Dammam is the capital of the Eastern Province and represents its major seaport. Its population is about 768,602 inhabitants. It presents at 26.43°N latitude, and 50.11°E longitude, and at 10 m above the sea level. Khobar is the second important large city in this region. Its population is about 165,799 inhabitants. It presents at 26.28°N latitude, and 50.21°E longitude. Its height above sea level is similar to that of Dammam. Due to the presence of several industrial, commercial, educational and recreational areas, there is an increase in the migration of people to these two governorates with a subsequent increase in the human and traffic activities. Consequently, a change in the air quality level is expected (El-Sharkawy & Zaki, 2012).

Air pollution becomes a significant challenge all over the world, especially in the developing countries (C. K. Chan & Yao, 2008). In recent years, particulate matter (PM) is considered the most important air pollutant from the public health point of view (Hu, Jia, Wang, & Pan, 2013; Qiu et al., 2012). Respirable ($PM_{10}$), and fine ($PM_{2.5}$) particulate matters are suspended particles with aerodynamic diameters ≤ 10 μm and 2.5 μm respectively. Their multiple sources include natural, industrial and traffic (Tian, Qiao, & Xu, 2014).

Many scientific studies have linked particulate matters' breathing to a series of significant health problems, including asthma aggravation, increase in respiratory symptoms, reduced lung function, cardiovascular disease, and premature death. The excess of daily mortality and morbidity are associated with exposure to respirable and fine particulates (Pandey et al., 2013; Reyna, Bravo, López, Nieblas, & Nava, 2012; Valavanidis, Vlachogianni, Fiotakis, & Loridas, 2013). In addition to health hazards, respirable and fine particulates play a vital role on climate change through their impact on radiative balance and aerosol–cloud interaction (Trivedi, Ali, & Beig, 2014; Vellingiri et al., 2014). In addition, PM can contribute to the variation of the visual range, which is the most obvious sign of atmospheric pollution to the public(Cheung, Wang, Baumann, & Guo, 2005; Yang et al., 2007).

The air quality situation of an area is largely dependent on the emission strength in combination with meteorology. The fates of air pollutants are highly determined by meteorological parameters such as wind speed, wind direction, air temperature, humidity, barometric pressure and height of the mixing layer. Moreover, they control natural emissions, transport, chemistry and deposition. Changing meteorological conditions on short and long time scales may affect the atmospheric pollutants' concentrations (Tai, Mickley, & Jacob, 2010; F. Zhang, Wang, Lv, Krafft, & Xu, 2011). For particulate matter, the limited number of studies do not agree on the direction of the anticipated change with meteorological factor (Jacob & Winner, 2009).The importance of air pollution attracts many studies in the recent

decades towards understanding the spatio-temporal distribution and the effect of meteorology on the evolution of particulate matters (Ali, Budhavant, Safai, & Rao, 2012; Gugamsetty, 2012). Since particulate matter consists of many components with different physical and chemical properties, the effect of the meteorological parameters on the individual components varies and is more uncertain than for other pollutants (e.g. ozone)(Dayan et al., 2011; Mues et al., 2012; Whiteman, Hoch, Horel, & Charland, 2014).

The present study was aimed to assess the effect of meteorological factors on the daily average levels of respirable and fine particulate matters in the Eastern Province of Saudi Arabia during year 2012.

## Materials and Method

This study was a cross-sectional analytical study, in which two different locations were selected as fixed air pollution monitoring stations in the Eastern Province of Saudi Arabia (Figures 1 and 2). Station No. 1 was located in the west municipality of Dammam at 26.40˚N latitude, 50.04˚E longitude, while station No. 2 was located at El-Khobar housing region at 26.06˚N latitude, and 50.21˚E longitude.

The study period extended from January 1, 2012 to December 31, 2012. The concentration of respirable ($PM_{10}$), and fine particulates ($PM_{2.5}$) were measured and recorded by the Horiba APDA-371 Continuous Particulate Monitor(Ielpo, Paolillo, de Gennaro, & Dambruoso, 2014; Solomon, Hopke, Froines, & Scheffe, 2008)using the beta attenuation principle. This monitor depends on collection of particulates on glass-fiber filter. The carbon-14 ($C_{14}$) represents a continuous source of high-energy electrons (beta rays), which attenuates as they collide with the clean filter. These beta rays are detected and counted by a sensitive scintillation detector to determine a zero reading. The Monitor automatically advances this spot of tape to the sample nozzle, where a vacuum pump then pulls a measured and controlled amount of dust-laden air through the filter tape, loading it with ambient dust ($PM_{2.5}$ or $PM_{10}$, depending upon the sampling head). At the end of an hour, this dirty spot is placed back between the beta source and the detector thereby causing an attenuation of the beta ray signal, which is used to determine the mass of the particulate matter on the filter tape and the mass concentration of particulate matter in the ambient air. The decrease of the signal scintillation counter is inversely proportional to the mass loading on the filter. For quality control, the monitor was automatically calibrated, and the zero testing of blank filter paper is performed at the beginning and end of the measurement period(CPCB, 2011).

The meteorological parameters were simultaneously recorded by the WS600-UMB weather parameters' sensors that compact weather station measures air temperature, relative humidity, precipitation quantity, air pressure, wind direction, and wind speed. Temperature was measured using a highly accurate NTC-resistor, while humidity was measured using a capacitive humidity sensor. Both sensors were located in a ventilated radiation shield to reduce the effects of solar radiation. Absolute air pressure was measured using a built-in MEMS sensor. The wind sensor used four ultrasound sensors, which take cyclical measurements in all directions. The resulting wind speed and direction were calculated from the measured run-time sound differential.

The above instruments were adjusted to save the measured concentrations and meteorological data as one-hour averages in the character-separated values (csv) format that easily transformed to excel sheet. The daily averages' concentrations and meteorological parameters, including prevailing wind directions were subsequently calculated. Local daily wind speed was then classified according to the Beaufort's wind force scale(Y. Zhang, Duc, Corcho, & Calbimonte, 2012) into light, and gentle-moderate.

The data were entered and statistically analyzed using the Statistical Package for the Social Sciences (IBM SPSS Statistics-21). The $PM_{10}$, $PM_{2.5}$, and the meteorological parameters (numeric variables) were classified according to the sampling station, season, local wind speed, and its prevailing direction (categorical variables) and expressed as [median (Inter quartile range[1])]. The Kolmogorov-Smirnov Z test was used to check normality of the numeric data. Mann-Whitney, Kruskal-Wallis H tests

[1] the difference between the first and third quartiles of a set of data

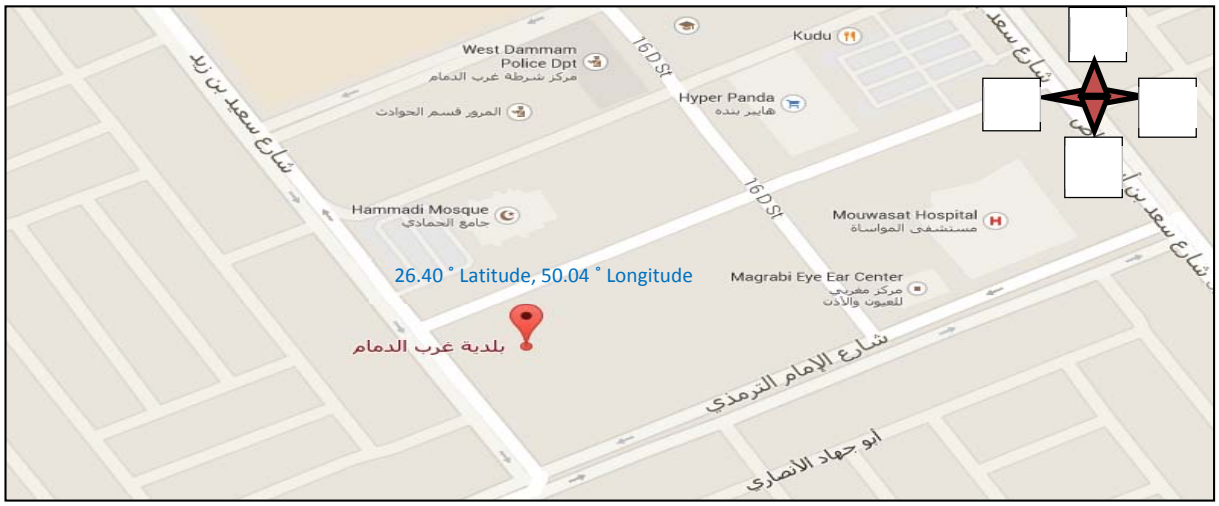


**Figure 1**: Location of Dammam Particulate Matter Monitoring Station


**Figure 2**: Location of El-Khobar Particulate Matter Monitoring Station

were used to check the significance of discrepancy in case of variables with two, and more classes respectively. The power, significance, and direction of relationships between two variables were tested using Spearman's rho correlation coefficient (Ott; & Longnecker., 2010; Peng; & Dominici., 2008).

## Results

There were totally 618 measurement days, 308 for station-1 in Dammam and 310 for station-2 in El-Khobar. Levels of $PM_{10}$ and $PM_{2.5}$ in Dammam were higher than the Saudi National Ambient Air Quality Standards for 60 (19.48%), and 141 (45.78%) measurement days, while those in El-Khobar exceeded this standard for 84 (27.1%), and 112 (36.13%) measurement days (Table 1). The $PM_{10}$ and $PM_{2.5}$ showed non-parametric behavior (highly significant Kolmogorov-Smirov test of normality). The [Median (Interquartile range)] for $PM_{10}$ and $PM_{2.5}$ in Dammam station [81.72 (92.20) µg/m$^3$] and [32.96 (31.52) µg/m$^3$] were higher than those in El-Khobar [80.81 (127.34) µg/m$^3$] and [27.17(32.62) µg/m$^3$] respectively (Table 2). These levels had a positive weak highly significant Spearman's rho correlation coefficients with local wind speed [0.272, 0.172] and air temperature [0.282, 0.300] at 0.001 level. They exhibited negative greatly significant coefficients with prevailing wind direction [-0.383, -0.308 respectively], relative humidity [-0.538, -0.180], and barometric pressure [-0.517, -0.468]. The precipitation exhibited very weak negative correlation coefficient with $PM_{10}$ [-0.109] and $PM_{2.5}$ [0.079] [Figure 3].

The overall data indicates that the highest daily $PM_{10}$ concentration [116.4 (117.7) µg/m$^3$] was found during

the fall season with the lowest relative humidity [18.5 (11.6)%], followed by summer [91.9 (136.9) µg/m$^3$], spring [76.4 (80.7) µg/m$^3$]. While the lowest mean level was recorded during winter.

**Table 1**: Days of daily average concentrations of respirable and fine particulates higher than the Saudi National Ambient Air Quality Standards

| | Station-1 (the west municipality of Dammam at 26.40 ˚ latitude, 50.04 ˚ longitude) | Station-2 (El-Khobar housing region at 26.06˚ latitude, and 50.21˚ Longitude) |
|---|---|---|
| | No (%) | |
| Number of days of daily average $PM_{10}$>150µg/m$^3$ | 60 (19.48%) | 84 (27.10%) |
| Number of days of daily average $PM_{10}$<150µg/m$^3$ | 248 (80.52%) | 226 (72.90%) |
| **Total** | **308** | **310** |
| Number of days of daily average $PM_{2.5}$>35µg/m$^3$ | 141(45.78%) | 112 (36.13%) |
| Number of days of daily average $PM_{2.5}$<35µg/m$^3$ | 167 (54.22%) | 198 (63.87%) |
| **Total** | **308** | **310** |

[45.0 (74.7) µg/m3] of maximum relative humidity (55.5%). There was highly significant PM10 variation at different seasons. The maximum PM2.5 was recorded during summer season [40.1 (62.5) µg/m3], followed by winter [29.5 (25.8) µg/m3], fall [29.5 (24.5) µg/m3], and spring [27.9 (20.4) µg/m3]. The fine particulate concentrations had non-significant variation with seasons. Generally, the PM10, and PM2.5 were higher at gentle-moderate winds than at light ones (Table-2).

In Dammam station, the "southeast light wind" was the most frequent (34.2% of the total measurement days), followed by the "southeast gentle-moderate" (17.9%), "south light" (16.0%), and "southwest light" (11.4 %). The maximum $PM_{10}$ level was at the "southern gentle-moderate wind" [**215.1 (154.2)** µg/m$^3$**]** during summer, while the minimum one [**21.1 (13.6)** µg/m$^3$] ) was at the "western gentle moderate wind" during winter. The highest $PM_{2.5}$ [84.0 (23.0) µg/m$^3$] was at the "southeast light wind" during fall, and the lowest [16.9 (13.8)µg/m$^3$] was at the "south light wind" during spring (Table 3).

In El-Khobar station, the "southeast light" winds were the most frequent (47.5%), followed by "south light" (18%), and "southeast gentle-moderate" (11.8%). Winter season recorded the highest $PM_{10}$ and $PM_{2.5}$ [218.6 (124.4), 91.5 (167.5) µg/m$^3$] at "southeast gentle-moderate winds", and "southwest gentle-moderate winds" respectively. The $PM_{10}$, and $PM_{2.5}$ were of the lowest values at the "southeast light winds" during the summer season (Table 4).

## Discussion

Dammam is the capital of the Eastern Province of Saudi Arabia, and its area is bigger than El-Khobar. In addition; the industrial, commercial, educational, recreational and traffic activities in Dammam are higher than those in El-Khobar(Al-Homaidan, 2008).. For this reason, the daily $PM_{10}$ and $PM_{2.5}$ levels in Dammam were the highest in Dammam. This finding is in accordance to the results of another study, which was previously conducted in the same two cities (El-Sharkawy & Zaki, 2012).

In the present study, the $PM_{10}$ and $PM_{2.5}$ levels had a positive weak highly significant Spearman's rho correlation coefficient with air temperature. This may be due to the increased road dust re-suspension, and contribution of secondary particles on the relatively warm sunny days. This result is consistent with the results of similar studies in different areas of the world such as Athens (Vardoulakis & Kassomenos, 2008), China (Trivedi, et al., 2014), and United States (Tai, et al., 2010). On the other hand, this positive correlation is contradictory to other studies in Brimingham ammonium nitrates on particulates, and the reduced particulate matter dispersion under cold stable meteorological conditions may be the main cause of the negative correlation.

The positive statistically significant correlation of $PM_{10}$ and $PM_{2.5}$ with local wind speed may be related to dust excitation at the stronger winds that may carry PM from other areas (southeast is the daily prevailing wind direction in the two sampling stations in 53.5% of the measurement days). This result is in accordance with the result of the Buenos Aires study during summer (Bogo et al., 2003; Trivedi, et al., 2014). On contrary, other studies in Athens and Brimingham (Vardoulakis & Kassomenos, 2008),

**Table 2**: Spatial and seasonal variation of the daily average $PM_{10}$, and $PM_{2.5}$ concentrations and meteorological factors of Dammam and El-Khobar monitoring stations, 2012

| | | 24-Hour Average $PM_{10}$ Concentration ($\mu g/m^3$) | | | | | | 24-Hour Average $PM_{2.5}$ Concentration ($\mu g/m^3$) | | | | | | Meteorological Factors as [Median (IQR)] | | | | | |
|---|---|---|---|---|---|---|---|---|---|---|---|---|---|---|---|---|---|---|---|
| | | N[1] | Median[2] | $Q_1$[3] | $Q_3$[4] | IQR[5] | P-Value | N | Median | $Q_1$ | $Q_3$ | IQR | P-Value | Wind Speed (m/sec) | Wind Direction (°) | Prevailing Wind Direction | Air Temperature (°C") | Relative Humidity (%) | Pressure (hpa) | Precipitation (mm) |
| Spatial variation | Station-1[6] | 308 | 81.7 | 41.7 | 133.9 | 92.2 | >0.05[7] | 308 | 33.0 | 23.0 | 54.5 | 31.5 | <0.05 | 2.7 (1.1) | 146.9 (27.2) | SE | 33.0 (13.3) | 27.9 (25.5) | 998.7 (9.4) | 0.0 (0.0) |
| | Station-2[8] | 310 | 80.8 | 32.5 | 159.8 | 127.3 | | 311 | 27.2 | 14.0 | 46.6 | 32.6 | | 2.3 (1.3) | 147.7 (27.9) | SE | 32.2 (8.9) | 24.7 (24.1) | 999.5 | 0.0 (0.0) |
| Seasonal Variation | Fall | 172 | 116.4 | 49.1 | 166.8 | 117.7 | <0.05[9] | 172 | 29.5 | 19.8 | 44.3 | 24.5 | >0.05 | 2.5 (1.0) | 158.1 (65.7) | SE | 27.6 (10.1) | 18.5 (11.6) | 997.6 (4.1) | 0.0[10] |
| | Winter | 160 | 45.0 | 26.6 | 101.3 | 74.7 | | 160 | 29.5 | 19.5 | 45.3 | 25.8 | | 2.5 (1.5) | 202.2 (68.2) | S | 19.0 (7.4) | 55.3 (29.6) | 1013.9 (7.3) | 0.0 (0.0) |
| | Spring | 163 | 76.4 | 46.6 | 127.3 | 80.7 | | 163 | 27.9 | 19.8 | 40.2 | 20.4 | | 2.5 (1.7) | 144.9 (13.2) | SE | 32.0 (6.9) | 29.5 (19.9) | 1003.1 (5.1) | 0.0 (0.0) |
| | Summer | 123 | 91.9 | 19.3 | 156.2 | 136.9 | | 123 | 40.1 | 7.6 | 70.1 | 62.5 | | 2.7 (1.3) | 143.1 (7.1) | SE | 36.5 (3.1) | 27.7 (19.9) | 995.9 (4.3) | 0.0[10] |

[1] Number of measurement day

[2] The middle number between the smallest and the highest numbers

[3] The middle number between the smallest number and the median of the data set (the first quartile).

[4] The middle number between the median and the highest number of the data set (the third quartile).

[5] Interquartile Range.

[6] Atthe west municipality of Dammam at 26.40 ˚ latitude, 50.04 ˚ longitude

[7] P-value using Mann-Whitney test

[8] El-Khobar housing region at 26.06˚ latitude, and 50.21˚ Longitude

[9] P-value using Kruskal-Wallis H test

[10] Precipitation is constant during fall, and summer seasons (zero mm)

**Table 3**: Wind speed and prevailing wind direction as related to the particulate matter concentrations in Dammam air monitoring station at 26.40 ˚ latitude, 50.04 ˚ longitude, Saudi Arabia, 2012

| Season | Prevailing Local Wind Direction | No[1] | Light wind (<3.1 m/sec) | | | | Gentle-Moderate wind (3.1-7.8 m/sec) | | | | |
|---|---|---|---|---|---|---|---|---|---|---|---|
| | | | PM10 Concentration (µg/m$^3$) | P-Value[2] | PM2.5 Concentration (µg/m$^3$) | P-Value | No | PM10 Concentration (µg/m$^3$) | P-Value | PM2.5 Concentration (µg/m$^3$) | P-Value |
| Fall | SE[3] | 14 | 170.0 (64.8) | <0.05 | 84.0 (23.0) | <0.05 | 1 | -- | <0.05 | -- | <0.05 |
| | S[4] | 24 | 115.8 (57.7) | | 34.7 (21.4) | | 5 | 179.5 (72.7) | | 73.1 (45.2) | |
| | SW[5] | 15 | 46.1 (76.6) | | 32.6 (10.0) | | 6 | 126.6 (82.3) | | 26.9 (56.4) | |
| | W[6] | 5 | 91.2 (84.6) | | 36.4 (13.0) | | 4 | 119.8 (194.5) | | 30.9 (96.7) | |
| | NW[7] | 3 | -- | | -- | | 4 | 149.7 (53.3) | | 28.7 (55.8) | |
| Winter | E[8] | 0 | -- | >0.05 | -- | >0.05 | 2 | -- | >0.05 | -- | >0.05 |
| | SE | 6 | 25.5 (28.3) | | 19.5 (9.5) | | 2 | -- | | -- | |
| | S | 19 | 35.2 (20.7) | | 27.7 (13.1) | | 0 | -- | | -- | |
| | SW | 12 | 31.6 (22.1) | | 20.7 (19.0) | | 6 | 25.7 (23.1) | | 17.1 (4.0) | |
| | W | 12 | 30.0 (23.4) | | 24.9 (22.6) | | 13 | 21.1 (13.6) | | 18.2 (6.9) | |
| | NW | 1 | -- | | -- | | 0 | -- | | -- | |
| Spring | SE | 38 | 69.7 (52.8) | <0.05 | 26.5 (14.8) | <0.05 | 36 | 131.2 (102.6) | <0.05 | 42.1 (39.2) | <0.05 |
| | S | 6 | 26.8 (22.4) | | 16.9 (13.8) | | 1 | -- | | -- | |
| | SW | 8 | 51.2 (16.1) | | 35.9 (5.6) | | 0 | -- | | -- | |
| | W | 2 | -- | | -- | | 0 | -- | | -- | |
| Summer | SE | 47 | 95.2 (35.6) | - | 54.7 (32.8) | - - | 16 | 215.1 (154.2) | | 80.8 (63.6 | -- |

Jinan, China (Yang, et al., 2007), and Milan, Italy (Marcazzan M. Grazia, Vaccaro, Valli, & Vecchi, 2001)revealed a negative correlation between $PM_{10}$ concentration and the wind speed. The better dispersion and the consequent PM dilution at higher wind speed are the main cause of the negative relation.

The particulates' concentrations disclosed negative correlation with relative humidity because of the settlement and removal of particulate matter, especially coarse size out of the humid atmosphere. This negative relation is compliant with those of the Delhi (Trivedi, et al., 2014), and European studies (Vardoulakis &

[1] Number of measurement days

[2] P-value using Kruskal-Wallis H test

[3] South-East

[4] South

[5] South-West

[6] West

[7] North-West

[8] East

Kassomenos, 2008), while it is contradictory to studies that have been conducted in Jinan, China(Yang, et al., 2007)and Hangzhou, China(Jian, Zhao, Zhu, Zhang, & Bertolatti, 2012). This discrepancy is due to the formation of secondary particles at high relative humidity.

Due to the limited amount of rainfall in Saudi Arabia all over the year, levels of $PM_{10}$ and $PM_{2.5}$ showed a negative weak correlation coefficient with the precipitation which usually acts as a scavenging sink for particulates. This result is consistent with that of the European (Vardoulakis & Kassomenos, 2008), Beijing (Tian, et al., 2014), and United States (Tai, et al., 2010) studies.

**Table 4**: Local Wind speed and prevailing wind direction as related to the particulate matter concentrations in El-Khobar air monitoring station at 26.06˚ latitude, and 50.21˚ Longitude, Saudi Arabia, 2012

| Season | Prevailing Local Wind Direction | Light wind (<3.1 m/sec) | | | | | Gentle-Moderate wind (3.1-7.8 m/sec) | | | | |
|---|---|---|---|---|---|---|---|---|---|---|---|
| | | No[1] | PM10 Concentration (µg/m$^3$) | P-Value[2] | PM2.5 Concentration (µg/m$^3$) | P-Value | N | PM10 Concentration (µg/m$^3$) | P-Value | PM2.5 Concentration (µg/m$^3$) | P-Value |
| Fall | N[3] | 2 | -- | | -- | | 0 | -- | | -- | |
| | E[4] | 1 | -- | | -- | | 0 | -- | | -- | |
| | SE[5] | 48 | 38.2 (109.3) | | 18.4 (19.4) | | 6 | 172.1 (205.8) | | 42.7 (53.4) | |
| | S[6] | 18 | 168.3 (106.8) | <0.05 | 26.8 (44.3) | >0.05 | 2 | -- | | -- | <0.05 |
| | SW[7] | 5 | 131.6 (95.9) | | 24.2 (17.0) | | 0 | -- | | -- | |
| | W[8] | 4 | 139.3 (38.8) | | 25.1 (16.3) | | 0 | -- | | -- | |
| | NW[9] | 5 | 148.2 (100.2) | | 31.8 (11.1) | | 0 | -- | | -- | |
| Winter | N | 2 | -- | | -- | | 0 | -- | | -- | |
| | NE | 2 | -- | | -- | | 0 | -- | | -- | |
| | E | 20 | 91.7 (66.2) | | 46.9 (25.3) | | 0 | -- | | -- | |
| | SE | 62 | 64.9 (110.1) | <0.05 | 22.0 (28.5) | <0.05 | 15 | 218.6 (124.4) | <0.05 | 75.8 (47.2) | <0.05 |
| | S | 34 | 113.6 (155.5) | | 30.5 (24.6) | | 9 | 135.3 (127.1) | | 36.6 (27.6) | |
| | SW | 14 | 43.9 (107.7) | | 21.1 (11.5) | | 4 | 205.9 (500.4) | | 91.5 (167.5) | |
| | W | 8 | 78.3 (95.0) | | 30.8 (13.8) | | 1 | -- | | -- | |
| | NW | 5 | 148.2 (100.2) | | 31.8 (11.1) | | 2 | -- | | -- | |
| Spring | SE | 43 | 78.6 (81.7) | [illegible] | 25.2 (21.5) | | 7 | 137.9 (90.0) | [illegible] | 39.7 (13.7) | [illegible] |

[1] Number of measurement days

[2] P-value using Kruskal-Wallis H test

[3] North

[4] East

[5] South-East

[6] South

[7] South-West

[8] West

[9] North-West

| | | | | | | | |
|---|---|---|---|---|---|---|---|
| | S | 18 | 42.3 (46.9) | 17.9 (12.7) | 3 | -- | 24.4 (6.7) |
| | SW | 1 | -- | -- | 0 | -- | -- |
| Summer | SE | 37 | 12.0 (35.0) | 3.3 (15.2) | 19 | 143.3 (251.2) | 41.5 (78.8) |
| | S | 2 | -- | -- | 1 | -- | -- |

On the other hand, the concentrations of the two PM types showed a negative highly significant coefficient with barometric pressure. This is similar to the Beijing study (Tian, et al., 2014), and non-compliant with the European study (Vardoulakis & Kassomenos, 2008).

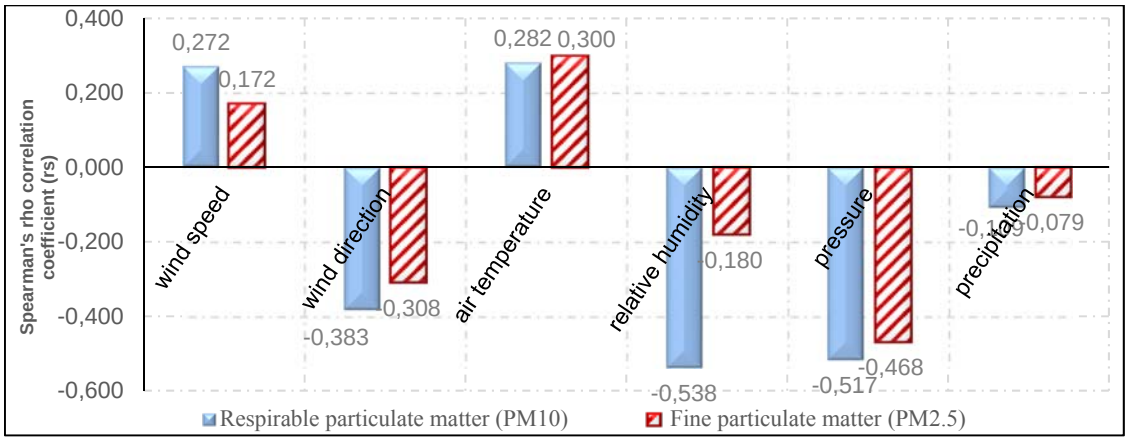


**Figure 3**: Spearman's rho correlation coefficient of $PM_{10}$, $PM_{2.5}$ and the major meteorological factors

The overall data of the present study indicates that the fall season was of the highest PM10 concentrations due to the lowest relative humidity. The winter season had the lowest PM10levels because of the maximum relative humidity and wet deposition, in addition to the highest barometric pressure. The Italian study (Marcazzan, Vaccaro, Valli, & Vecchi, 2001) stated that the winter values of particulate matter were higher those of summer due to the frequent persistent thermal inversions during winter, and the greater wind speed that broadens the mixing layer and improves air quality during summer.

The highest PM2.5 level that has been recorded during the summer season in the present study may be attributed to the highest air temperature and the lowest atmospheric pressure, while the lowest PM2.5value was recorded during the spring season. Based on several studies, the seasonal variation differs from one location to another. For example; A Buenos Aires study indicated higher PM2.5 during the summer season (congruent with this study) due to the slightly higher wind speed that may generate more PM2.5(Bogo, et al., 2003). While the Korean and Hong Kong studies revealed that the highest PM2.5was during winter because of the thermal inversion (L. Y. Chan & Kwok, 2001; Vellingiri, et al., 2014).

In Dammam station, the maximum $PM_{10}$ concentration [215.1 (154.2) µg/m$^3$] was recorded at the "southeast gentle-moderate wind" during summer. This may be due to the high wind speed, in addition to the highest air temperature, and the lowest pressure. The lowest level of $PM_{10}$ [21.1 (13.6) µg/m$^3$**]** was found at the

"western gentle moderate wind" during winter because of the high relative humidity and the very low human activities at the western area. As for $PM_{2.5}$, the highest concentration which was found at the "southeast light wind" during fall is due to the presence of dense population and high traffic activity in this direction.

In El-Khobar, the winter season recorded the highest PM10, and PM2.5 levels at gentle-moderate southeastern and southwestern directions. This may be owing to thermal inversion during this cold season. The lowest levels of both PM types that were found during the summer season at the "light southeast winds" can be attributed to the higher air temperature and lower atmospheric as stated in the Italian and European studies(Marcazzan, et al., 2001; Vardoulakis & Kassomenos, 2008).

## Conclusions

Concentrations of both $PM_{10}$, and $PM_{2.5}$ have the positive weak highly significant Spearman's rho correlation coefficients with local wind speed and air temperature, while they have negative significant coefficients with prevailing wind direction, relative humidity, and barometric pressure. In addition, precipitation has a very weak negative coefficient with the two types.

## Acknowledgements

The authors would like to thank the Municipality of Eastern Province in Dammam, KSA for their administrative support and information given during this study, which was a part of a long-period term project for continuous assessment of air quality level in the Eastern Province of KSA.

## References

Al-Homaidan, A. A. (2008). Accumulation of nickel by marine macroalgae from the Saudi coast of the Arabian Gulf. *Journal of Food Agricultura and Environment, 6*(1), 148.

Ali, K., Budhavant, K. B., Safai, P. D., & Rao, P. S. P. (2012). Seasonal factors influencing in chemical composition of total suspended particles at Pune, India. *The Science Of The Total Environment, 414*, 257-267. doi: 10.1016/j.scitotenv.2011.09.011

Bogo, H., Otero, M., Castro, P., Ozafrán, M. J., Kreiner, A., Calvo, E. J., & Negri, R. M. n. (2003). Study of atmospheric particulate matter in Buenos Aires city. *Atmospheric Environment, 37*(8), 1135-1147. doi: 10.1016/s1352-2310(02)00977-9

Chan, C. K., & Yao, X. (2008). Air pollution in mega cities in China. [Article]. *Atmospheric Environment, 42*(1), 1-42. doi: 10.1016/j.atmosenv.2007.09.003

Chan, L. Y., & Kwok, W. S. (2001). Roadside suspended particulates at heavily trafficked urban sited of Hong Kong — Seasonal variation and dependence on meteorological conditions. [Article]. *Atmospheric Environment, 35*(18), 3177.

Cheung, H.-C., Wang, T., Baumann, K., & Guo, H. (2005). Influence of regional pollution outflow on the concentrations of fine particulate matter and visibility in the coastal area of southern China. [Article]. *Atmospheric Environment, 39*(34), 6463-6474. doi: 10.1016/j.atmosenv.2005.07.033

CPCB. (2011). Guidelines for the Measurement of Ambient Air Pollutants Vol. Volume II. M. o. E. F. Central Pollution Control Board, Govt. of India (Ed.) *Guidelines for Real Time Sampling & Analyses* Retrieved from http://cpcb.nic.in/NAAQSManualVolumeII.pdf

Dayan, U., Erel, Y., Shpund, J., Kordova, L., Wanger, A., & Schauer, J. J. (2011). The impact of local sources and meteorological factors on nitrogen oxide and particulate matter concentrations: A case study of the Day of Atonement in Israel. [Article]. *Atmospheric Environment, 45*(19), 3325-3332. doi: 10.1016/j.atmosenv.2011.02.017

El-Sharkawy, M. F., & Zaki, G. R. (2012). Traffic pollutants levels at different designs of King Fahd Road, Saudi Arabia: comparative study. *The Online Journal of Science and Technology, 2*(1).

Gugamsetty, B. (2012). Source Characterization and Apportionment of PM10, PM2.5 and PM0.1 by Using Positive Matrix Factorization. *Aerosol and Air Quality Research*. doi: 10.4209/aaqr.2012.04.0084

Hu, M., Jia, L., Wang, J., & Pan, Y. (2013). Spatial and temporal characteristics of particulate matter in Beijing, China using the Empirical Mode Decomposition method. *The Science Of The Total Environment, 458-460*, 70-80. doi: 10.1016/j.scitotenv.2013.04.005

Ielpo, P., Paolillo, V., de Gennaro, G., & Dambruoso, P. R. (2014). PM10 and gaseous pollutants trends from air quality monitoring networks in Bari province: principal component analysis and absolute principal component scores on a two years and half data set. [Article]. *Chemistry Central Journal, 8*(1), 1-25. doi: 10.1186/1752-153x-8-14

Jacob, D. J., & Winner, D. A. (2009). Effect of climate change on air quality. [Article]. *Atmospheric Environment, 43*(1), 51-63. doi: 10.1016/j.atmosenv.2008.09.051

Jian, L., Zhao, Y., Zhu, Y.-P., Zhang, M.-B., & Bertolatti, D. (2012). An application of ARIMA model to predict submicron particle concentrations from meteorological factors at a busy roadside in Hangzhou, China. *The Science Of The Total Environment, 426*, 336-345. doi: 10.1016/j.scitotenv.2012.03.025

Marcazzan, G. M., Vaccaro, S., Valli, G., & Vecchi, R. (2001). Characterisation of PM10 and PM2. 5 particulate matter in the ambient air of Milan (Italy). *Atmospheric Environment, 35*(27), 4639-4650.

Marcazzan M. Grazia, Vaccaro, S., Valli, G., & Vecchi, R. (2001). Characterisation of PM10 and PM2.5 particulate matter in the ambient air of Milan (Italy). *Atmospheric Environment, 35*, 4639–4650.

Mues, A., Manders, A., Schaap, M., Kerschbaumer, A., Stern, R., & Builtjes, P. (2012). Impact of the extreme meteorological conditions during the summer 2003 in Europe on particulate matter concentrations. [Article]. *Atmospheric Environment, 55*, 377-391. doi: 10.1016/j.atmosenv.2012.03.002

Ott;, R. L., & Longnecker., M. (2010). *An Introduction to Statistical Methods and Data Analysis* (6th Edition ed.). Canada: Brooks/Cole, Cengage Learning.

Pandey, P., Patel, D. K., Khan, A. H., Barman, S. C., Murthy, R. C., & Kisku, G. C. (2013). Temporal distribution of fine particulates (PM 2.5, PM 10 ), potentially toxic metals, PAHs and Metal-bound carcinogenic risk in the population of Lucknow City, India. [Article]. *Journal of Environmental Science & Health, Part A: Toxic/Hazardous Substances & Environmental Engineering, 48*(7), 730-745. doi: 10.1080/10934529.2013.744613

Peng;, R. D., & Dominici., F. (2008). *Statistical Methods for Environmental Epidemiology with R: A Case Study in Air Pollution and Health*. Washington: Springer.

Qiu, H., Yu, I. T.-S., Tian, L., Wang, X., Tse, L. A., Tam, W., & Wong, T. W. (2012). Effects of coarse particulate matter on emergency hospital admissions for respiratory diseases: a time-series analysis in Hong Kong. *Environmental Health Perspectives, 120*(4), 572-576. doi: 10.1289/ehp.1104002

Reyna, M. A., Bravo, M. E., López, R., Nieblas, E. C., & Nava, M. L. (2012). Relative risk of death from exposure to air pollutants: a short-term (2003–2007) study in Mexicali, Baja California, México. [Article]. *International Journal of Environmental Health Research, 22*(4), 370-386. doi: 10.1080/09603123.2011.650153

Solomon, P. A., Hopke, P. K., Froines, J., & Scheffe, R. (2008). Key Scientific Findings and Policy- and Health-Relevant Insights from the U.S. Environmental Protection Agency's Particulate Matter Supersites Program and Related Studies: An Integration and Synthesis of Results. [Article]. *Journal of the Air & Waste Management Association (Air & Waste Management Association), 58*, S:3-S:92. doi: 10.3155/1047-3289.58.13.s-3

Tai, A. P. K., Mickley, L. J., & Jacob, D. J. (2010). Correlations between fine particulate matter (PM2.5) and meteorological variables in the United States: Implications for the sensitivity of PM2.5 to climate change. *Atmospheric Environment, 44*(32), 3976-3984. doi: 10.1016/j.atmosenv.2010.06.060

Tian, G., Qiao, Z., & Xu, X. (2014). Characteristics of particulate matter (PM10) and its relationship with meteorological factors during 2001-2012 in Beijing. *Environmental Pollution (Barking, Essex: 1987), 192*, 266-274. doi: 10.1016/j.envpol.2014.04.036

Trivedi, D. K., Ali, K., & Beig, G. (2014). Impact of meteorological parameters on the development of fine and coarse particles over Delhi. [Article]. *Science of the Total Environment, 478*, 175-183. doi: 10.1016/j.scitotenv.2014.01.101

Valavanidis, A., Vlachogianni, T., Fiotakis, K., & Loridas, S. (2013). Pulmonary oxidative stress, inflammation and cancer: respirable particulate matter, fibrous dusts and ozone as major causes of lung carcinogenesis

through reactive oxygen species mechanisms. *International Journal Of Environmental Research And Public Health, 10*(9), 3886-3907. doi: 10.3390/ijerph10093886

Vardoulakis, S., & Kassomenos, P. (2008). Sources and factors affecting PM10 levels in two European cities: Implications for local air quality management. *Atmospheric Environment, 42*(17), 3949-3963.

Vellingiri, K., Kim, K.-H., Ma, C.-J., Kang, C.-H., Lee, J.-H., Kim, I.-S., & Brown, R. J. C. (2014). Ambient particulate matter in a central urban area of Seoul, Korea. *Chemosphere, 119C*, 812-819.

Whiteman, C. D., Hoch, S. W., Horel, J. D., & Charland, A. (2014). Relationship between particulate air pollution and meteorological variables in Utah's Salt Lake Valley. [Article]. *Atmospheric Environment, 94*, 742-753. doi: 10.1016/j.atmosenv.2014.06.012

Yang, L.-X., Wang, D.-C., Cheng, S.-H., Wang, Z., Zhou, Y., Zhou, X.-H., & Wang, W.-X. (2007). Influence of meteorological conditions and particulate matter on visual range impairment in Jinan, China. *The Science Of The Total Environment, 383*(1-3), 164-173.

Zhang, F., Wang, W., Lv, J., Krafft, T., & Xu, J. (2011). Time-series studies on air pollution and daily outpatient visits for allergic rhinitis in Beijing, China. [Article]. *Science of the Total Environment, 409*(13), 2486-2492. doi: 10.1016/j.scitotenv.2011.04.007

Zhang, Y., Duc, P. M., Corcho, O., & Calbimonte, J.-P. (2012). Srbench: a streaming rdf/sparql benchmark *The Semantic Web–ISWC 2012* (pp. 641-657): Springer.

# Fitting The Cogeneration Plant To Energy Needs

Francesco Piccininni

Department of Civil Engineering and Architecture Via Orabona, 4, 70100 Bari, Italy
francesco.piccininni@poliba.it

**Abstract** This paper proposes a scheme of cogeneration plant that allows to minimize the surplus of thermal energy and electricity produced. Using the data of consumption of thermal energy and electricity of a hospital in south Italy, it was proposed a cogeneration plant added by compression refrigerators and heat pumps and absorption refrigerators. After analyzing the thermodynamic parameters to assess the energy savings achieved as a reduction of primary energy n passing from conventional energy production to in cogeneration with integration of auxiliary machines.
It was suggest to adapt, according to the type of energy to be supplied, the components added by assessing the reduction of primary energy obtained with a scheme of this type adapted to the energy requirements monthly. The results obtained were assessed with efficiency values lower than those attributed to thermal machines to take into account that these machines are used partialized working because it supplies a power reduced with respect to the maximum possible value, then, with efficiency values lower. The results obtained have confirmed the need to fit the system to the energy requirements for the minimum consumption of thermal plants..

**Key words:** Cogeneration. Energy saving. Primary energy. Efficiency, Energy conversion.

## Introduction

The cogeneration system uses an engine that supplies, in addition to the electricity produced, thermal energy that is rejected in traditional systems. With this kind of power plant is possible arise the efficiency up to '80% of the energy supplied to the system. These high efficiency values are valid only if the two forms of energy are used completely. Their report precise values such as 37% of electricity and 45% of thermal energy while it is hard to find users who are in need of electricity and thermal energy in the same proportion. It must take into account also that the energy needs change during the year requiring the need to heating load in winter and cooling in summer, while the ratio of the two forms of energy produced is, of course, the same. The fitting of the cogeneration plant to actual consumption of energy enables the use of cogeneration high efficiency only if there are no surplus energy. In the analysis of plant performance will not be taken into consideration opportunities, as a heat recovery system that may be not available if the cogeneration system is used in the event of refurbishing and/or the possibility of supplying any surplus of electricity to the grid because these facilitations depend on the place and the economic situation: both solutions, if active, reduce the surplus of energy and thus increase its efficiency.

The main aim is to compare the efficiency of the plant calculated in the design phase with the efficiency of the system in actual operation. It becomes important, therefore, to analyze more deeply the various configurations of the machines involved in a cogeneration plant to evaluate in a more reliable the reduction of energy consumption for the efficient evaluation of the economic convenience of the cogeneration plant.

The use of a PLC to control and manage whole the machines which constitute the cogeneration plant allows to address the energy, heat and electricity, produced to supply energy to heat pumps and refrigerators, both in compression and absorption, to maximize the reduction of energy produced. The change of the energy needs both in quantity along the hours of the day and in quality along the months of the year requires to analyze the most common configurations in order to evaluate their effects on energy consumption. To analyze the efficiency of various configurations are taken into account, in addition to the internal combustion engine as the primary source of cogeneration, absorption chillers and reverse cycle compression machines, refrigerators and heat pumps. The PLC allows also to monitor the connections of the various machines, the operating times and, therefore, to assess the effective efficiency of the whole plant with the capability to modify the intervention strategy, if necessary.

The average values and the modulation of these parameters are important in the system configuration. The electricity consumption are easily derived from the bills and the thermal one are evaluated through the amount of fuel supplied. The consumption associated with both thermal requirement that the electric ones are differentiated from the point of view of quality. With reference to the way with which the energy is transformed and the temporal variability with which they control the consumption same.

**Nomenclature**

| | |
|---|---|
| COP | heat pump efficiency |
| $E_{CCS}$ | conventional electrical output, |
| $E_{CCU}$ | cogeneration electrical output, |
| $E_{CoGe}$ | primary energy demand by the cogeneration plant, |
| $E_E$ | electricity produced, |
| $EER_{ARS}$ | absorption refrigerating system efficiency |
| $EER_{CRS}$ | compression refrigerating system efficiency |
| $E_{HP}$ | electricity power to driving the heat pumps |
| $E_{CoGe}$ | electricity actually used. |
| $E_{Tc}$ | civil heat produced, |
| $E_{Ti}$ | industrial heat produced, |
| $Q_{ARS}$ | engine thermal power for absorption refrigerators driving |
| $Q_{EC}$ | primary energy of conventional cooling |
| $Q_{CoGe}$ | primary energy for the cogeneration plant, |
| $Q_{CP}$ | heat power to driving absorption refrigerating system |
| $Q_H$ | primary energy for conventional boiler |
| $Q_{ICE}$ | heating capacity, |
| $Q_P$ | primary energy demand for cogeneration |
| $Q_{UC}$ | cold actually used, |
| $Q_{UH}$ | heat actually used, |
| $\eta_B$ | heating burner efficiency |
| $\eta_{EL}$ | electricity generation efficiency |
| $\eta_{Tc}$ | civil thermal production efficiency, |
| $\eta_{Ti}$ | industrial thermal production efficiency, |

## The cogeneration plant

The cogeneration or Combined Heat and Power (CHP) is substantially an engine capable to produce mechanical power and can arrange the recovery of heat from the engine in order to use it for the technological applications for high, medium and low temperatures.

The installation of a cogeneration plant becomes more convenient when you must proceed to the replacement or installation of new heat generators or motors for the production of electricity. it should be specified that in the case of civil users and unlike industrial utilities with energy demands practically constant, the analysis is complex due to the strong variations of thermal loads and electrical and non-coincidence of variation for both energies. In the face of significant changes, the cogeneration plant cannot be sized for the maximum load to avoid incurring the penalties for lower yields at partial load.

One solution is the construction of the cogeneration plant using a group of machines having powers such that their sum is equal to the maximum power. In this way, the reduction of the thermal load is answered by turning off one or more of the units allowing the others machine to operate at the maximum load leaving only one operating in partial load thus reducing losses related to the reduction in yield due to partial load. This, however, leads to an increase in the cost of the system and an amortization period longer.

The achievement of high overall performance typical of cogeneration is subject to the effective use of heat

generated from the production of electricity and thus to maintain the relationship between electricity and thermal energy demand. For this purpose it would be necessary diagrams of the electrical power demand during the day type summer and winter. It is possible, then, define the trend of the annual frequency of the power produced and the power absorption. Even at this stage have a fractionation in different machines operating in parallel would help to regulate the production of energy to the request of the same. This would be possible if it remains more or less constant ratio between electricity and thermal energy produced and absorbed.

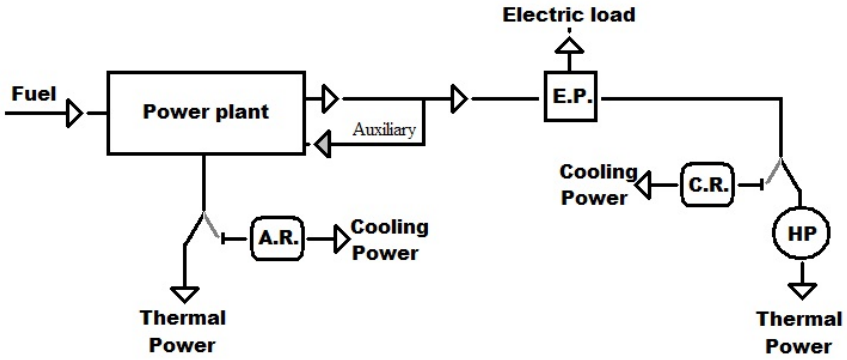


**Figure 1:** Schematic representation of the proposed cogeneration plant

In hospitals the production of cold is done with compression refrigerators electrically operated. This means that during the hottest hours of summer days there are high demands for electric power, not necessary in the rest of the year, that would not be possible to satisfy. It would be necessary to take such power from the electrical grid undergoing paying high rates normally linked to consumption peaks. The cogeneration plant during the summer days has a surplus of heat that can be suitably converted into cold with the use of absorption machines that can produce the necessary cold to satisfy the summer thermal load. From a thermodynamic point of view there is an increase of the quality of the system because the thermal energy produced in the summer, to be considered completely lost, is recovered in the percentage of the cooling efficiency of the absorption machine.

On cold winter days the increase of the thermal power needed to satisfy the heat load can be reduced using the more electric power produced for driving heat pumps that can provide heat in the percentage amount of the efficiency parameter, COP. Even in this case, the reduction of produced and not used energy increases the thermodynamic efficiency of the plant. Any increase in thermodynamic efficiency results in a reduction of primary energy required by the thermal plant.

To increase the flexibility of the cogeneration plant it is possible to alter the relationship between electrical and thermal energy. is possible to use compression heat pumps (moved by an electric motor) and absorption refrigeration machines. In this way if there is a greater demand of thermal energy, an increase of power supplied by the cogeneration plant would result in a surplus of electrical energy whose disposal may even lead to the disposal environment by reducing the efficiency of the plant. using the most electricity to power a heat pump of sufficient value of the COP, it is possible to reduce the power increase using the surplus of electricity supplying it to heat pump with COP value more of $1/\eta_{EL}$. reducing the power increase without any waste of energy produced. In case of increase in the demand for electricity for air conditioning in summer can be avoided by increasing proportionally the electric power generated. This would result in an increase of heat cannot be used resulting in a reduction in the efficiency of the system.

## Parameters for evaluating the cogeneration effectiveness

The evaluation of the efficiency of a plant that produces heat, cold and electricity must be taken into account the efficiency with which these products are energy. The heat produced is directly characterized the performance of the burner, $\eta_B$, while the production of cold depends on the efficiency of refrigerators, EER; the

obtained mechanical/electrical power is related to the energy supplied to the engine through the thermodynamic efficiency of the engine, $\eta_{EL}$. When evaluating the efficiency of energy production in a cogeneration plant production efficiencies are not directly comparable. For this reason the most effective parameter for evaluating any higher efficiency of a cogeneration plant is to evaluate the percentage of the reduction of primary energy when a cogeneration plant is involved to satisfy the heat, cold and electricity needs instead of a conventional one.

The primary energy required by a conventional system designed to produce heat, cold and use electricity is equal to the sum of primary energies required by production of the three types of energy:

$$PE_{Conv} = \frac{\sum Q_H}{\eta_B} + \frac{\sum Q_C}{EER_{CRS} \cdot \eta_{EL}} + \frac{E_{CCS}}{\eta_{EL}} \qquad (1)$$

where

$\frac{\sum Q_H}{\eta_B}$ is the primary energy demand for furnace with performance $\eta_B$,

$\frac{\sum Q_C}{EER_{CRS} \cdot \eta_{EL}}$ is the primary energy demand for refrigerators compression with efficiency parameter $EER_{CRS}$ driven by electricity produced with performance $\eta_{EL}$,

$\frac{E_{CCS}}{\eta_{EL}}$ is the primary energy demand from the production of electricity with performance $\eta_{EL}$.

The primary energy of the cogeneration power plant is the energy supplied in order to produce electric and thermal energy; as noted above cooling can be produced using heat to drive absorption refrigerator or electricity to drive compression one.

The real energy savings can be evaluated through the parameter named Primary Energy Savings defined by the following formula:

$$PES = \frac{PE_{Conv} - PE_{CoGe}}{PE_{Conv}} \qquad (2)$$

This parameter represents the reality of the energy consumption for the same meeting the energy needs satisfying; the greater thermodynamic efficiencies and/or management are these involve an actual reduction of primary energy.

European law (DIRECTIVE 2004/8/EC) states that a cogeneration plant can be regarded as a "high efficiency" in order to take advantage of incentives and facilities if the value of the parameter PES is greater than zero for power plants less than 1.0 MW and greater than 10% for power plants greater than or equal to 1.0 MW.

By inserting in the formula the values of the efficiencies of heat and electricity production the PES can be wrote as the following formula also named FERS (Fuel Energy Saving Ratio):

$$PES = 1 - \frac{Q_{CoGe}}{\frac{Q_{Tc}}{\eta_{Tc}} + \frac{E_E}{\eta_E}} \qquad (3)$$

The thermodynamic efficiency of a cogeneration system depends on the efficiency of the three components such as heat, cold and electricity. The efficiency values depend on the value of the instantaneous power because the choking of the power produced will reduce the values. The energy produced and not used cannot be taken into consideration to assess its efficiency bearing in mind that the relationship between the thermal power and the electric power generated is constant.

Using all the efficiency parameters and the percentages of the thermal energy produced by the internal combustion engine used to driving the absorption refrigerating system ($Q_{EC}/Q_{ICE}$) and the percentage of electricity produced by the internal combustion engine used to driving heat pump ($E_{HP}/E_{CCU}$) it's possible evaluate directly the variation of primary energy achievable with a cogeneration plant.

$$PES = 1 - \frac{\left[1 + \frac{E_{CCU}}{Q_{ICE}}\right]}{\left(\frac{Q_{ICE} + E_{CCU}}{Q_p}\right) \cdot \left[\left(\frac{E_{CCU} - E_{HP}}{\frac{Q_{ICE}}{\eta_{El}}}\right) + \left(\frac{1 + \left\{\frac{E_{HP}}{E_{CCU}} \cdot \frac{E_{CCU}}{Q_{ICE}}\right\} + \frac{Q_{EC}}{Q_{ICE}} \cdot EER_{ARS}}{\eta_B}\right) + \left(\frac{\frac{Q_{EC}}{Q_{ICE}} \cdot EER_{ARS}}{\eta_{El} \cdot EER_{CRS}}\right)\right]} \quad (4)$$

The cogeneration plants must be able to meet the heat demand of the technological and heat for heating, electricity for technological needs and for the production of cold necessary for the air conditioning in summer. The formula (4) expresses the possible reduction percentage of primary energy when energy needs are met with the CHP. This formula takes into account the yield at which the various forms of energy are produced. It should be noted that obtaining a reduction of primary energy used is an energy saving even in the presence of surplus energy not directly usable by the user. In this case one can think of using storage systems with regard to thermal energy or to direct any surplus electric power to the overall network.

## Case of study

The object of the study hospital has about 850 beds, situated in the south of Italy consumes in a year about 1,750,000 litres of diesel and 5,000 MWh of electricity. The thermal power plant, equipped with traditional boilers, providing steam to 1.0 MPa at about 175 °C to meet the typical hospital services such as laundry, kitchen and sterilizers for both generic services such as hot water and heating in winter. There is no centralized air-conditioning plant but a room small air-conditioning.

The choice to study the application of a cogeneration system for a hospital derives from fairy for this type of users, there is well-known in literature. The thermal requirements related to heating were obtained by subtracting the heat consumption winter the heat consumption of the summer months representing the consumption of thermal energy for hospital purposes.

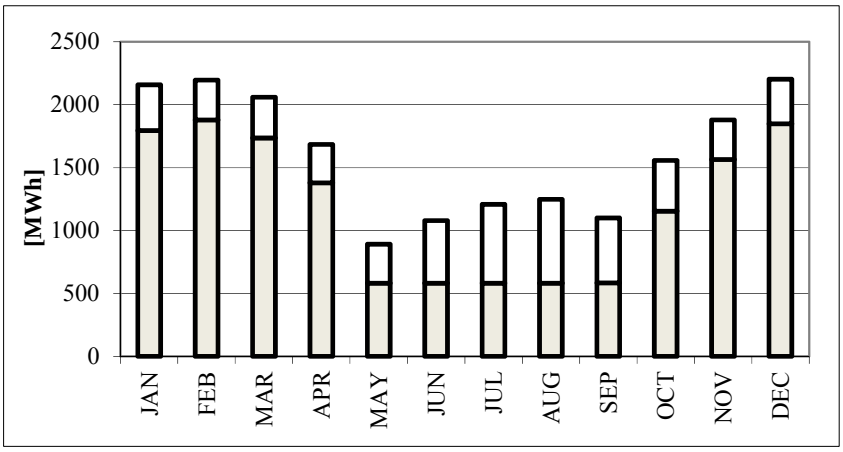


**Figure 2:** The thermal and electrical consumption of hospital

The monthly average thermal energy consumption (grey) and electrical ones (white) are shown in Figure 3. From the same figure is shown the increase in electricity consumption in the summer months due to the use of air conditioning. The relationship between the electrical power and thermal power is a key parameter to determine the pattern of the cogeneration plant. The plants of this type have a relationship between the two energies fairly constant which can be very different from the relationship of the needs of the hospital.

In the particular case considered is added that for security reasons, a hospital must have an ability to self-

production of heat and power for the continuity of emergency services in case of power failure. This involves an economic advantage in buying, and management, the apparatus of self-production.

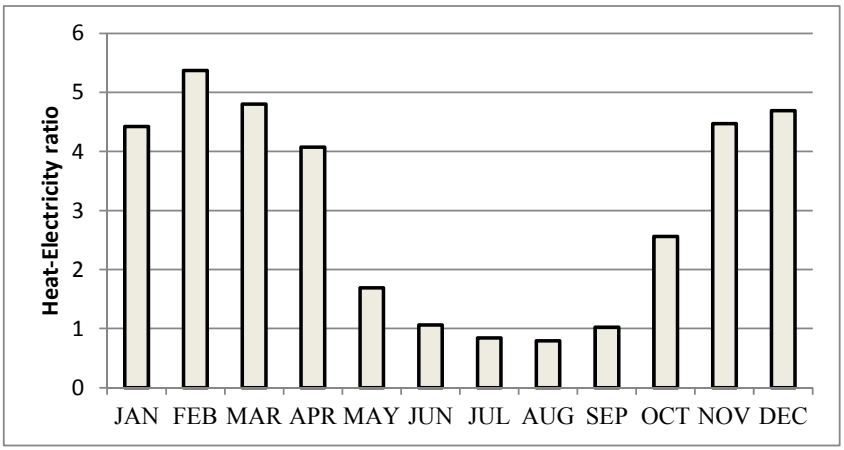


**Figure 3:** The ratio between the thermal and electrical energy

It is felt important to emphasize that this ability to produce energy is becoming paramount also for office buildings as the spread of the apparatuses TLC (router, wifi, and the computer itself) requires the availability of electricity is no longer available directly on the line telephone as is present on traditional phone lines.

As regards the value of the temperatures at which the heat is supplied as it is energetically more valuable the higher the temperature at which it is supplied. It is recalled that the sterilization requires 140 ° C 190 ° around the ironing, cooking little more than 100 ° C, hot water at 50 ° C and heating to around 80 ° C as well as absorption refrigeration machines. In Figure 4 shows the thermal energy at high enthalpy and the low enthalpy where we see that the heating requirements of high enthalpy is relatively low compared to that of low enthalpy.

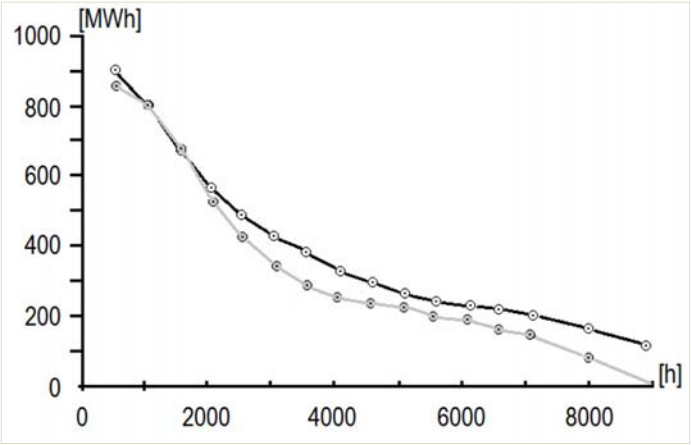


**Figure 4:** Total heat energy needs (black curve) and the low enthalpy thermal energy needs (gray curve).

On average, the heat consumption is divided in half between the heating and the hot water, for general uses. As regards the hot water, the percentages of utilization and the uses are indicated in the figure below.

CHP gives the ability to produce heat and electricity using about 90% of the energy supplied. The heat produced is about 58% while the electricity produced is about 32% with a ratio heat electricity equal to 1.37:1.

This high efficiency of transformation is only valid if all the electricity and all the thermal energy produced

is used. If the energy requirements of thermal energy and electricity have a relationship other than that of cogeneration, the fulfillment of one leads to an imbalance of the other.

The ratio of heat and electricity energy needs required is almost always different from the relationship of cogeneration (surely it is during the day and between days) so it is needs to adapt the system to the energy requirements because the production of not used energy results as a reduction in system efficiency.

Regarding the hospital object of our analysis, in the winter period a part of the thermal power is used for technological purposes (the same throughout the year) and a part for room heating. By adjusting the heat output of CHP in order to satisfy the thermal load can have a ratio greater than the ratio heat-electricity cogeneration thus producing a surplus of electricity. Using the surplus of electrical energy to drive a heat pump would be obtained rate of heat which would reduce the thermal power produced by the motor up to the coincidence of the thermal power produced (engine plus heat pump) with the heat load, minimizing the electricity surplus.

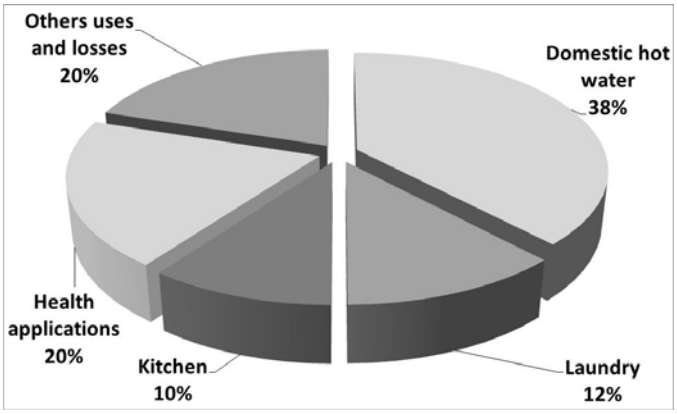


**Figure 5:** Percentages of the thermal energy needs in hospitals

In summer time the electricity demand is used to meet both the needs of technology (the same throughout the year) and the electrical load to produce cold for room conditioning. By adjusting the thermal power cogeneration to meet the electrical load can have a ratio less than the ratio heat-electricity cogeneration producing a surplus of thermal energy. Using the excess heat to power an absorption refrigerator is possible to satisfy a portion of the refrigeration load. Even in this case, reducing the power produced by the cogeneration engine it's possible to meet the electrical, heat and cold loads minimizing the surplus of produced energy. The primary energy can be reduced leading toward zero thermal energy surplus realizing energy savings

The consumption data collected for technological hospital every month serve 525 MWh of thermal power and 310 MWh of electrical power at a ratio heat and power equal to 1.76:1 ratio already exceeds the cogeneration 1.37:1.

**Table 1**: Values of the efficiencies used in the assessment of energy consumption.

| Name | Symbol | Value |
|---|---|---|
| Absorption refrigerating system efficiency | $EER_{ARS}$ | 0,60 |
| Heat pump efficiency | COP | 3.50 |
| CHP heat generation efficiency | $\eta_{CHP\_B}$ | 0.47 |
| Heating burner efficiency | $\eta_B$ | 0.90 |
| CHP Electricity generation efficiency | $\eta_{EL}$ | 0.38 |
| Grid Electricity generation efficiency | $\eta_{EL\_TR}$ | 0.49 |

In the summer time using the same energy source of the conventional unit in a cogeneration plant to meet the electrical load there is an overproduction of heat (over 525 MWh per month). The highest demand for electricity (the part that exceeds 310 MWh per month ) is bound to summer conditioning.

In the winter using the same energy source of the conventional unit in a cogeneration plant to meet the thermal load there is an overproduction of electricity (over 310 MWh per month). The reduction of primary energy does not prevent the fulfilment of energy needs. Knowing the monthly consumption of diesel and electricity, considering an efficiency of electricity production (domestic) by 42%, it's possible calculate the primary energy required monthly.

The evaluations of the values of PES was made assuming a classic cogeneration system capable of converting into electricity for 38% of primary energy into heat and 48% of the same. After verifying the satisfaction of the thermal energy and electricity needed to operate the hospital as such were evaluated excess energy produced. As evidenced by the data shown in Figure 2, the hospital for proper operation monthly needs 525 MWh of thermal energy and 310 MWh of electricity. In the winter months it has the majority required to provide heat to heat the building, while in summer the majority request concerns the electricity for the production of cold for the summer cooling of the building. The values of the efficiency of the machines used in the installation of cogeneration, complete with heat pump and absorption refrigerators, are shown in Table 1.

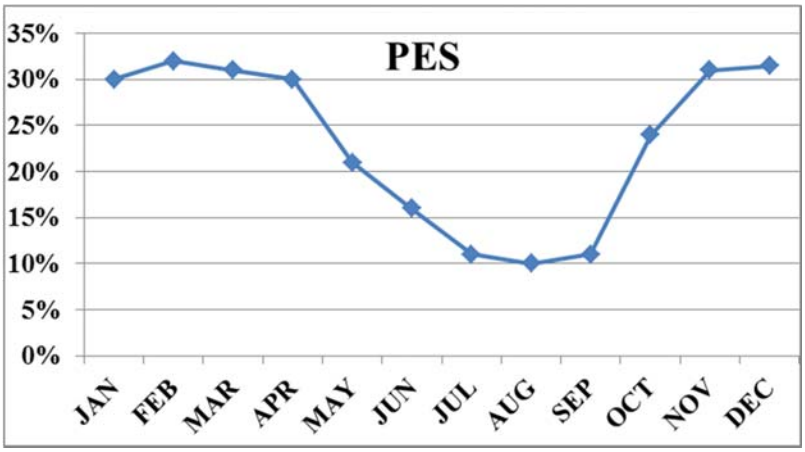


**Figure 6:** Primary energy savings achievable

In the first case there is a surplus of electrical energy that is converted into heat through the use of a heat pump because of the relatively high value of conversion of electrical energy into thermal energy values of primary energy savings are much higher than the higher the demand for thermal energy with the peak in the month of February.

In the summer months the surplus concerns the thermal energy. A part of this is converted into cold using double-effect absorption refrigerators. Because of the low conversion value, the reduction of primary energy consumption takes values significantly lower than those in winter, reaching the lowest value in the month of August, the hottest month of the year in southern Italy.

## Conclusions

The use of a cogeneration system to replace the traditional plant of which you know the monthly consumption of heat and electricity in a hospital in southern Italy has allowed the evaluation of the primary energy savings achievable. Assuming the use of heat pumps and absorption refrigerators has been possible to vary the ratio heat-mechanical power of a cogeneration plant adapting the cogeneration plant to the energy needs of the hospital. Energy saving is verified even in the summer months when it is not dropped below 10%.

In the calculations were assessed excess energy use of which has not been taken into account, but they might find an opportunity to further reduce primary energy consumption by using recovery systems. In the summer months, when the PES reaches the lowest values, it's possible get better results by using photovoltaic panels that

produce electricity synchronously with the requirement of the cold.

The possibility of having energy, especially the electric one, even in case of black-out is essential for a hospital that obtains by cogeneration plant the economic savings of purchase of engines for the production of electricity in case of emergency. The availability of self-produced electricity represents a condition of safety for office buildings which make use of a high communications now totally entrusted to the web.

The increasing energy supply in the presence of economic development would avoid loading all the electricity needs on the existing thermal power plants given the enormous difficulties to create new power plants in a densely populated country like Italy.

## References

HavelskyÂ V. (1999). Energetic efficiency of cogeneration systems for combined heat, cold and power production, *International Journal of Refrigeration* 22 (pp. 479-485)

Lucas, K. (2000). On the thermodynamics of cogeneration. *International Journal of Thermal Sciences,* 39, (pp. 1039–1046)

Malinowska W., Malinowski L., Green M.A. (2003): Parametric study of exergetic efficiency of a small-scale cogeneration plant incorporating a heat pump, *Applied Thermal Engineering* 23 (pp. 459–472)

DIRECTIVE 2004/8/EC OF THE EUROPEAN PARLIAMENT AND OF THE COUNCIL of 11 February 2004 on the promotion of cogeneration based on a useful heat demand in the internal energy market and amending Directive 92/42/EEC

Verbruggen A. (2008). The merit of cogeneration: Measuring and rewarding performance. *Energy Policy* 36 3059–3066

Kanoglu, M., Dincer I. (2009). Performance assessment of cogeneration plants. *Energy Conversion and Management* 50 (pp. 76–81)

# Iteration Free Fractal Image Compression For Color Images Using Vector Quantization, Genetic Algorithm And Simulated Annealing

A R Nadira Banu Kamal

Dept of Computer Science, TBAK College for Women, Kilakarai, Tamil Nadu, India
nadirakamal@gmail.com

**Abstract:** This research paper on iteration free fractal image compression for color images using the techniques Vector Quantization, Genetic Algorithm and Simulated Annealing is proposed, for lossy compression, to improve the decoded image quality, compression ratio and reduction in coding time. Fractal coding consists of the representation of image blocks through the contractive transformation coefficients, using the self-similarity concept present in the larger domain blocks. Fractal coding achieves high compression ratio but it consumes more time to compress and decompress an image. Different techniques are available to reduce the time consumption and improve the decoded image reliability. But most of them lead to a bad image quality, or a lower compression ratio. Usage of synthetic codebook for encoding using Fractal does not require iteration at decoding and the coding error is determined immediately at the encoder. The techniques Vector Quantization, Genetic Algorithm and Simulated Annealing are used to determine the best domain block that matches the range blocks. The proposed algorithm has the better performance in terms of image quality, bit rate and coding time for Color images. Only the encoding consumes more time but the decoding is very fast.

**Key words: Fractal code, Iteration free, Vector quantization, Genetic algorithm, Simulated annealing**

## Introduction

With the recent rapid growth of multimedia applications and digital transmission, image compression techniques have become a very important subject. A digital image obtained by sampling and quantizing a continuous tone picture requires an enormous storage. For instance, a 24 bit color image with 512x512 pixels will occupy 768 Kbytes storage on a disk and a picture twice of this size will not fit in a single floppy disk. To transmit such an image over a 28.8 Kbps modem would take almost 4 minutes (Vivek Arya et al., 2013). Thus image compression addresses the problem of reducing the amount of data required to represent a digital image, so that it can be stored and transmitted more efficiently. Fractal compression is one of the methods and this method is used in this research work to achieve improved image quality, compression ratio and reduction in coding time. The proposed method has the advantages such as low time consumption for decoding and less memory requirements for storage, which is most needed in today's communication.

Fractal coding consists of the representation of image blocks through the contractive transformation coefficients, using the self-similarity concept present in the larger domain blocks. Fractal coding achieves high compression ratio but the time required to compress and decompress an image is time consuming. There are many modified versions proposed to improve the fractal coding techniques (Ghazel et al., 2005, Mohsen et al., 2003). Most of the studies focus on

- refining the block transformation (Chong and Minghong, 2001)
- reducing of the complexity of the encoding process (Chen et al., 2002)
- speeding up the process (Hau-Jie and Wang, 2005, Riccardo et al., 2006)

An iteration-free fractal image coding for color images using the techniques Vector Quantization (VQ), Genetic Algorithm (GA) and Simulated Annealing (SA) is proposed for lossy compression in this research work to improve decoded image quality, compression ratio and to reduce the coding time. The major problems with a VQ encoder are the codebook search complexity and the memory required to store the codebook. Both the codebook search complexity and storage requirements increase exponentially with the vector dimension (Jeng et al., 2003). Therefore the size of the VQ blocks is usually kept very small which in turn results in a high statistical correlation between adjacent blocks. In this research work the size of the vector is limited to 64 ie., 8x8 blocks. The searching process of the reproduction vector for an input vector using full search requires intensive computations. Many algorithms are proposed to speed up the searching process. The algorithm given by Jim and Yi (2004) uses the vector's features (mean value, edge strength, and texture strength) to delete impossible codewords that cannot be rejected by the DHSS algorithm using three projections. Two additional inequalities, one for terminating the searching process and another to reject impossible codewords, were presented to reduce the distortion computations. This algorithm is better than the DHSS algorithm and Pan's method (Pan et al., 2003) in terms of computing time and the number of distortion calculations hence this

algorithm was included in the present research work for eliminating the domain blocks while searching for the optimal solution in the proposed method using the technique VQ. As genetic algorithms and Simulated Annealing are global search and optimization method, it can be applied to the proposed method to find the optimal domain block for each range block in iteration-free fractal color image coding. The problems faced in GA are encoding the solution, fixing the size of the population, choosing the crossover and its probability, mutation and its probability and selection procedure. Similarly the problems faced in SA are generating a candidate solution, problem-specific cooling schedule, objective function and Metropolis-step in which the algorithm decides if a solution is accepted or rejected. The selection of these parameters greatly affects the solution. The proposed method using the VQ technique aims to design an efficient domain pool for the fractal coding schemes and it also introduces the optimization techniques like GA and SA to improve the quality of the decoded image and for speeding the encoding time in generating the fractal codes. This research work of introducing VQ, GA and SA reduces the computational complexity, improves the image quality and reduces the coding time.

## Algorithm of the proposed method

Usage of synthetic codebook for encoding using Fractal does not require iteration at decoding and the coding error is determined immediately at the encoder (Chang and Chung, 2000). Hence there is a reduction in decoding time. In the proposed method a synthetic codebook is created as the domain pool using the mean image, whose pixel values are the block means of all the range blocks. This code book is used as the domain pool for genetic algorithm and simulated annealing techniques. As these techniques have become an efficient tool for search and optimization, they can be used to find the better domain block from the domain pool that matches the range block of the image in fractal coding.

**Parameters for VQ**

In the iteration-free fractal image coding using vector quantization the domain pool was classified and pruned for each range block for each RGB component before the comparison for the identification of the better domain block from the codebook for the range block in order to reduce the computational time (Jim and Yi, 2004). The proposed methodology using the VQ technique reduces the coding process time and intensive computation tasks by pruning the domain block for each range block. The redundancies in the domain pool are first reduced by the Linde Buzo Gray (LBG) Algorithm. Further redundancy in the domain block for each range block was achieved using the vector features such as mean value, edge strength, and texture strength (Nadira and Priyanga, 2014a). A pruning condition for terminating the searching process to find the best domain block from the domain pool has been used in this proposed research work.

**Parameters of GA**

Crossover is made in hope that new chromosomes will contain good parts of old chromosomes and therefore the new chromosomes will be better. However, it is good to let some part of old populations survive to next generation. The crossover probability is chosen as 0.85 in the proposed method. Mutation generally prevents the GA from falling into local extremes. Mutation should not occur very often, because GA will in fact then change to random search. The mutation probability is chosen to be 0.06 in the proposed method (Nadira and Priyanga, 2014). Research shows that after some limit (which depends mainly on encoding and the problem) it is not useful to use very large populations because it does not solve the problem faster than moderate sized populations. In the proposed method the size of the population is chosen to be 40. There are many methods in selecting the best chromosomes. Examples are Roulette wheel selection, Boltzmann selection, Tournament selection, Rank selection, Steady state selection and some others. Roulette wheel selection is used in the proposed method.

**Parameters of SA**

At each step, the SA heuristic considers some neighbors of the current state **s**, and probabilistically decides between moving the system to state **s'** or staying back in state **s**. The probabilities are chosen so that the system ultimately tends to move to states of lower energy. Boltzmann's Probability is used in the proposed method. In the present problem the neighbor of a state is any domain block from the domain pool. The probability of making the transition to the new state **s'** is a function P(δE, T) of the energy difference δE = E(s') - E(s) between the two states, and of a global time-varying parameter T called the control parameter (Nadira , 2012). In the proposed method T is made to vary from 1 to 0. Initially, T is set to a high value (or infinity), and it is decreased at each step according to some annealing schedule. Various cooling schedules are suggested in

literature. In the proposed method $T_i = T_0 - i\frac{T_0 - T_{N2}}{N2}$ is used as it leads to better solution (Nadira and Thamaraiselvi, 2006a).

The sender sends the color image for compression. In the preprocessing stage, the input MxNx3 image under coding is divided into non-overlapping square blocks of BxBx3 pixels called the range blocks. Then the mean and variance of each range blocks are determined. After the mean of all the range blocks are obtained, a mean image of size M/B x N/B x 3 with each pixel corresponding to the block mean is generated. The mean image must be larger than the size of the range block i.e. M/B x N/B x 3 > B x B x 3. The maximum size of B is limited to 8 in order to produce a good quality of the decoded image. The higher the resolution of the input image (MxNx3) more blocks can be generated for the domain pool which helps to find a good mapping between the domain and range blocks. The initial domain pool with blocks of the same size as the range is generated using the mean image. In the encoder if the variance of the range block is smaller than the threshold value *E*, the range block is coded by the mean, or else the range block will be coded by the contractive affine transformation (Chang, 2001). The aim of the proposed scheme is to find the domain block for each image range block and the transformation parameters that minimize the distortion between the image block and the transformed domain block in a minimized time. This process of finding the best domain block makes use of the techniques like VQ, GA and SA. In the decoder, the mean information of each range block is extracted from the fractal codes. Using this information the mean image is constructed. This mean image is partitioned into blocks of the same size as the input image. This forms the domain pool for GA and SA search methods but for VQ the domain pool is constructed from the mean image blocks (same size as that of the input) using LBG algorithm. The decompressed image is constructed block by block by applying the transformation parameters to the selected domain block from the domain pool as per the code.

## Implementation

For implementation of the proposed algorithms, four 512 x 512 benchmark color images of Lena, Pepper, Tajmahal and Cauliflower [shown in Figure 1 (a) to (d)] with twenty four bit color resolution were used. In the simulation, the images were partitioned into range blocks with the block size, 8x8 or 4x4 or 2x2. The maximum block size is set to 8x8 because for a range block size greater than 8x8 the determination of the proper domain block was difficult and the quality of the image reconstructed was poor. The threshold value for the variance of range blocks was chosen by trial and error basis to be of size 20 for block size 8x8, 10 for 4x4 and 5 for 2x2 that results in good compression ratio and PSNR. The number of blocks in the mean image is the size of the domain pool. These algorithms were implemented using the software Matlab 7.12 on the Intel (R) Core[TM] 2 E7500 systems with 2.93 GHz and 1.96 GB of RAM.

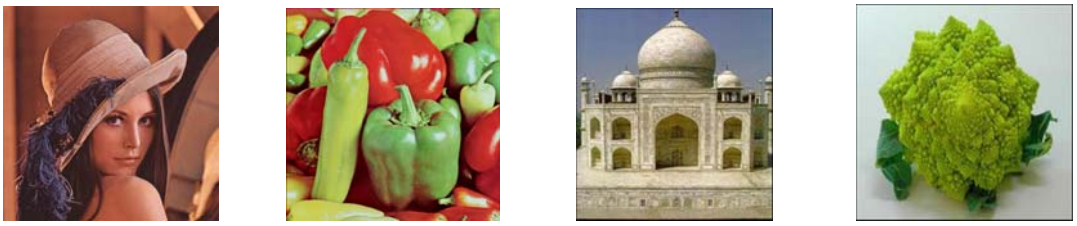

(a) Lena (b) Pepper (c) Tajmahal (d) Cauliflower

**Figure 1:** Original (512 X 512x3, 24 Bit/Pixel) Images.

The range block with a size 8x8, 4x4 and 2x2 was considered for simulation. The length of the attached header to the proposed iteration-free fractal code for each range block was one bit because it only denoted whether or not the range block was coded by the mean. For an image partitioned by 4x4 range blocks, every block mean was calculated and a 128x128 mean image was obtained. Figure 2 (b) shows the mean image of Lena got by this partition and it is very similar to its original image except its size. Therefore the domain pools of different sizes namely 16, 32 and 64 using the LBG-based method from the mean image was constructed for VQ. For GA and SA the range block with a size 8x8, 4x4 & 2x2 was considered for simulation. Here the total number of range blocks for the block size 4x4 for each color component was n = 16384 and total number of domain blocks (m) to search were (128 / 4) x (128 / 4) = 32 x 32. Thus, the cardinality (N1) of the search spaces for this case was 8 x 4 x 1024.The string length n was taken to be 15 (3 + 2 + 10). In GA out of these $2^{15}$ binary strings, forty strings (S = 40) were selected randomly to construct an initial population. A high crossover probability, say $p_c = 0.85$, was taken for the crossover operation. For mutation operation, $p_m$ was 0.06. Roulette-wheel selection procedure

was used. The fitness value of a string between the given range block and the obtained range block for each RGB color component is taken to be the MSE given in Eq. 1.

$$MSE\ (R, \hat{R}) = \frac{1}{B^2} \sum_{0, i, j \le B} \left( r_{i,j} - \hat{r}_{i,j} \right)^2 \qquad (1)$$

The probability of selection of a string in the population to the mating pool was inversely proportional to its fitness value because the present optimization problem is a minimization problem. The total number of generations (iterations) considered in the GA was T = 60. Hence, the search space reduction ratio was approximately 14. For the block size 8x8, the total number of range blocks for each RGB component was n = 4096 and total number of domain blocks to search was (64 / 8) x (64 / 8) = 8 x 8. Thus, the cardinality (N1) of the search spaces for this case was 8 x 4 x 64. The string length n was taken to be 11 (3 + 2 + 6). For the block size 2x2, the total number of range blocks was n = 65536 and total number of domain blocks to search was (256 / 2) x (256 / 2) = 128 x 128. Thus, the cardinality (N1) of the search spaces for this case was 8 x 4 x 16384.The string length n was taken to be 19 (3 + 2 + 14). The domain pool was found and the coding performance using the above parameters was simulated. Using SA for the block of size 8x8, 4x4 and 2x2 the solution configuration length was taken to be 11, 15 and 19 respectively. Knuth random numbers were globally generated for the rearrangement of the solution so that most possible solutions were considered. The seed value was chosen to be as 0.5. In the simplest form of the problem, the objective function *was* taken as the Mean Square Error (MSE). Some random rearrangement of the solution was first generated, and used them to determine the range of values the objective function encountered from move to move. Choosing a starting value for the parameter $T_0$ which was considerably large say 1, and process was conducted downward each amounting to a decrease in *T*. Each new value of *T* was kept constant for, say, *N* (N=40) reconfigurations and store the configuration which produces minimum value for the objective function. If the terminating condition was not reached, the parameter for *T* was reduced and the next trial was started with the configuration that produced minimum value for the objective function. The equation for the parameter *T* was chosen as

$$T_i = T_o - i \frac{T_o - T_N}{N} \qquad (2)$$

where $T_o$ = 1 and $T_N$ = 0 and *i* is the iteration number. The coding performance with the contractive affine transformation under the different sizes for the domain pool on the parameters like coding time, image quality and bit rate was determined.

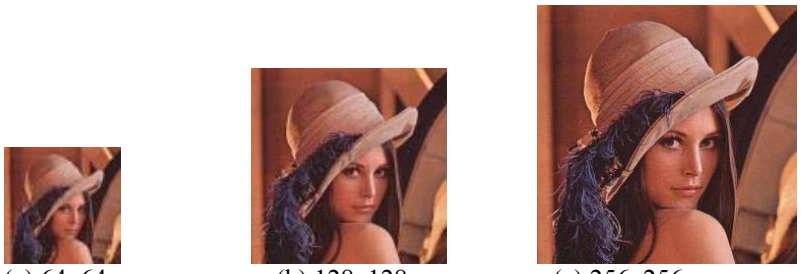

(a) 64x64 (b) 128x128 (c) 256x256

**Figure 2:** Mean Images Of Lena.

## Results and Discussions

The range blocks were classified before coding [Yung et al., 2003]. Range blocks were grouped into two sets according to the variability of the pixel values in these blocks. If the variability of a block was low, i.e., if the variance of the pixel values in the block was below a fixed value, called the threshold, the block is called smooth type range block. Otherwise, it is called a rough type range block.

**Table 1:** Classification of blocks and bit rate using different types of encoding on the chosen images using the proposed techniques.

| Image | Range Block size | No of Range Blocks for GA/SA | | Bit Rate | | Compression ratio | | PSNR | | |
|---|---|---|---|---|---|---|---|---|---|---|
| | | | | GA / SA | VQ | GA / SA | VQ | | | |
| | | Smooth | Rough | | | | | GA | SA | VQ |
| Lena | 2 * 2 | 43927 | 21611 | 7.56 | 7.47 | 3.17 | 3.20 | 41.60 | 35.41 | 31.55 |
| | 4 * 4 | 8394 | 7992 | 1.95 | 2.04 | 12.26 | 12 | 33.12 | 31.68 | 27.84 |
| | 8 * 8 | 1559 | 2539 | 0.48 | 0.54 | 49.82 | 44.50 | 28.76 | 28.36 | 25.16 |
| Pepper | 2 * 2 | 51409 | 14129 | 7.02 | 7.16 | 3.41 | 3.35 | 39.84 | 36.24 | 30.78 |
| | 4 * 4 | 9851 | 6535 | 1.87 | 1.99 | 12.81 | 12.06 | 33.52 | 32.20 | 26.92 |
| | 8 * 8 | 1638 | 2460 | 0.47 | 0.53 | 50.16 | 45.19 | 27.84 | 27.84 | 23.91 |
| Cauliflower | 2 * 2 | 49433 | 16105 | 7.16 | 7.04 | 3.34 | 3.40 | 37.63 | 37.44 | 27.03 |
| | 4 * 4 | 8640 | 7746 | 1.94 | 1.87 | 12.34 | 12.77 | 29.49 | 28.31 | 23.45 |
| | 8 * 8 | 1682 | 2416 | 0.47 | 0.49 | 50.36 | 48.87 | 24.23 | 24.88 | 21.97 |
| Tajmahal | 2 * 2 | 44672 | 20866 | 7.51 | 7.35 | 3.19 | 3.26 | 42.83 | 39.90 | 22.50 |
| | 4 * 4 | 6624 | 9762 | 2.05 | 1.98 | 11.65 | 12.07 | 33.86 | 32.32 | 25.49 |
| | 8 * 8 | 1018 | 3080 | 0.50 | 0.57 | 47.58 | 44.44 | 26.64 | 26.52 | 30.42 |

The purpose of choosing this block classification was for two reasons. One is to get higher compression ratio, and the other is to reduce the coding time. The threshold value that separates the range blocks into two types was chosen as stated earlier. After classification, VQ-based, GA-based and SA-based coding was adopted for the rough type range blocks only. All the pixel values in a smooth type range block were replaced by the mean of its pixel values. [Table 1] gives the classification of blocks and bit rate using different types of encoding using the proposed techniques on the images chosen for simulation. From the results tabulated in [Table 1], it is observed that for the images which have the number of smooth blocks significantly high has a high compression ratio.

**Figure. 3.** Decompressed Images of Lena, Pepper, Cauliflower and Tajmahal using VQ for block size 8x8 using 16 level

**Figure 4:** Decompressed Images of Lena, Pepper, Cauliflower and Tajmahal using VQ for block size 4x4 using 32 level

The decompressed image of Lena, Pepper, Cauliflower and Tajmahal for the block partition of sizes 8 x8 using 16 level, 4x4 using 32 level and 2x2 using 64 level for the technique VQ is shown in Figure 3,4and 5 respectively.

**Figure 5:** Decompressed Images of Lena, Pepper, Cauliflower and Tajmahal using VQ for block size 2x2 using 64 level

(a) Block size 8x8 (b) Block size 4x4 (c) Block size 2x2

**Figure 6 :** Decompressed Image Of Lena For Block Size 8x8, 4x4 And 2x2 Using The Proposed GA Technique.

(a) Block size 8x8 (b) Block size 4x4 (c) Block size 2x2

**Figure 7:** Decompressed Image Of Cauliflower For Block Size 8x8, 4x4 And 2x2 Using The Proposed GA Technique.

(a) Block size 8x8 (b) Block size 4x4 (c) Block size 2x2

**Figure 8:** Decompressed Image Of Pepper For Block Size 8x8, 4x4 And 2x2 Using The Proposed GA Technique.

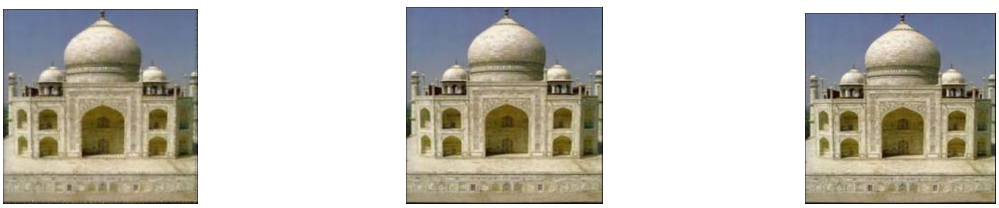

(a) Block size 8x8 (b) Block size 4x4 (c) Block size 2x2

**Figure 9:** Decompressed Image Of Tajmahal For Block Size 8x8, 4x4 And 2x2 Using The Proposed GA Technique.

The decompressed image of Lena, Cauliflower, Pepper and Tajmahal for the block partition of sizes 8 x8, 4x4 and 2x2 using the technique GA is shown in Figure 6,7,8 and 9 respectively. The decompressed image of Cauliflower, Lena, Pepper and Tajmahal for the block partition of sizes 8 x8, 4x4 and 2x2 using the technique SA is shown in Figure 10,11,12 and 13 respectively.

(a) Block size 8x8 (b) Block size 4x4 (c) Block size 2x2

**Figure 10:** Decompressed Cauliflower Image for Block Size 8x8, 4x4 And 2x2 Using the Proposed SA Technique

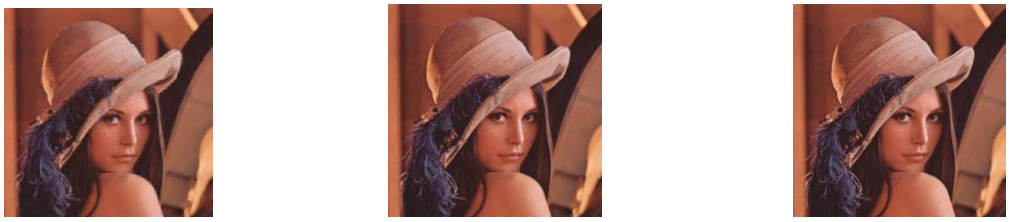

(a) Block size 8x8 (b) Block size 4x4 (c) Block size 2x2

**Figure 11:** Decompressed Lena Image for Block Size 8x8, 4x4 And 2x2 Using the Proposed SA Technique

(a) Block size 8x8 (b) Block size 4x4 (c) Block size 2x2

**Figure 12:** Decompressed Pepper Image for Block Size 8x8, 4x4 And 2x2 Using the Proposed SA Technique

(a) Block size 8x8 (b) Block size 4x4 (c) Block size 2x2

**Figure 13:** Decompressed Tajmahal Image for Block Size 8x8, 4x4 And 2x2 Using the Proposed SA Technique

The Encoding time of the proposed techniques using GA, SA and VQ values are reported in the [Table 2]. These results of encoding time using block sizes 8x8, 4x4, 2x2 are plotted in the graph and shown in Figure 14 and the and their PSNR values are plotted in the graph shown in figure 15.

**Table 2:** Results of the Proposed Iteration-Free Fractal Method Using the Techniques VQ, GA and SA

| Image | Range Block Size | Using GA | | Using SA | | Using VQ | | | | | |
|---|---|---|---|---|---|---|---|---|---|---|---|
| | | RMS | Coding Time (secs) | RMS | Coding Time (secs) | Codebook size 16 | | Codebook size 32 | | Codebook size 64 | |
| | | | | | | RMS | Coding Time (secs) | RMS | Coding Time (secs) | RMS | Coding Time (secs) |
| Lena | 8x8 | 9.29 | 31250 | 9.64 | 17784 | 14.06 | 5941.4 | 14.30 | 6374.3 | 14.29 | 7009.6 |
| | 4x4 | 5.62 | 63871 | 6.64 | 51921 | 10.33 | 23272 | 10.14 | 70142 | 10.19 | 31386 |
| | 2x2 | 2.12 | 110330 | 4.32 | 106660 | 6.74 | 79228 | 6.69 | 104390 | 6.57 | 153450 |
| Pepper | 8x8 | 10.84 | 36276 | 10.33 | 17076 | 16.24 | 5855 | 16.38 | 6756.4 | 16.57 | 6881 |
| | 4x4 | 5.37 | 52157 | 6.25 | 22802 | 11.50 | 21268 | 11.23 | 24023 | 11.35 | 28241 |
| | 2x2 | 2.59 | 77985 | 3.92 | 70342 | 7.37 | 55990 | 7.30 | 160930 | 7.23 | 109640 |
| Cauliflower | 8x8 | 15.39 | 34054 | 14.52 | 17743 | 20.31 | 4562.8 | 20.29 | 4789.2 | 20.34 | 5265.7 |
| | 4x4 | 8.54 | 50683 | 9.78 | 20484 | 17.12 | 16334 | 16.92 | 18459 | 16.77 | 22585 |
| | 2x2 | 3.34 | 84643 | 3.42 | 64120 | 11.34 | 49001 | 11.31 | 66905 | 11.25 | 96249 |
| Tajmahal | 8x8 | 11.86 | 31250 | 12.02 | 28842 | 19.11 | 8817.3 | 19.49 | 5616.4 | 19.52 | 6408.1 |
| | 4x4 | 5.16 | 64737 | 6.16 | 17794 | 13.53 | 14163 | 13.39 | 24725 | 13.39 | 31149 |
| | 2x2 | 1.84 | 110470 | 2.57 | 60320 | 7.68 | 38014 | 7.52 | 95678 | 7.39 | 138210 |

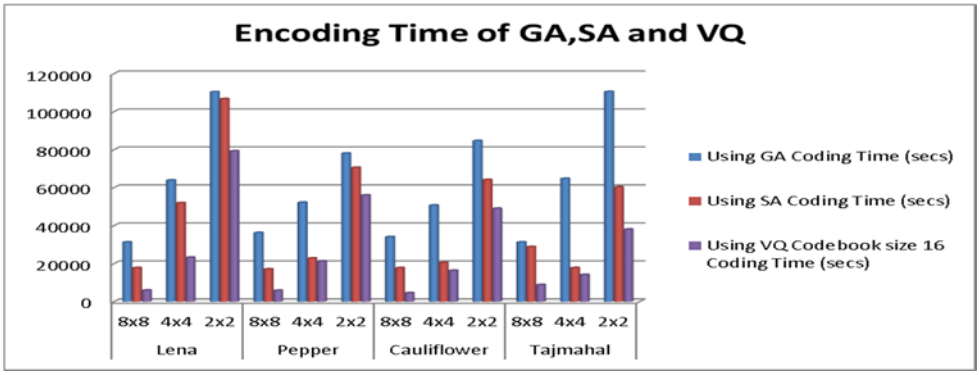


**Figure 14:** Encoding Time of GA, SA and VQ

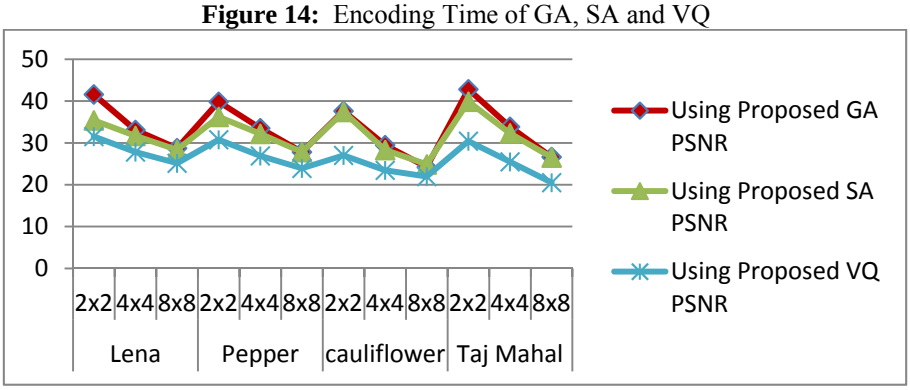


**Figure 15:** PSNR Of Lena, Pepper, Cauliflower and Tajmahal for Block Size 8x8, 4x4 and 2x2 Using the Technique GA, SA And VQ.

From the results obtained, it is obviously clear that GA technique for iteration-free fractal coding is preferred for better image quality whereas VQ is preferred for reduced coding time and SA is preferable for optimal image quality and time. The proposed methods using VQ, GA and SA are found to provide computational efficiency, thereby drastically reducing the cost of coding. [Table 3] gives the result of similar methods found in the literature and the proposed methods for the bench mark image of Lena and Pepper (512 x 512, 24 bit color image). In the proposed method using SA, GA and VQ the PSNR is highly effective when compared to the existing fractal methods given in references (Somasundaram, 2011) and (Nileshsingh and Kakde, 2007)

**Table 3:** PSNR of some methods for 512x512 color images

| Image | Range | SA | GA | VQ | RGB & Gray Scale Component On MPQ-BTC In Image Compression (Somasundaram, 2011) | Color Image Compression with Modified Fractal Coding on Spiral Architecture (Nileshsingh and Kakde, 2007) |
|---|---|---|---|---|---|---|
| Lena | 4 x 4 | 31.68 | 33.12 | 27.84 | 24.1209 | 29.05 |
| Pepper | 4 x 4 | 32.20 | 33.52 | 26.92 | 24.1531 | - |

## Conclusion

In this Work, a fast-encoding algorithm for fractal image coding is proposed and implemented using Genetic Algorithm, Simulated Annealing and Vector Quantization for still color images. First the range blocks were classified as either smooth or rough depending on the variance of the block. This classification was very useful when the image had lot of smooth blocks. So depending on the image and the partition, a high compression ratio was achieved. Only the encoding consumes more time but the decoding is very fast. GA technique for iteration-free fractal coding is preferred for better image quality whereas VQ is preferred for reduced coding time and SA is preferable for optimal image quality and time. The proposed methods using VQ, GA and SA are found to provide computational efficiency, thereby drastically reducing the cost of coding. The execution time can further be reduced by implementing the proposed method in parallel for encoding. Color images are commonly used in most of the application now-a-days. Applications where images can be stored in a compressed form, which require faster retrieval, like medical images and photographs for identification can use the proposed method.

## Acknowledgment

This research work is supported by the UGC, New Delhi, India

## References

Chang and Chung, (2000) .Hsuan T. Chang and Chung J. Kuo. Iteration-Free Fractal Image Coding Based on Efficient Domain Pool Design. IEEE Trans. Image Processing, **9(3)**, 329-339, Mar 2000.

Chang, (2001). Hsuan T. Chang. Variance-Based Domain Blocks for Non-Iterative Fractal Image Compression. Journal of Chinese Institute of Electrical Engineering (EI), **8(2)**, 159-169, April 2001.

Chen et al., (2002). Chen Yisong; Wang Guoping; Dong Shihai. Feature Difference Classification Method in Fractal Image Coding. Proceedings of the 6th International Conference on Signal Processing, **1**, 26-30 Aug. 2002, 648 – 651, 2002.

Chong and Minghong, (2001). Chong Sze Tong and Minghong Pi. Fast Fractal Image Encoding Based on Adaptive Search. IEEE Transactions on Image Processing, **10(9)**, 1269-1277, September 2001.

Ghazel et al.,( 2005). M.Ghazel, R. K. Ward, R. Abugharbieh,E. R. Vrscay, G. H. Freeman. Simultaneous Fractal Image Denoising and Interpolation. 0-7803-9195-0/05/$20.00 ©2005 IEEE, 558-561, 2005.

Hau-Jie and Wang, (2005). Hau-Jie Liang and Shuenn-Shyang Wang. Architectural Design Of Fractal Image Coder Based On Kick-Out Condition. 0-7803-8834-8/05 $20.00 © 2005 IEEE, 1118-1121, 2005.

Jeng et al.,( 2003). Jeng -Shyang Pan, Zhe-Ming Lu and Sheng-He Sun. An Efficient Encoding Algorithm for Vector Quantization Based on Subvector Technique. IEEE Transactions on Image Processing. **12(3)**, 265-270, March 2003.

Jim and Yi,( 2004) .Jim Z. C. Lai and Yi-Ching Liaw. Fast-Searching Algorithm for Vector Quantization Using Projection and Triangular Inequality. IEEE Transactions on Image Processing, **13(12)**, 1554-1558, December 2004.

Mohsen et al., (2003). Mohsen Ghazel, George H.Freeman and Edward R.Vrscay. Fractal Image Denoising, IEEE Trans. Image Processing, **12(12)**, 1560–1578, Dec. 2003.

Nadira and Thamaraiselvi, (2006a) .A.R.Nadira Banu Kamal and Dr S. Thamarai Selvi. Iteration-Free Fractal Coding For Image Compression Using Simulated Annealing. Proceedings of the IET International Conference on Visual Information Engineering 2006, Institute of Engineering and Technology, United Kingdom, 189-194, Sep 2006.

Nadira ,(2012). A.R.Nadira Banu Kamal, "Iteration Free Fractal Compression Using Simulated Annealing for still Colour Images", UACEE International Journal of Artificial Intelligence and Neural Networks,**2(3),**10-14,Dec 2012.

Nadira and Priyanga, (2014). A.R.Nadira Banu Kamal and P.Priyanga, "Iteration Free Fractal Compression Using Genetic Algorithm for still Colour Images", ICTACT Journal on Image and Video Processing,**4(3),** 785-790, Feb 2014.

Nadira and Priyanga, (2014a). A.R.Nadira Banu Kamal and P.Priyanga, "Iteration Free Fractal Color Image Compression Using Vector Quantization", International Journal of Advanced Research in Computer and Communication Engineering, **3(1),** 5154-5163, Jan 2014.

Nileshsingh and Kakde, (2007) .Nileshsingh V. Thakur and Dr.O.G Kakde, "Color Image Compression with Modified Fractal Coding on Spiral Architecture" Journal of Multimedia, **2(4):** 55-66, Aug 2007.

Pan et al.,( 2003) .T.S.Pan, Z. M. Lu and S.H. Sun. An Efficient Encoding Algorithm for Vector Quantization Based on Subvector Techniques, IEEE Trans. Image Processing **12(3),** 265 – 270, 2003.

Riccardo et al., (2006) .Riccardo Distasi, Michele Nappi, and Daniel Riccio. A Range/Domain Approximation Error-Based Approach for Fractal Image Compression, IEEE Transactions on Image Processing, **15(1)**, 89- 97**,** January 2006.

Somasundaram ,(2011). K. Somasundaram and P.Sumitra, "RGB & Gray scale Component on MPQ-BTC in Image Compression", International Journal on Computer Science and Engineering,.**3(4):**1462-1467, Apr 2011.

Vivek Arya et al., (2013). Vivek Arya, Dr.Priti Singh, Karamjit Sekhon, RGB Image compression using Two Dimensional Discrete Cosine Transform, International Journal of Engineering Trends and Technology, **4(4),**828-832,April 2013.

Yung et al., (2003) .Yung -Gi, Wu, Ming-Zhi, Huang, Yu-Ling, Wen. Fractal Image Compression with Variance and Mean, ICME 2003, I- 353 to I-356, 2003.

# Toxic heavy metal chromium remediation by processed low cost adsorbent- Green coconut shell

Seema Tharannum, Krishna Murthy V, Nandini.V, Shruthi.P.T

Department of Biotechnology, PES Institute of Technology, Bangalore, India
seema@pes.edu

**Abstract**: In recent years industrialization, consequent urbanization and increasing population, has lead to pollution of basic amenities of life air, water and soil. The major pollutants from the industrial complexes are effluents with heavy metals. Chromium is a highly toxic element and major pollutant present in the environment. Chromium (III) and (VI) are mainly found in chrome plating, dyes and pigments, leather tanning, and wood preserving. Chromium (VI) is mobile and easily soluble into cells of an organism. There are many methods like ion exchange, ultra filtration, reverse osmosis etc by which chromium (VI) can be removed but they are quiet expensive and have many other disadvantages. In our present study, natural products considered to be wastes were used as adsorbents because of its high availability and low-cost. Low cost adsorbent used was Green coconut shell in a processed form in order to compare the efficiency. This study, reports the efficiency of low cost biosorbents in remediation of chromium (VI). It is seen that the biosorbents, green coconut shell has showed high biosorption capacity as it reduced 50% of 100mg/L concentration of chromium in a span of 24 hrs. The obtained results showed that incubation time and size of adsorbent affected the uptake capacity of biosorbent. As the time increased the percentage of adsorption increased till 264 hours. Smaller the size more efficient is the adsorption capacity. Hence, low cost biosorbents can be potential agents of bioremediation of heavy metals which are toxic to all life forms especially to humans.

**Key words:** Biomass, Waste, Biosorption, Effluent, Industrial, Heavy metals, Toxic.

## Introduction

In the wake of industrialization, consequent urbanization and increasing population, the basic amenities of life i.e. air, water and soil are being polluted continuously. Industrial complexes have become the focus of environmental pollution. The major pollutants from the industrial complexes are effluents with heavy metals. Chromium, a highly toxic element is a major pollutant present in the environment, are mainly found in chrome plating, dyes and pigments, leather tanning, and wood preserving (Anyakora et al., 2011). Chromium (Cr) is a heavy metal that can exist in six valence states, 0, II, III, IV, V and VI, which represent the number of bonds an atom is capable of making. Trivalent (Cr-III) and hexavalent (Cr-VI) are the most common chromium species found environmentally. Trivalent is the most stable form and its compounds are often insoluble in water. Hexavalent Chromium is the second most stable form, and the most toxic. Many of its compounds are soluble. Most chromium VI in environment is due to anthropogenic activities. Occupational exposure is via inhalation. Cr (III) is poorly absorbed, whereas Cr (VI) is readily absorbed.. Exposure to chromium leads to nasal irritation, nasal ulcers, and perforation of nasal septum and hypersensitivity reactions and chronic holes of the skin (Holmes et al., 2008). World Health Organization and Indian Standard Institution has the desirable limit for Cr (VI) in drinking water is 0.05mg/L and With reference to Central pollution control board, the allowable chromium concentration in effluents is 2.0-5.0 mg/L. The techniques conventionally used for removal of heavy metals from contaminated sites include: reverse osmosis, electro dialysis, ultra filtration, ion-exchange, chemical precipitation, phytoremediation, etc. Each of these methods has its own merits and demerits (Hima et al., 2007) the methods suggested are being time consuming and needs expertise. Bioremediation is a process of removal of toxic metals using living organisms. Bioaccumulation is the widely used bioremediation technique which involves the accumulation of heavy metals in the organism. Though the technique is widely used, has its own pros and cons. Biosorption is a physicochemical process that occurs naturally in certain biomass which allows it to passively concentrate and bind contaminants onto its cellular structure. The most frequently studied biosorbents are Bacteria, Fungi and Algae. But more recently, the search for new cost effective biosorbents has directed attention and natural sorbents which can effectively remove toxic metals (Senthilkumar et al., 2000). A successful biosorption process requires preparation of good biosorbent. The process starts with selecting various types of biomass. Pretreatment and immobilization are done to increase the efficiency of the metal uptake. The adsorbed metal is removed by desorption process and the biosorbent can be reused for further treatments ( Hima et al.,2007). In our study, biomass of Green coconut shell considered as waste and disposed to the environment without any further usage, was used as adsorbent because of its high availability and low-cost.

## Materials and Method

### Sampling

The adsorbent Green coconut shell waste was collected from coconut vendors , sun dried for 2 days and was blended in a mixer. The blended powder was sieve separated on the basis of particle size of 719 microns and 250 microns and pre treated with 0.1 M NaOH for 3 hours and then washed with distilled water to remove the traces of NaOH( Rosa et al.,2010).The sample was filtered and then dried at 50°c in Hot air oven .

### Estimation of Chromium (VI)

Chromium estimation was carried out by spectrophotometric method using Diphenylcarbazide (APHA 2005). Chromium (VI) was determined colorimetrically by reaction with diphenylcarbazide in acid solution. A pink colour complex was formed, absorbance was read at 540nm. Chromium standard of 100mg/L was prepared using potassium di chromate. Optical density of known standard samples was recorded and Graph of absorption versus amount of chromium (µg) was plotted.

### Batch Studies

The batch studies were carried in 250ml conical flasks at Room Temperature (RT) by shaking at an interval of two hours. 0.5g of biosorbent Green coconut shell waste was mixed with 100ml of standard chromium solution(100mg/L) in 250ml conical flask. After a known contact period of 24, 48, 72, 96 hours (h), 0.5ml of solution was collected from conical flask and centrifuged at 6000rpm for 5 minutes at 4°c. The supernatant thus collected was estimated for chromium by DPC method (Shankar Congeevaram., 2006). Adsorption studies were conducted in triplicates.

### Column Studies

A borosilicate column (21cm X 2.2cm) was filled with adsorbent Green coconut shell waste corresponding to 3cm bed heights. The adsorbent was initially heated with distilled water to 80°C to remove the lipids. The bed was then filled with 10ml of chromium solution (100mg/L). After a known contact period of 24, 48, 72, 96 hours (h), 0.5ml of solution was collected and estimated for chromium by DPC method The amount of chromium before and after adsorption was determined by DPC method.

## Results and Discussion

### Sampling

The Green coconut shell samples of different sized particles obtained by sieve method were collected processed and stored at room temperature for analysis.

### Estimation of Chromium(VI)

The hexavalent chromium was determined calorimetrically by reaction with diphenylcarbazide in acid solution. Absorbance at 540nm was found to increase as the as the chromium concentration increases. The results are as plotted in Figure 1.

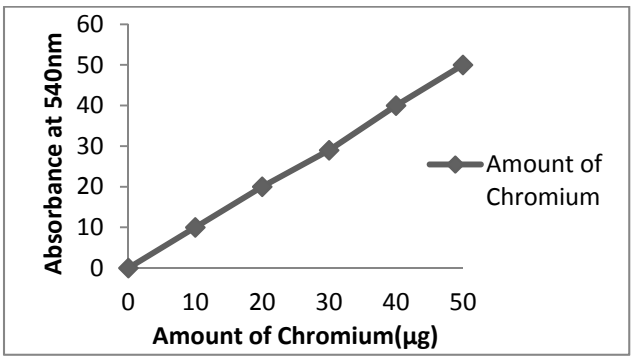


**Figure1:** Standard Chromium curve by DPC method.

### Batch Studies

The amount of chromium decreased from day 1 to day 8. Sample of particle size 719 microns was found to adsorb 90mg of chromium from the solution, whereas, that of particle size 250 microns was found to remove chromium completely from the solution on day 8. Comparisons of amount of chromium in the solution with both the particle sizes are as depicted in Figure 2 ( 2a and 2b)

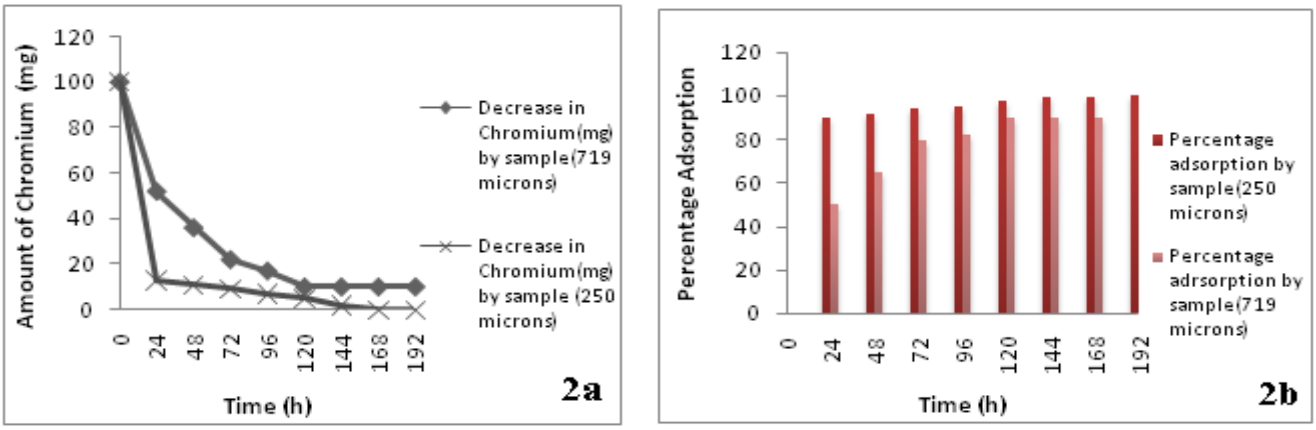


**Figure 2:** Effect of Particle size on Adsorption in Batch studies 2a: Chromium removal capacity of green coconut shell. 2b: Percentage adsorption of green coconut shell

**Column Studies**

The amount of chromium was found to reduce gradually and total amount of chromium was to be absorbed in 30h. Sample of particle size 250 microns was found to adsorb chromium completely in a short contact time(42h), whereas, the same of particle size 719 microns showed 100% adsorption by the end of 48h. percentage adsorption by sample of both particle sizes are compared in Figure 3 (3a and 3b).

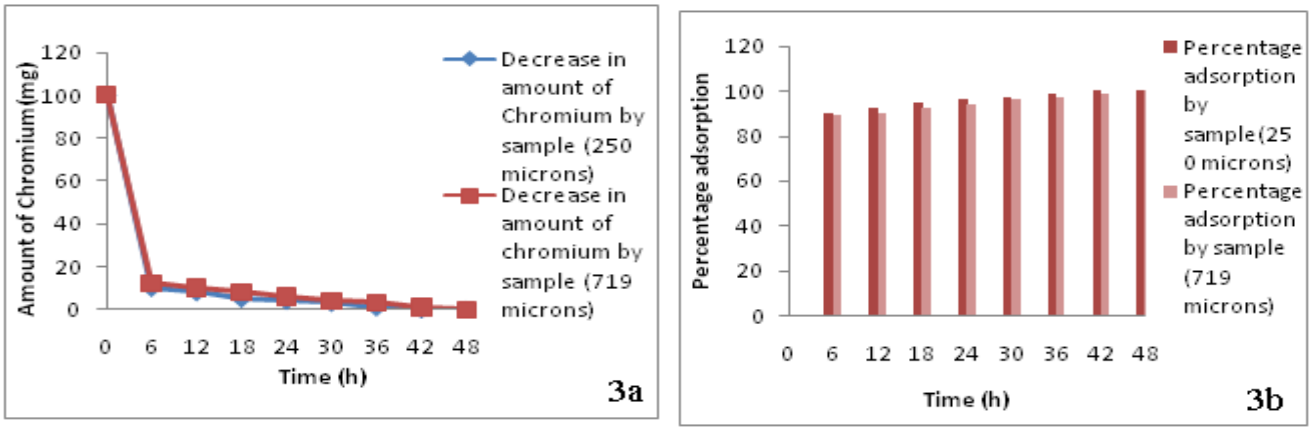


**Figure 3:** Effect of Particle size on Adsorption in column studies 3a: Chromium removal capacity of green coconut shell. 3b: Percentage adsorption of green coconut shell

**SEM and EDS Analysis**

Scanning electron microscope evaluated the morphological characteristics of coconut. The micrographs of coconut shell powder before metal uptake and the respective EDS (Energy Dispersive Spectroscopy) analyses are presented in Fig 4a and 5 respectively. Fig 4b and 6 show the same for coconut shell after chromium uptake.

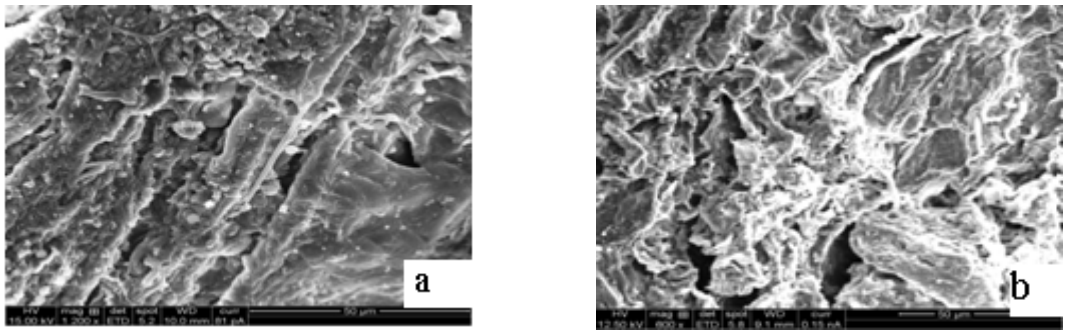


**Figure 4:** Scanning electron micrograph of coconut shell a) Before and b)after Cr biosorption.

Figure 4 a shows a quite irregular and porous material. This surface characteristic would be substantiating the high adsorption observed for particles of larger size, through mass transport inside the sorbent. Figure 4 b shows no significant difference between the surface of particles loaded with metal ions and the particles that does not suffer the biosorption process .

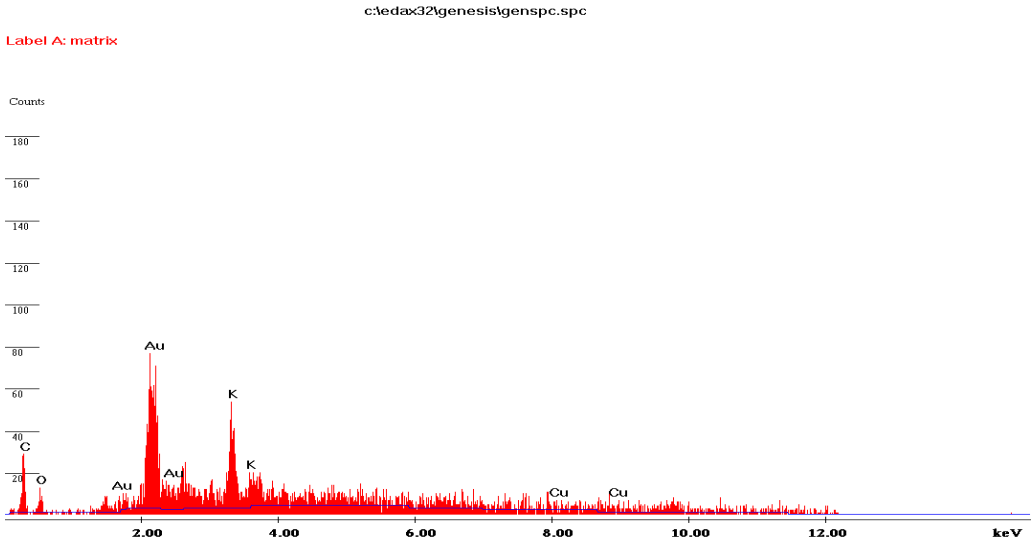


**Figure 5:** EDS diffractogram of micrographs of coconut shell before Cr uptake.

The EDS analysis presented in Figure 5 shows the presence of Cu, K, O and C as natural species on the coconut shell, as already expected. The presence of these elements could influence on the adsorption mechanism thought ionic exchange interactions.

The EDS analysis in the particle loaded with chromium presented in Figure 6, shows the presence of chromium bands, and the absence of Ca, K, Na, O and Mg bands. This could be indicative of ionic exchange mechanism involvement between these elements and Cr on the surface of particles. The band of Au appears in the EDS, a time that the metalizing of the samples was carried through with this element.

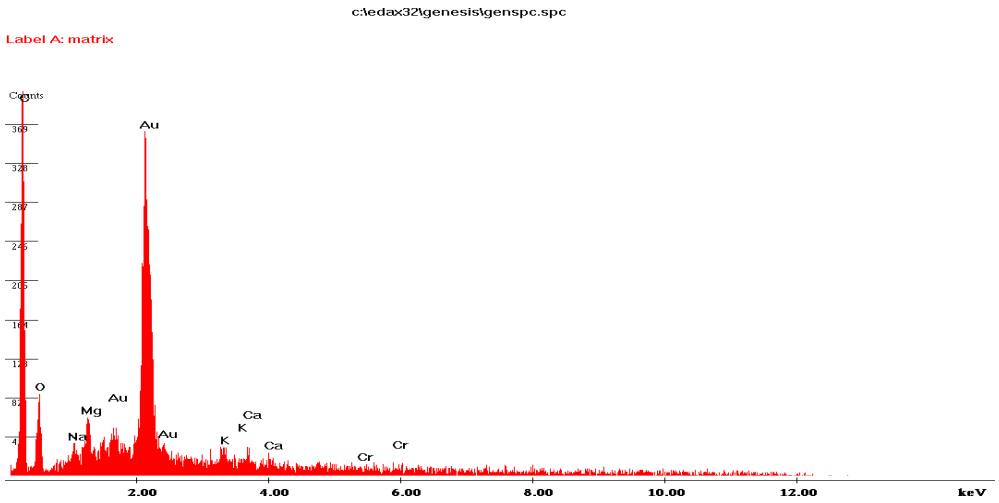


**Figure 6**:EDS diffractogram of micrographs of coconut shell after Cr biosorption.

## Conclusions

The study establishes the role of low cost adsorbent like green coconut shell in biosorption, accumulation and remediation of chromium (VI). Heavy metals can be toxic to all the life forms especially to humans due to their strong affinity to form complexes with the constituents of cell membrane, causing impairment of their functions and loss of integrity. However, low cost adsorbents can be potential agents for bioremediation of heavy metal pollution.
The study when conducted in batch revealed that capacity of green coconut shell to biosorb the heavy metal chromium (VI). Sample G showed to absorb 50% of chromium with an incubation of 24h and 90% adsorption in 144hrs.

The results obtained showed that incubation time affected the uptake capacity of biosorbent. As the time increased the percentage of adsorption increased till 264 hours. Another important parameter was the influence of the particle size (719 and 250 microns) used to uptake chromium. It showed increase in chromium adsorption with decrease of particle size of biomass. Later, a column study was performed in which Sample G and was found to adsorb maximum amount of chromium. So finally, green coconut shell powder of 250 microns showed better results than 719 microns. The analyses accomplished by MEV-EDS proved the presence of chromium in the biomass particles i.e green coconut shell powder after biosorption. The micrographs obtained show a quite irregular and porous material. This surface characteristic would be substantiating the high adsorption observed for particles of larger size, through mass transport inside the sorbent.

## Acknowledgements

The authors wish to thank management, PES Institute of Technology, Bangalore for providing research facility to carry out present work.

## References

Ahalya N, T.V. Ramachandra, RD Kanamadi(2003). Biosorption of heavy metals: Review. *Research journal of chemistry and environment*, Vol 7(4): 71-79.

Ahmed Ahmed Gaballa, Ranya Amer, Hany Hussein, Hassan Moawad and Soraya Sabry(2003). Heavy metal resistant pattern in moderately halophilic bacteria. *Arab Journal of biotech.*Vol2:267-278

Aksu Z and Acikel U. (2000). Modelling of a single-staged bioseparation process for simultaneous removal of iron (III) and Chromium(VI) by using Chlorella vulgaris. *Biochem Eng. J,* 4:229-238.

Alice Wang and Kevin Lin(2001). Effects of N-Acetylglucosamine and alpha methylglucoside on bacteriophage T4adsorption of E.coli B23.*Journal of Experimental Microbiology and Immunology (JEMI)* .Vol. 1:54-63

Alok Prasad Das and Susmita Mishra(2010). Biodegradation of the metallic carcinogen hexavalent chromium (VI) by an indigenously isolated bacterial strain. *Journal of carcinogenisis*. Vol 9:1-7.

Ansari M I and Mallik A. (2007). Biosorption of nickel and cadmium by metal resistant bacterial isolates from agricultural soil irrigated with industrial wastewater. *Bioresource Technol*, 56(6):3149-3153.

APHA: Standard methods for the examination of water and wastewater. 21st Edn. Washington, D.C. (2005).

Asha Latha Singh(2007).Removal of Chromium from waste water with the help of microbes. e- journal of science and technology.21:361-370.

Bai, R. S., Abraham, T. E., (2001). Biosorption of Cr(VI) from aqueous solution by *Rhizopus nigrificans*. *Bioresources Technology.,* 79: 73-81.

Chimezie Anyakora, Kenneth Nwaeze, Olufunsho Awovedele, Chinwe Nwadike, Mohsen Arbabi and Herbert coker (2011). Concentrations of heavy metals in some pharmaceutical effluents in Lagos, Nigeria. *Journal of Environmental Chemistry and ecotoxicity,* Vol 3, No. 2: 25-31.

Deans J R and Dixon B G. (1998). Uptake of Pb2+and Cu2+ by novel biopolymers. Wat. Res,26:469-472.

Emine Malkov and Yasar Nuhoglu(2007). Potential of tea factory waste for chromium(VI) removal from aqueous solutions:thermodynamic and kinetic studies. *Journal of separation and purification technology*, Vol 54:291-298.

Francisco W.Sousa, Andre G.Oliveira, Jefferson P.Ribeiro, Morsyleide F.Rosa, Denis Keukeleire, Ronaldo F.Nascimento (2010). Green coconut shells applied as adsorbent for removal of toxic metal ions using fixed bed column technology. *Journal of environmental management,* Vol 91:1634-1640.

Gabriela Huama Pino, Luciana Maria Souza de Mesquita,Mauricio Leonardo Torem, Gustavo Adolfo Saavedra Pinto (2006). Biosortion of Cadmium by green cocnut shell powder. *Journal of Mineral engineering*, Vol 19:380-387.

Gadd G M. (1990). Heavy metal accumulation by bacteria and other microorganisms *Experentia. Biochem Eng. J*, 46:834-840.

Guixia Zhao, Xilin Wu, Xiaoli Tan and Xiangke Wang. (2011). Sorption of Heavy metal ions from Aqueous Solutions: A Review. *The Open Colloid Science Journal*, 4: 19-31.

Hima Karnika Alluri, Srinivasa Reddy Ronda, Vijaya Saradhi Settalluri, JayakumarSingh(2007). Biosorption: an ecofriendly alternative for heavy metal removal. *African jounal of biotechnology*, Vol 6, No. 25:2924-2931.

Holmes A.L., Wise S S and Wise J P(2008). Carcinogenicity of hexavalent chromium. *Indian journal of medical research*. Vol 128:353-378.

Jianlong Wang, Can Chen(2008).biosorbents for heavy metals removal and their future. *Journal of biotechnology advances.*Vol 22:196-222.

# Simple Harmonic Motion Experiment Using Force Sensor: Low Cost and Single Setup

**Siti Nurul Khotimah[1], Luman Haris, Sparisoma Viridi, Widayani, and Khairurrijal**
Department of Physics, Faculty of Mathematics and Natural Sciences
Institut Teknologi Bandung
Jalan Ganesha No. 10, Bandung 40132, Indonesia
[1]e-mail: nurul@fi.itb.ac.id

**Abstract:** A method of simple harmonic motion (SHM) experiment is proposed. The SHM of a load-spring system is observed through the use of force sensor to measure the force acting on the spring. The data will then be further analyzed to derive the kinematic of load. Through the enforcement of Newton's second law of motion, this method is able to produce two out of three kinematic quantities; $x(t)$ and $a(t)$. It will then be completed through numerical approach such as Euler method and central finite difference. The experimental data are used to determine appropriate initial conditions for numerical approach, and initial phase angle for constructing the theoretical kinematics. The result was further validated through the ellipse trajectory in phase-space. Hence, the experiment proved to be capable of producing simple harmonic motion without raising the complexity level. It can also produce all of the necessary quantities needed to provide SHM kinematics in the form of both graphs and equations.
**Keywords**: simple harmonic motion, oscillation, force sensor, Euler method, phase space

## Introduction

There are many objects around us that exhibit oscillation behavior such as the beatings of butterfly wing, trembling building due to earthquakes, pendulum motion of grandfather clock, and the motion of rodeo cowboy while riding hopping bull. However, most of natural oscillations are nonlinear which is formed by an infinite number of harmonics (Beléndez et al, 2007). Simple harmonic motion (SHM) is a basic type of oscillations where each motion is mathematically expressed in a sinusoidal function of time with a single frequency (Halliday et al, 2011).

Although kinematics of an object undergoing simple harmonic motion has been established, the mathematical formulas (position, velocity, and acceleration) are still in general solution. Hence, students may have difficulties either with the determination of its phase constant or the initial conditions for the corresponding kinematic quantities. Therefore, laboratory work is necessary to support the theoretical literature.

However, there are other problems occurring in SHM experiments. Laboratory work is designed to provide students the opportunity to acquire the necessary skills and techniques in manipulating apparatus as well as ample understanding of the instruments themselves (Tyler, 1967). In other words, the experiment should be carefully carried out in order to ensure the validity of the obtained data. Thus, it would be better if the system is equipped with apparatus to record the raw data as a function of time. This would enable them to focus on data interpretation and analysis instead of wasting most of their time collecting data (Thornton and Sokoloff, 1990).

There are several ways of observing simple harmonic motion, and determining oscillation period is one of them. Some experiments utilize photogate as a means of measurement (Triana and Fajardo, 2012). Another way of observing SHM is through the trajectory of the object in which video recording is commonly used. This method captures the object movement whose image will be processed through a certain image processing algorithm and pixel conversion. However, this method can only produce one out of three kinematic quantities which is position of load.

The previously established methods for SHM experiment require several correction and approximation. Some still debating over the use of static spring constant and dynamic one since it was proved that the two quantities have different values although still fall within agreeable uncertainties (Baylor University, 2010). Another chose to consider the effect of spring mass resulting in approximation and rules (Eduardo and Gabriel, 2007). Meanwhile, Pasco used both force sensor and motion sensor to observe SHM; obtaining all of the SHM kinematics (Pasco, 2014).

In developing countries, equipment for physics experiment is usually inadequate. So with provided tools, the same output must be produced as if the experiment is carried out using more complete equipment. Therefore, a SHM experiment is proposed using only force sensor. It is used to measure the spring restoring force which is displayed as a

function of time. It also requires the use of numerical approach as a complementary means of obtaining the kinematics equation. It will be shown that this method is comparable to others in obtaining kinematics quantities in the form of both graphs and equations.

## Theory

For every system which exhibits simple harmonic motion of amplitude $A$, the position is given by the following equation.

$$x(t) = A\cos(\omega t + \varphi) \quad (1)$$

Where angular frequency $\omega$ is a measure of the oscillations rapidity, and initial phase $\varphi$ is determined from the initial condition of the system. Furthermore, velocity and acceleration are given as follows:

$$v_x(t) = -A\omega\sin(\omega t + \varphi) \quad (2)$$

$$a_x(t) = -A\omega^2\cos(\omega t + \varphi) \quad (3)$$

Meanwhile, a relation between angular frequency $\omega$ and period $T$ is given by

$$\omega = \frac{2\pi}{T} \quad (4)$$

Mechanical energy $E$ of a simple oscillating object having mass $m_b$ is

$$E = \frac{1}{2}m_b\omega^2A^2 \quad (5)$$

In accordance with the concept on mechanical energy, a relation between speed and position of the system is formulated as (Kaiser, 1990):

$$|v_x(t)| = \omega A\sqrt{1-\left(\frac{x(t)}{A}\right)^2} \quad (6)$$

and an equation for its trajectory in phase-space (position-momentum space) is

$$\frac{x^2}{\left(2E/m_b\omega^2\right)} + \frac{\left(m_bv_x\right)^2}{\left(2m_bE\right)} = 1 \quad (7)$$

which is an ellips with area of $\frac{2\pi E}{\omega}$.

## Experiment

A load-spring system and the measurement apparatus were arranged as shown in Figure 1. The force sensor is hung on the top of the stand, while the system was hung on the hook below the sensor. The sensor was connected to an analog channel of an interface from Vernier which is connected to a computer through USB port. Once the oscillation occurred, the force acting on the spring will be measured every 0.01 second, and stored within a file using Logger Pro. This setup was chosen such that the data could smoothly form sinusoidal pattern.

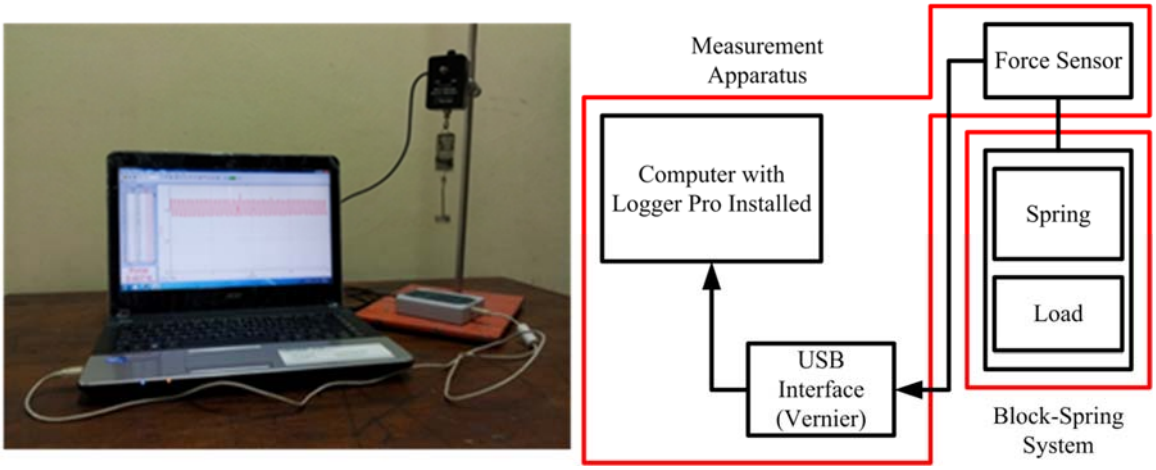


Figure 1. The experimental setup for observing simple harmonic motion which consists of load-spring system and measurement apparatus (Vernier Software & Technology, 2014).

The sensor reading $F_R$ must then be processed further to obtain the actual spring force on the load $F$ . The process is based on the illustration of three different position shown in Figure 2. While the load is at equilibrium position (Figure 2a), the sensor reading $F_R(t)$ shows the weight of both load and spring, i.e. $F_R = (m_b + m_s)g$ . Once the load is pulled down from its equilibrium position (Figure 2b), the spring stretches. As a result, the load is pulled upward by the spring while the spring pulled the sensor down. Similar explanation can also be applied to the last state (Figure 2c). In summary, the spring force $F(t)$ on the load is equal to the difference between the new reading and the reading at equilibrium position. Hence, at any time $t$ , the spring force on the load is the same as the difference of the sensor reading with respect to the reading in equilibrium state.

$$F(t) = F_R(t) - (m_b + m_s)g \tag{8}$$

Moreover, Hooke's Law may be applied to equation (8) yielding the position of the load at any time $t$ .

$$x(t) = -\frac{F_R(t) - (m_b + m_s)g}{m_b \omega^2} \tag{9}$$

Angular frequency $\omega$ may be obtained through equation (4) while the oscillation period $T$ is determined by plotting $F_R(t)$ as shown in Figure 3. Meanwhile, equilibrium position is also obtained when the $F_R(t) = 0.61\,\mathrm{N}$ which corresponds to equation (9) when $x(t) = 0$. Furthermore, plotting $x(t)$ in equation (9) yields oscillation amplitude $A$ . On the other hand, in accordance with Newton's second law of motion, equation (8) yields the acceleration of the load.

$$a_x(t) = \frac{F_R(t) - (m_b + m_s)g}{m_b} \tag{10}$$

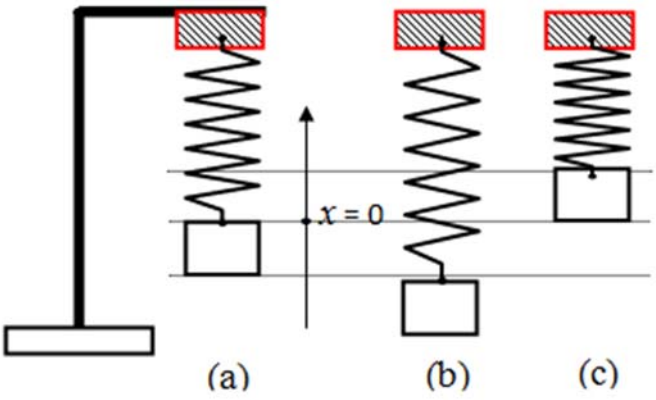


Figure 2. Three different positions of load: (a) at equilibrium $(x = 0)$, (b) at negative $x$ , and (c) at positive $x$ .

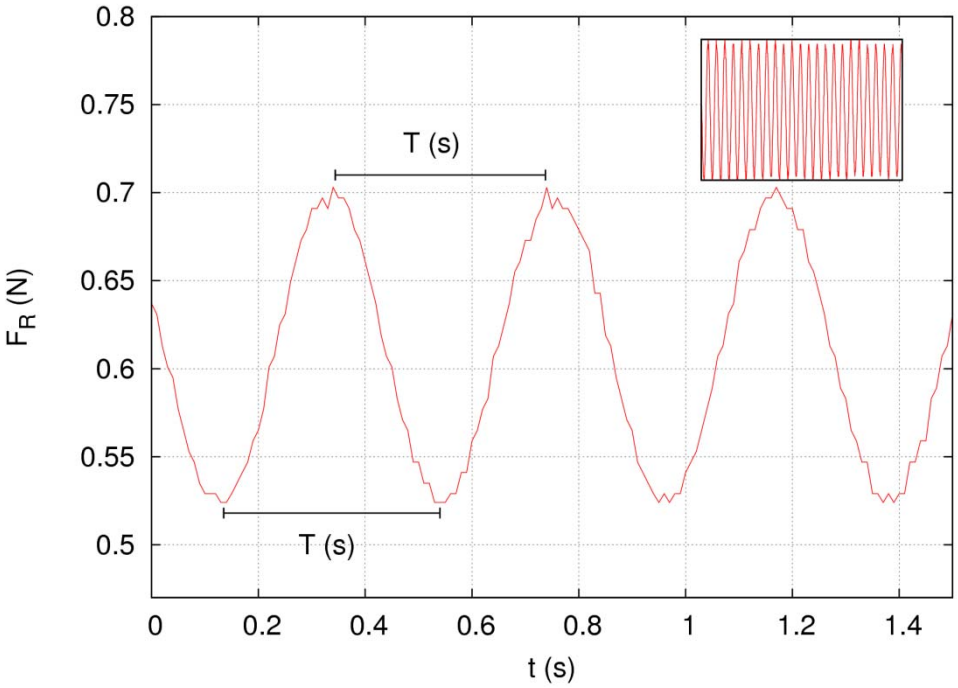


Figure 3. A sample of sensor readings was taken from the whole data (upper right) to determine oscillation period $T$ . The sensor reading is centered at about 0.61 N which corresponds to equation (9) when $\boldsymbol{x(t) = 0}$ .

## Numerical Approach

Numerical approach was used to support the results obtained by the experiment. It was used to obtain velocity of load since equation (6) is only capable of yielding speed. It is based on the standard kinematics and motion equations. Newton's second law of motion gives:

$$m_b \frac{dv_x}{dt} = -m_b \omega^2 x \tag{11}$$

Based on equation (11), numerical formulation of velocity of the load can be derived. Euler method yields:

$$v_x(t + \Delta t) = v_x(t) - \omega^2 x(t)\Delta t \tag{12}$$

$$x(t + \Delta t) = x(t) + v_x(t + \Delta t)\Delta t \tag{13}$$

Note that equation (12) requires initial conditions obtained from the experiment. The rest is generated numerically using equation (13). On the other hand, the central finite difference (cfd) method yields:

$$v_x(t) = \frac{x(t + \Delta t) - x(t - \Delta t)}{2\Delta t} \tag{14}$$

This method generates velocity of load using the position of load obtained from equation (9).

## Results

Simple harmonic motion characteristics were obtained not only from experiment through several equations but also from numerical simulation. These characteristics and other information such as load mass and spring mass were provided within Table 1.

Table 1. SHM properties and the other parameter used in the experiment.
All quantities are given in mks unit.

| Quantities | Value | Note |
|---|---|---|
| $m_b$ | 0.057 | Data |
| $m_s$ | 0.00536 | Data |
| $T$ | 0.420 | Experimental result, Figure 3. |
| $\omega$ | 14.960 | Numerical calculation, equation (4) |
| $A$ | 0.0069 | Experimental result, Figure 4 |
| $x_0$ | -0.00198 | Experimental result, Figure 4 |
| $v_0$ | 0.099 | Numerical calculation, equation (6)* |
| $\varphi$ | -0.5926 $\pi$ | Numerical calculation, equations (1) and (2) at $t$ = 0 |

*equation (6) provides the initial speed at $t$ = 0, however the direction of $v_0$ is determined by observing $x_0$ and $a_0$ from Figure 4.

Finally, kinematics of the load can be written as:

$$x(t) = 0.0069\cos\left(\frac{2\pi}{0.420}t - 0.5926\pi\right)$$

$$v(t) = -0.1032\sin\left(\frac{2\pi}{0.420}t - 0.5926\pi\right)$$

$$a(t) = 1.5442\cos\left(\frac{2\pi}{0.420}t - 0.5926\pi\right)$$

## Discussion

Aside from the reason when input parameter for force sensor is determined, the time step $\Delta t = 0.01$ means that 42 data were used within one period which is sufficient to reconstruct sinusoidal curve. This is shown within Figure 4 up to Figure 6. On the other hand, the validity of this experiment can be proved by observing Figure 3 and Figure 4. In accordance with Hooke's law, it is known that spring force $F$ is proportional to the position of the load $x$. Hence, the oscillation can be observed directly from $F_R(t)$ instead of $x(t)$. The sensor reading $F_R(t)$ shows a sinusoidal motion which keeps repeated periodically. Furthermore, as seen within Figure 4, the kinematic quantities obtained from the experiment are well overlapping with those obtained theoretically.

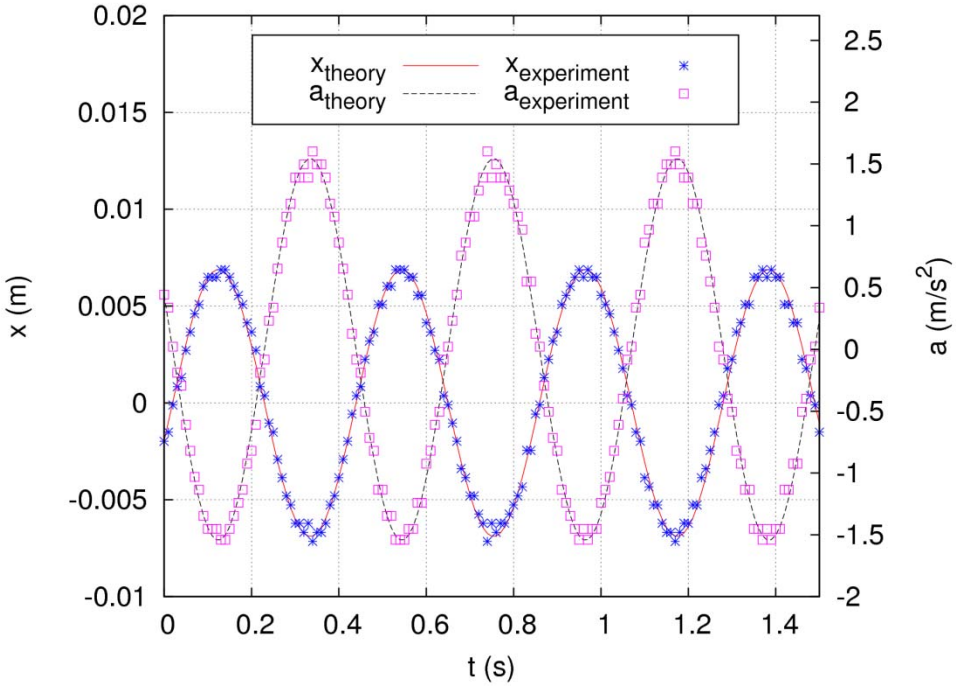


Figure 4. The acquired kinematic quantities compared to the theoretical one.

Since velocity cannot be obtained directly from the experiment, the velocity of the theoretical kinematics is compared to that obtained from the simulation. It can be seen from Figure 5 that equation (6) is actually enough to show that the proposed method is sufficient in producing simple harmonic motion. However, since it is a scalar quantity, then it lacks the direction. Hence, to complete the kinematic of simple harmonic motion, numerical method is used. Among two numerical methods that were used, it was decided that Euler method is most suitable to be used to complement the experiment. This decision was based on the comparison between the two numerical methods and the theoretical one as seen within Figure 6. As seen in equation (14), the velocity generated by cfd method is essentially the slope of position of load $x(t)$. Although the curve of $x(t)$ is continuous, its slope may become discontinue at critical points and turning points causing the value to blow up.

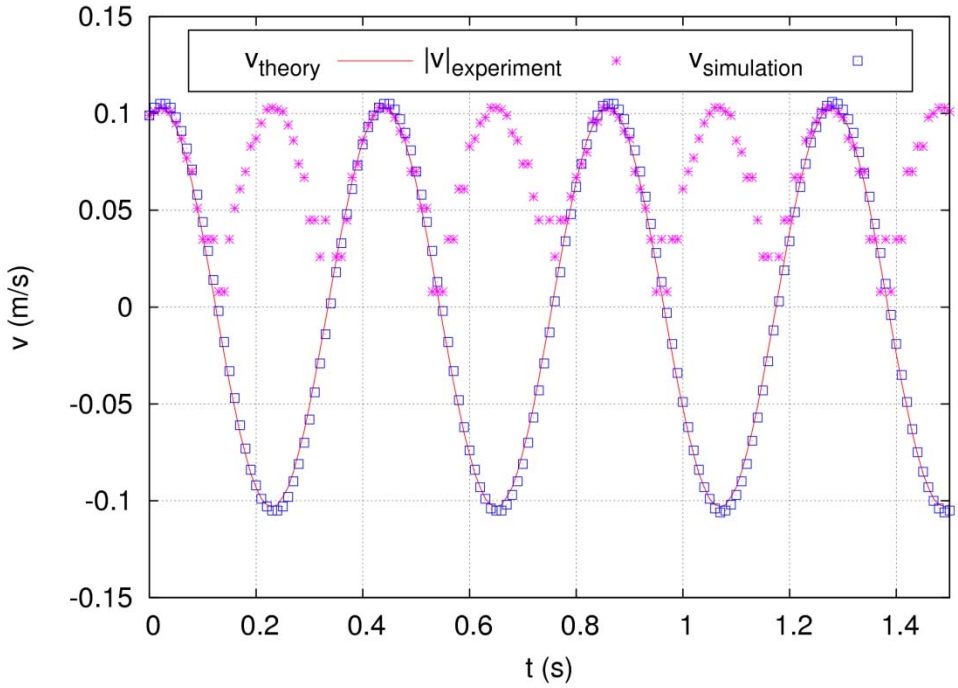


Figure 5. Numerically obtained velocity of load compared to the theoretical one. Additionally, the speed of load is also provided.

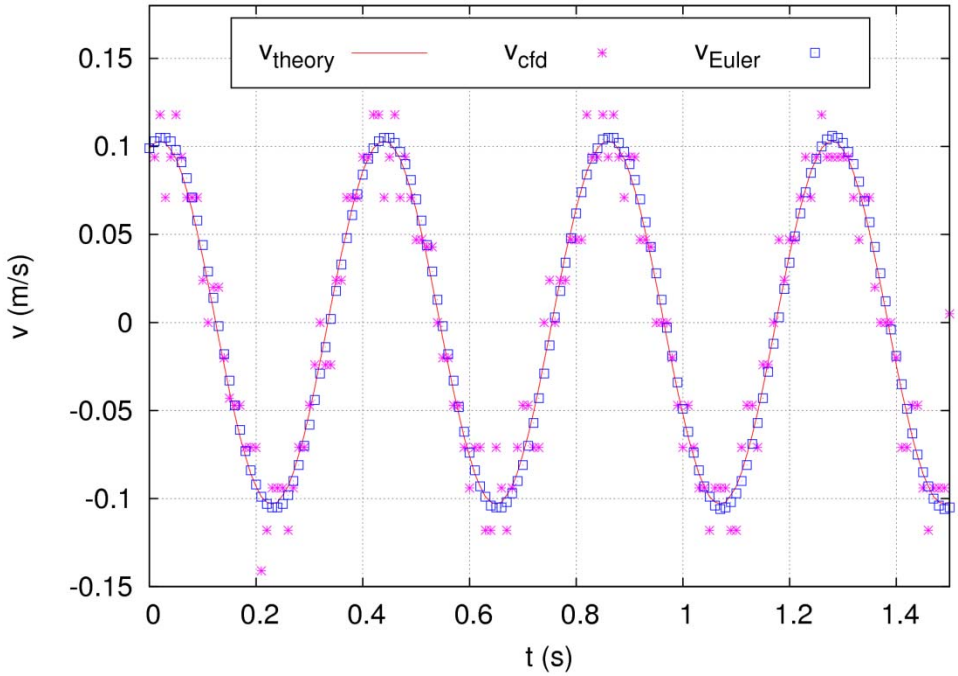


Figure 6. Velocity of load obtained from the numerical methods was compared with theory.

Figure 7 shows that experimental data of position $x(t)$ with respect to the corresponding numerical data of momentum $m_b v(t)$. Trajectory in phase-space of this SHM seems to appear as an ellipse which validate the experimental results.

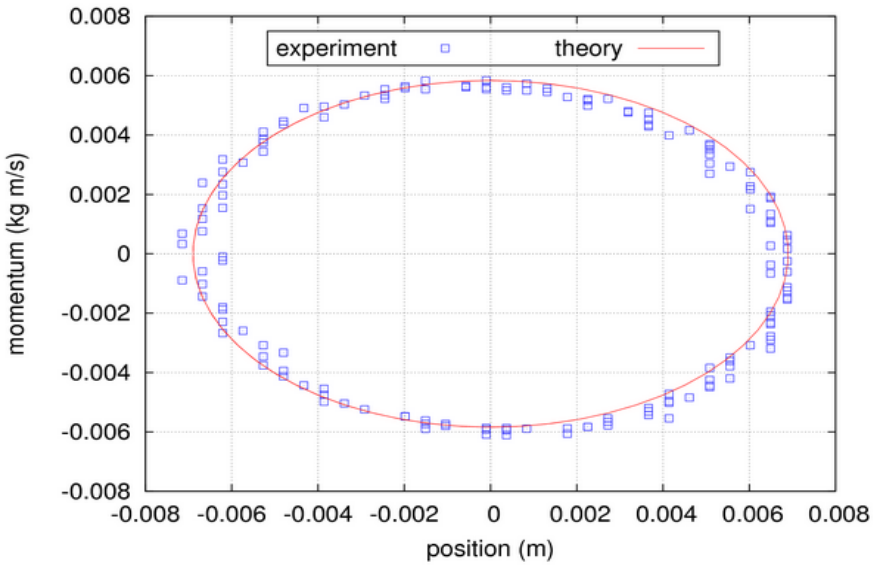


Figure 7. The plotting of SHM data for 3.5 periods in phase space forms an ellipse.

## Conclusion

The force-based SHM experiment proved to be able to produce simple harmonic motion without the use of complicated approximation and condition. The interpretation of the raw data is quite simple since it only involves analytical work. Complementing the method with Euler method allows it to produce all of the necessary quantities in the form of graphs and equations; including initial phase angle. They were also verified through the ellipse trajectory in phase-space.

## References

Beléndez A, Hernández A, Beléndez T, Neipp C, & Márquez A (2007). Application of Homotopy Perturbation Method to the Nonlinear Pendulum. Eur. J. Phys, 28 (1), 93-104.

Halliday David, Resnick Robert, & Walker Jearl (2011). Principles of Physics, 9th ed, International Student Version. Asia: John Wiley & Sons, Inc, 386-387.

Tyler F (1967). A laboratory Manual of Physics, 3th ed. London: Edward Arnold (Publishers) ltd, 1.

Thornton RK & Sokoloff DR (1990). Learning Motion Concepts using Real-Time Microcomputer-Based Laboratory Tools. Am. J. Phys., 58 (9), 858-867.

Triana CA & Fajardo F (2012). The Influence of Spring Length on the Physical Parameters of Simple Harmonic Motion. Eur. J. Phys., 33 (1), 219-229.

Baylor University (2010). Mechanical Behavior of a Spring. Sample Lab Report.

Eduardo E. Rodriguez & Gabriel A. Gesnouin (2007). Effective Mass of an Oscillating Spring. The Physics Teacher. 45, 100-103.

Pasco (2014). Simple Harmonic Motion. Teacher Information, 1-15.

Kaiser JF. (1990). On a Simple Algorithm to Calculate the `Energy' of a Signal. International Conference on Acoustics, Speech, and Signal Processing (ICASSP-90). 1, 381 – 384.

Vernier Software & Technology (2014). Computer Experiment 16: Simple Harmonic Motion, Evaluation Copy of the Vernier Student Lab. 16.1-16.5.